

EFFECT OF PLASTIC MEDIA ON MASS TRANSFER AND BUBBLE HYDRODYNAMIC
PARAMETERS IN BUBBLE COLUMN AND AIRLIFT REACTOR

Miss Nawaporn Thaphet

จุฬาลงกรณ์มหาวิทยาลัย
CHULALONGKORN UNIVERSITY

A Thesis Submitted in Partial Fulfillment of the Requirements
for the Degree of Master of Science Program in Environmental Management
(Interdisciplinary Program)

Graduate School

บทคัดย่อและแฟ้มข้อมูลฉบับเต็มของวิทยานิพนธ์ตั้งแต่ปีการศึกษา 2554 ที่ให้บริการในคลังปัญญาจุฬาฯ (CUIR)

เป็นแฟ้มข้อมูลของนิสิตเจ้าของวิทยานิพนธ์ที่ส่งผ่านทางบัณฑิตวิทยาลัย

Copyright of Chulalongkorn University

The abstract and full text of theses from the academic year 2011 in Chulalongkorn University Intellectual Repository (CUIR)
are the thesis authors' files submitted through the University Graduate School.

ผลกระทบของตัวกลางพลาสติกต่อตัวแปรด้านการถ่ายเทมวลสารและอุทกพลศาสตร์ของ
ฟองอากาศในถังปฏิกรณ์แบบฟองอากาศและแบบอากาศยก



นางสาวนวพร ทาเพชร

จุฬาลงกรณ์มหาวิทยาลัย
CHULALONGKORN UNIVERSITY

วิทยานิพนธ์นี้เป็นส่วนหนึ่งของการศึกษาตามหลักสูตรปริญญาวิทยาศาสตรมหาบัณฑิต
สาขาวิชาการจัดการสิ่งแวดล้อม (สหสาขาวิชา)
บัณฑิตวิทยาลัย จุฬาลงกรณ์มหาวิทยาลัย
ปีการศึกษา 2556
ลิขสิทธิ์ของจุฬาลงกรณ์มหาวิทยาลัย

นภาพร ทาเพชร : ผลกระทบของตัวกลางพลาสติกต่อตัวแปรด้านการถ่ายเทมวลสารและอุทกพลศาสตร์ของฟองอากาศในถังปฏิกรณ์แบบฟองอากาศและแบบอากาศยก (EFFECT OF PLASTIC MEDIA ON MASS TRANSFER AND BUBBLE HYDRODYNAMIC PARAMETERS IN BUBBLE COLUMN AND AIRLIFT REACTOR) อ.ที่ปรึกษาวิทยานิพนธ์หลัก: รศ. ดร. พิสุทธิ์ เพียรมนกุล, 119 หน้า.

งานวิจัยนี้มีวัตถุประสงค์เพื่อศึกษาและเปรียบเทียบผลกระทบของตัวกลางพลาสติกที่มีต่อตัวแปรด้านการถ่ายเทมวลสารและอุทกพลศาสตร์ของฟองอากาศในถังปฏิกรณ์แบบฟองอากาศและแบบอากาศยก โดยพิจารณาจากตัวแปรด้านการถ่ายเทมวลสาร ได้แก่ สัมประสิทธิ์ $K_L a$ และ K_L และตัวแปรด้านอุทกพลศาสตร์ฟองอากาศ ได้แก่ ขนาดฟอง ความเร็วการไหลขึ้นของฟอง และพื้นที่ผิวสัมผัสจำเพาะ ตัวแปรด้านอุทกพลศาสตร์วัดได้โดยกล้องความเร็วสูง (350 รูป/วินาที) และโปรแกรมวิเคราะห์ภาพถ่าย ถังปฏิกรณ์แบบฟองอากาศที่ใช้มีขนาดเส้นผ่านศูนย์กลาง 14 เซนติเมตร สูง 100 เซนติเมตร สำหรับถังปฏิกรณ์แบบอากาศยก แผ่นอะคริลิกทรงสี่เหลี่ยมถูกแทรกลงในถังปฏิกรณ์แบบฟองอากาศเพื่อแบ่งถังเป็นสองส่วนคือ ส่วนโรเตอร์และส่วนดาวน์คัมเมอร์ ใช้หัวกระจายอากาศแบบแข็งและเฟสของเหลวคือ น้ำประปา ทำการเดินระบบภายใต้อุณหภูมิห้องที่อัตราการไหลของแก๊สเท่ากับ 2.5, 5, 7, 10, 12, 15 และ 20 ลิตรต่อนาที ตัวกลางพลาสติกที่ใช้ในงานวิจัยนี้คือ โพลีไวนิลคลอไรด์ (PVC) อคริโลไนไตรล์ บิวตะไดอินสไตรีน (ABS) และโพลีโพรพิลีน (PP) และปริมาณตัวกลางพลาสติกที่ใช้คือ 2-15 %v/v จากผลการทดลองแสดงให้เห็นว่า ค่าสัมประสิทธิ์ $K_L a$ เพิ่มขึ้นตามอัตราการไหลของแก๊สเข้าถังปฏิกรณ์ทั้งสองแบบ โดยถังปฏิกรณ์แบบอากาศยก ($0.89-3.47 \text{ min}^{-1}$ สำหรับส่วนโรเตอร์ และ $0.91-3.48 \text{ min}^{-1}$ สำหรับส่วนดาวน์คัมเมอร์) มีค่าสัมประสิทธิ์ $K_L a$ มากกว่าถังปฏิกรณ์แบบฟองอากาศ ($0.53 \text{ and } 2.03 \text{ min}^{-1}$) ซึ่งเกิดจากการไหลเวียนของฟองอากาศและของเหลว(น้ำประปา) ที่เกิดขึ้นในถังปฏิกรณ์แบบยก นอกจากนี้การเติมตัวกลางพลาสติกที่มีชนิดและปริมาณที่เหมาะสม (PP ปริมาณ 15 % v/v) สามารถเพิ่มค่าสัมประสิทธิ์ $K_L a$ ได้โดยการทำให้อัตราการไหลขึ้นของฟองลดลง ซึ่งส่งผลให้ค่าพื้นที่ผิวสัมผัสจำเพาะและค่าสัมประสิทธิ์ $K_L a$ เพิ่มขึ้น สำหรับการประยุกต์ใช้ถังปฏิกรณ์แบบยกเพื่อดูดซับแก๊สเบนซีน พบว่าการเติมตัวกลางพลาสติก PP ปริมาณ 15 % v/v ร่วมกับการเติมแอกทิเวตเตดคาร์บอน (GAC) ปริมาณ 195 กรัม ลงในน้ำประปาในถังปฏิกรณ์แบบยกสามารถให้ประสิทธิภาพการดูดซับเบนซีนมากถึง 88%

สาขาวิชา การจัดการสิ่งแวดล้อม

ปีการศึกษา 2556

ลายมือชื่อนิสิต

ลายมือชื่อ อ.ที่ปรึกษาวิทยานิพนธ์หลัก

5587557520 : MAJOR ENVIRONMENTAL MANAGEMENT

KEYWORDS: BUBBLE COLUMN / INTERNAL LOOP AIRLIFT REACTOR / MASS TRANSFER
PARAMETER / BUBBLE HYDRODYNAMIC PARAMETER / PLASTIC MEDIA / BENZENE

NAWAPORN THAPHET: EFFECT OF PLASTIC MEDIA ON MASS TRANSFER AND BUBBLE
HYDRODYNAMIC PARAMETERS IN BUBBLE COLUMN AND AIRLIFT REACTOR. ADVISOR:
ASSOC. PROF. PISUT PAINMANAKUL, Ph.D., 119 pp.

The objective of this work was to study and compare the mass transfer and bubble hydrodynamic parameters obtained with a bubble column reactor (BC) and internal loop airlift reactor (ILALR), as well as, analyze the effect of different types and amounts of plastic media presence in the reactors. More over the best reactor and plastic media (Type and concentration) observed in this work was applied for design the benzene absorption control system. The BC was made of Plexiglas with 14 cm in diameter and 100 cm in height. For an ILALR system, the rectangular Plexiglas baffle (with 13 cm width, 80 cm height, and 0.5 cm thickness) was installed within the BC in order to divide the cross section into a riser zone and a down-comer zone. Moreover, Polypropylene (PP), Poly Vinyl Chloride (PVC) and Acrylonitrile Butadiene Styrene (ABS) were applied as the plastic media with different concentrations of 2-15 %v/v. The mass transfer parameters (overall mass transfer coefficient; $K_L a$ and liquid-side mass transfer coefficient; K_L) and the bubble hydrodynamic parameters (bubble size; D_b , terminal bubble rising velocity; U_b , and specific interfacial area; a) were determined for providing a better understanding on mass transfer mechanism. It can be noted that the $K_L a$ values were determined by using dissolved oxygen electrode; whereas the D_b and U_b values were determined by using a high speed camera (350 frames/sec) with an image analysis program. The result has shown that the $K_L a$ coefficients obtained with both reactors increased with gas flow rate (Q_G). The values of $K_L a$ in case of ILALR (0.89-3.47 min^{-1} and 0.91-3.48 min^{-1} for riser zone and down-comer zone, respectively) were greater than those in case of BCR (0.53 and 2.03 min^{-1}). The gas (bubble) and liquid recirculation occurred in ILALR system can be defined as one of the important factors in this study. Moreover, the $K_L a$ coefficients can be clearly enhanced by adding the suitable type and concentration of plastic media (15 %v/v of PP): the modification of terminal bubble rising velocity and specific interfacial area should be responsible for these results. Finally, for benzene absorption, the highest benzene removal efficiency in this work was obtained with 15% of PP and 195 g Granular activated carbon (GAC) addition into tap water in the ILALR.

Field of Study: Environmental Management

Student's Signature

Academic Year: 2013

Advisor's Signature

ACKNOWLEDGEMENTS

I wish to express my profound gratitude and sincerest appreciation to my advisor Assoc. Prof. Dr. Pisut Painmanakul for his precious guidance, shape advice, helpful suggestions, and continuous encouragement throughout this research. He gave me the useful knowledge and systematic thinking for the environmental application and management. He has always taught several important points to gain the completion to work without his creative ideas and devotion, this study would not been successful. I also would to extend my profound gratitude to Assist. Prof. Dr. Chanta Tongcumpou, Chairman of the committee, Assoc. Prof. Dr. Jin Anotai, Assist. Prof. Dr. Patiparn Punyapalakul, and Dr. Marupatch Jamnongwong members of thesis committee.

This research was financially supported by the Center of Excellence on Hazardous Substance Management (HSM). Without this scholarships, this research would not been achieved.

I would like to thank laboratory staffs and students in Environmental Engineering, Chulalongkorn University for their support, kindness, and friendship which give me relax and familiar workplace surrounding.

Finally, deepest and most sincere appreciation is extended to my parents for their support, love and encouragement.

CONTENTS

	Page
THAI ABSTRACT	iv
ENGLISH ABSTRACT	v
ACKNOWLEDGEMENTS	vi
CONTENTS	vii
LIST OF TABLES	x
LIST OF FIGURES	xi
CHAPTER I	1
INTRODUCTION.....	1
1.1 Statement of problem.....	1
1.2 Objectives.....	2
1.3 Scopes of the Study.....	3
1.4 Hypotheses:.....	4
CHAPTER II.....	5
BACKGROUND AND LITERATURE REVIEW	5
2.1 Volatile organic compounds.....	5
2.2 Control of gaseous benzene	6
2.3 Absorption process.....	7
2.4 Mass transfer theory.....	13
2.5 Bubble hydrodynamic.....	17
2.6 Airlift reactor	21
2.7 Plastic media.....	23
2.8 Surfactant	25
2.9 Activated carbon	26
2.10 Literature reviews	27
2.11 Research focuses	31
CHAPTER III.....	32
METHODOLOGY.....	32

	Page
3.1 Research overview.....	32
3.2 Experimental set-up.....	33
3.3 Materials and methods.....	34
3.4 Analytical methods.....	37
3.5 Experimental procedure.....	40
CHAPTER IV	47
RESULTS AND DISCUSSIONS	47
4.1 Effect of plastic media on overall mass transfer coefficient in BC.....	47
4.2 Effect of plastic media on bubble hydrodynamic parameter in BC.	51
4.3 Study the oxygen mass transfer and bubble hydrodynamic parameters in ILALR.....	65
4.4 Effect of plastic media on oxygen mass transfer and bubble hydrodynamic parameters in ILALR.	72
4.5 Comparison the effect of best plastic media condition on mass transfer and bubble hydrodynamic parameters in BC and ILALR.	89
4.6 Application for benzene gas absorption.	96
CHAPTER V	101
CONCLUSIONS AND RECOMMENDATIONS.....	101
5.1 Conclusions	101
5.2 Recommendations for future work	105
REFERENCES	106
APPENDIX.....	108
VITA.....	119

LIST OF TABLES

	Page	
Table 2.1	Technology for removal benzene	7
Table 2.2	Henry's law coefficients of some common compounds.	9
Table 3.1	Physical and chemical properties of benzene	34
Table 3.2	Physical and chemical properties of Tween 80	35
Table 3.3	Types and properties of plastic media	36
Table 3.4	Variable of studying effect of plastic media on K_La coefficient in BC.	41
Table 3.5	Variable of studying effect of plastic media on bubble hydrodynamic parameter in BC.	42
Table 3.6	Variable of studying the oxygen mass transfer and bubble hydrodynamic parameters in ILALR.	43
Table 3.7	Variable of studying the effect of plastic media on oxygen mass transfer and bubble hydrodynamic parameters in ILALR.	44
Table 3.8	Variable of studying the oxygen mass transfer and bubble hydrodynamic parameters in BC and ILALR.	45
Table 3.9	Variable of studying application for benzene gas absorption.	46
Table 4.1	The overall results obtained in oxygen absorption part.	95
Table 4.2	Summary of K_La values for benzene absorption	97
Table 4.3	Summary of K_La benzene removal efficiency.	99

LIST OF FIGURES

		Page
Figure 2.1	Pate column	10
Figure 2.2	Packed towers	10
Figure 2.3	Spray towers	11
Figure 2.4	Bubble columns	12
Figure 2.5	Centrifugal contactors	12
Figure 2.6	Concentration gradients between two contacting phases.	15
Figure 2.7	Terminal rising bubble velocity of single gas bubbles.	18
Figure 2.8	Different types of airlift reactors	22
Figure 2.9	Symbols of surface active agent	26
Figure 3.1	Experimental framework	32
Figure 3.2	Bubble column (BC)	33
Figure 3.3	Internal loop airlift reactor (ILALR)	33
Figure 3.4	Rigid orifice gas diffuser	33
Figure 3.5	Benzene generator	36
Figure 3.6	High speed camera	38
Figure 3.7	Flow diagram for studying effect of plastic media on overall mass transfer coefficient in BC.	41
Figure 3.8	Flow diagram for studying effect of plastic media on bubble hydrodynamic parameter in BC.	42
Figure 3.9	Flow diagram for studying the oxygen mass transfer and bubble hydrodynamic parameters in ILALR.	43
Figure 3.10	Flow diagram for studying the effect of plastic media on oxygen mass transfer and bubble hydrodynamic parameters in ILALR.	44
Figure 3.11	Flow diagram for studying application for benzene gas absorption.	46

LIST OF FIGURES

		Page
Figure 4.1	Overall mass transfer coefficient versus gas flow rate in BC	47
Figure 4.2	Overall mass transfer coefficient versus gas flow rate in BC for different amount of PVC	48
Figure 4.3	Overall mass transfer coefficient versus gas flow rate in BC for different amount of ABS	49
Figure 4.4	Overall mass transfer coefficient versus gas flow rate in BC for different amount of PP	50
Figure 4.5	Bubble diameter versus gas flow rate in BC	51
Figure 4.6	Bubble formation photographs in BC at gas flow rate: (a) 2.5 L/min (b) 5 L/min, and (c) 20 L/min	52
Figure 4.7	Bubble size distribution measured in the BC at different gas flow rate	52
Figure 4.8	Bubble diameter versus gas flow rate in BC for different amount of PVC	53
Figure 4.9	Bubble size and bubble generator for: (a) No media (b) large PVC loadings	53
Figure 4.10	Bubble diameter versus gas flow rate in BC for different amount of ABS	54
Figure 4.11	Occurrence of bubbles and plastic media particles in BC for: (a) PVC, and (b) ABS	55
Figure 4.12	Bubble diameter versus gas flow rate in BC for different amount of PP	55
Figure 4.13	Occurrence of bubbles and plastic media particles in BC for PP	56
Figure 4.14	Bubble formation photographs in BC at gas flow rate 5 L/min for: (a) No plastic media (b) 15% PVC loading (c) 15% ABS loading, and (d) 15% PP loading	56
Figure 4.15	Terminal rising bubble velocity versus gas flow rate in BC	58
Figure 4.16	Terminal rising bubble velocity versus gas flow rate in BC for different amount of PVC	58

LIST OF FIGURES

	Page
Figure 4.17 Terminal rising bubble velocity versus gas flow rate in BC for different amount of ABS	59
Figure 4.18 Terminal rising bubble velocity versus gas flow rate in BC for different amount of PP	60
Figure 4.19 Specific interfacial area versus gas flow rate in BC	61
Figure 4.20 Specific interfacial area versus gas flow rate in BC for different amount of PVC	62
Figure 4.21 Specific interfacial area versus gas flow rate in BC for different amount of ABS	62
Figure 4.22 Specific interfacial area versus gas flow rate in BC for different amount of PP	63
Figure 4.23 Liquid film mass transfer coefficient versus gas flow rate in BC for different types of plastic media: (a) PVC, (b) ABS, and (c) PP	64
Figure 4.24 Overall mass transfer coefficient versus gas flow rate in BC and ILALR	66
Figure 4.25 Liquid and bubbles recirculation in BC and ILALR	67
Figure 4.26 Bubble diameter versus gas flow rate in BC and ILALR	67
Figure 4.27 Bubble formation photographs in ILALR at gas flow rate: (a) 2.5 L/min (b) 5 L/min, and (c) 20 L/min	68
Figure 4.28 Terminal rising bubble velocity versus gas flow rate in ILALR	68
Figure 4.29 Rising bubble in down-comer zone of ILALR at: (a) low gas flow rate (b) high gas flow rate	69
Figure 4.30 Specific interfacial area versus gas flow rate in BC and ILALR	70
Figure 4.31 Gas flow rate (Down-comer zone) versus gas flow rate (Riser zone) in ILALR	71
Figure 4.32 Gas flow rate (Down-comer zone and riser zone) of ILALR	72
Figure 4.33 Overall mass transfer coefficient versus gas flow rate in ILALR for different amount of PVC: (a) Riser zone, (b) Down-comer zone	73

LIST OF FIGURES

		Page
Figure 4.34	Overall mass transfer coefficient versus gas flow rate in ILALR for different amount of ABS: (a) Riser zone, (b) Down-comer zone	75
Figure 4.35	Overall mass transfer coefficient versus gas flow rate in ILALR for different amount of PP: (a) Riser zone, (b) Down-comer zone	76
Figure 4.36	Bubble diameter versus gas flow rate in ILALR for different amount of PVC: (a) Riser zone, (b) Down-comer zone	77
Figure 4.37	Bubble diameter versus gas flow rate in ILALR for different amount of ABS: (a) Riser zone, (b) Down-comer zone	78
Figure 4.38	Bubble diameter versus gas flow rate in ILALR for different amount of PP: (a) Riser zone, (b) Down-comer zone	79
Figure 4.39	Bubble formation photographs in ILALR (Riser zone) at gas flow rate 5 L/min for: (a) No plastic media (b) 15% PVC loading (c) 15% ABS loading, and (d) 15% PP loading	80
Figure 4.40	Terminal rising bubble velocity versus gas flow rate in ILALR for different amount of PVC: (a) Riser zone, (b) Down-comer zone	81
Figure 4.41	Terminal rising bubble velocity versus gas flow rate in ILALR for different amount of ABS: (a) Riser zone, (b) Down-comer zone	82
Figure 4.42	Terminal rising bubble velocity versus gas flow rate in ILALR for different amount of PP: (a) Riser zone, (b) Down-comer zone	83
Figure 4.43	Specific interfacial area versus gas flow rate in ILALR for different amount of PVC: (a) Riser zone, (b) Down-comer zone	84
Figure 4.44	Specific interfacial area versus gas flow rate in ILALR for different amount of ABS: (a) Riser zone, (b) Down-comer zone	85
Figure 4.45	Specific interfacial area versus gas flow rate in ILALR for different amount of PP: (a) Riser zone, (b) Down-comer zone	86
Figure 4.46	Gas flow rate (Down-comer zone) versus gas flow rate (Riser zone) in ILALR for different amount of PVC	87

LIST OF FIGURES

	Page
Figure 4.47 Gas flow rate (Down-comer zone) versus gas flow rate (Riser zone) in ILALR for different amount of ABS	88
Figure 4.48 Gas flow rate (Down-comer zone) versus gas flow rate (Riser zone) in ILALR for different amount of PP	89
Figure 4.49 Overall mass transfer coefficient versus gas flow rate in BC and ILALR	90
Figure 4.50 Bubble diameter versus gas flow rate in BC and ILALR	90
Figure 4.51 Specific interfacial area versus gas flow rate in BC and ILALR	91
Figure 4.52 Gas flow rate (Down-comer zone) versus gas flow rates (Riser zone) in the ILALR	92
Figure 4.53 Liquid film mass transfer coefficient versus gas flow rate in BC and ILALR	93
Figure 4.54 Absorbent versus time for benzene absorption	97
Figure 5.1 Schematic diagram of continuous ILALR system	105

CHAPTER I

INTRODUCTION

1.1 Statement of problem

Volatile organic compounds (VOCs) are organic chemicals that have high vapor pressures under normal conditions to rapidly vaporize and enter the atmosphere. The main component of VOCs is carbon atoms that bond to hydrogen and other elements. The VOCs have vapor pressure greater than about 0.0007 atm (70 Pa) and initial boiling points less than or equal to 250 °C (482 °F, 523 K) measured at a standard atmospheric pressure (101.3 kPa). The VOCs are both outdoor pollutants and indoor pollutants that emitted from manufacture process and the use of household products containing VOCs. These substances are able to participate in atmospheric photochemical reactions under certain condition to form smog or ozone, which is well known to cause adverse effects on plant and living things. The chemicals also have short- and long-term serious human health effects.

In this research work, benzene is chosen to represent a toxic VOC. The benzene molecule is a hexagon formed by six sets of carbon and hydrogen atoms bonded together with alternating single and double bonds. Due to their low boiling points, it is found most often in air as a result of emissions from burning coal and oil, gasoline vapors at gasoline service stations, motor vehicle exhaust, cigarette smoke, wood-burning fires, some adhesives, and other sources (EPA, 1998). Human exposure to benzene has been associated with a range of acute and long-term adverse health effects and diseases. For high concentrations exposure can result in death. Moreover, the U.S. EPA classified benzene as a human carcinogen for all routes of exposure. Therefore, the emissions of benzene to atmosphere are regulated to reducing their emission.

A number of methods for controlling benzene emissions have been developed. The chemical and physical properties of benzene are of primary concern in choosing the treatment system. Moreover, selecting a benzene abatement technology usually depends on their concentration and operation cost.

Absorption process is commonly used as a raw material or product recovery technique in the purification of gas streams containing high concentrations of VOC. However, it is also used as an emission control technique (EPA, 2009). The absorption is a diffusional mass-transfer operation by which a soluble gaseous component is removed from a gas stream by dissolution in a solvent liquid. The driving force for mass transfer is the concentration difference of the solute between the gaseous and liquid phases (Higbie, 1935).

Bubble column (BC) and airlift reactor (ALR) are multiphase absorption reactors in which a gas phase is dispersed in form of small bubbles into liquid phase. These gas-liquid reactors have been extensively used in emission control process due to their simple construction, ease of operation, flexibility, and relatively high mass transfer efficiency.

In recent years, the addition of solid phase in gas-liquid reactors has also attracted much attention due to their numerous advantages. The main advantages over conventional reactors include excellent contact among the gas-liquid-solid phases, which improve mass transfer rates.

1.2 Objectives

The purpose of this study was to determine the impact of plastic media on oxygen mass transfer and bubble hydrodynamic parameters at a variety of gas flow rate in a bubble column (BC) and an internal loop airlift reactor (ILALR). The different types and amount of small size plastic particles were added into the reactors, overall mass transfer coefficients, bubble diameters, terminal rising bubble velocity, specific interfacial area, and liquid film mass transfer coefficient were investigated. These experimental results can be applied for designing a high-efficiency benzene absorption system. Moreover, the most practical condition was determined. The scope of this work is as follows:

1. Effect of plastic media on overall mass transfer coefficient in BC.
2. Effect of plastic media on bubble hydrodynamic parameter in BC.
3. Study the oxygen mass transfer and bubble hydrodynamic parameters in ILALR.

4. Effect of plastic media on oxygen mass transfer and bubble hydrodynamic parameters in ILALR.

5. Comparison the effect of best plastic media condition on mass transfer and bubble hydrodynamic parameters in BC and ILALR.

6. Application for benzene gas absorption.

1.3 Scopes of the Study

1. This experiment is carried out in laboratory scale with the BC and ILALR at atmospheric pressure and water temperature $26 (\pm 1) ^\circ\text{C}$. The BC was made of Plexiglas with 14 cm in diameter and 100 cm in height. For ILALR system, the rectangular Plexiglas baffle (with 13 cm width, 80 cm height, and 0.5 cm thickness) is installed within the BC in order to divide the cross section into a riser zone and a down-comer zone.

2. Gas diffuser used in this work is rigid orifice diffuser and different gas flow rates (2.5, 5, 7, 10, 15, 20 L/min).

3. The experiment can be divided into two part; oxygen absorption and benzene absorption parts. For oxygen absorption part, the mass transfer parameters (overall mass transfer coefficient, $K_L a$; and liquid-side mass transfer coefficient, K_L) and the bubble hydrodynamic parameters (bubble size, D_B ; terminal bubble rising velocity, U_B ; and specific interfacial area, a) will be studied in BC and ILALR for with and without plastic media particles. For benzene absorption part, the best condition (most practical reactor, most practical types and amount of plastic media) obtained with oxygen absorption part will be applied for this part, the mass transfer parameters (overall mass transfer coefficient, $K_L a$) and benzene removal efficiency will be studied.

4. For oxygen absorption part, the liquid phase used in this study was tap water. Sodium sulfite was added into water to decrease the oxygen concentration in water. The overall mass transfer coefficients ($K_L a$) are determined by using the experimental data based on the variation of oxygen concentration in liquid phase with time. The oxygen concentrations obtained in this study are measured by dissolved oxygen electrode (DO electrode).

5. Specific interfacial area (a) is calculated by using experimental results of bubble diameter (D_B), and terminal rising bubble velocity (U_B). The D_B and U_B values are determined with photographic technique by using a high speed camera (350 images/second).

6. For benzene absorption part, the $K_L a$ values are determined by using the experimental data based on the variation of benzene concentration in liquid phase (absorbent) with time. The benzene concentrations obtained in this study are measured by UV-Visible Spectroscopy. Moreover, the benzene gas inlet and outlet of the reactor were collected into air bag at 5.0-5.5 minutes. The benzene gas concentrations were measured by the Agilent Technologies gas chromatograph (GC) 6890N equipped with flame ionization detector. The area under curve of benzene gas obtained with gas chromatography will applied to calculate the benzene removal efficiency.

1.4 Hypotheses:

1. Addition of plastic media in the reactors affect to oxygen mass transfer and bubble hydrodynamic parameters.
2. The most practical condition (Reactor, and types and concentration of plastic media) obtained with oxygen absorption part provides high efficiency of benzene removal.

CHAPTER II

BACKGROUND AND LITERATURE REVIEW

2.1 Volatile organic compounds

Volatile organic compounds (VOCs) are organic chemicals that have high vapor pressures under normal conditions to rapidly vaporize and enter the atmosphere. The main component of VOCs is carbon atoms that bond to hydrogen and other elements. The VOCs have vapor pressure greater than about 0.0007 atm (70 Pa) and initial boiling points less than or equal to 250 °C (482 °F, 523 K) measured at a standard atmospheric pressure (101.3 kPa). The VOCs are both outdoor pollutants and indoor pollutants that emitted from manufacture process and the use of household products containing VOCs. These substances are able to participate in atmospheric photochemical reactions under certain condition to form smog or ozone. Ozone is well known to cause adverse effects on plant and living things. The chemicals also have short- and long-term serious human health effects. Therefore, the emissions of VOCs to atmosphere are regulated to reducing their emission. The several VOCs treatment system has been studied in order to controlling their emission to meet the regulation standard.

In this research work, benzene is chosen to represent a toxic VOC. Benzene is found most often in air as a result of emissions from burning coal and oil, gasoline vapors, motor vehicle exhaust, wood-burning fires, and other sources. Human exposure to benzene has been associated with a range of acute and long-term adverse health effects and diseases. Moreover, the U.S. EPA classified benzene as a human carcinogen. Therefore, the study and development of benzene emission control technique is very important.

A number of methods for controlling benzene emissions have been developed. The chemical and physical properties of benzene are of primary concern in choosing the treatment system. Moreover, selecting a benzene abatement technology usually depends on their concentration and cost.

2.2 Control of gaseous benzene

There are many methods have been used for controlling benzene emission, which are including:

2.1.1 Combustion

Combustion process has been used in petrochemical and other industries for reducing benzene to non-hazardous compounds such as carbon dioxide and water. Efficiency of this abatement method depends on combustion temperature and burning duration.

2.1.2 Adsorption

Adsorption is primarily a physical process that a gas or liquid solute accumulates on the surface of a solid or a liquid (adsorbent) to form a molecular or atomic film (adsorbate). The process requires very large surface areas to be effective. Adsorption technology is usually applied for control of organic compounds. In case of benzene, the contaminated gas is trapped on the surface of solid adsorbent such as activated carbon, and synthetic resins. If a surface already heavily contaminated by adsorbate, it is hard to have much capacity for additional binding. Therefore, regeneration system is required to clean spent adsorbents.

2.1.3 Absorption

Absorption process was developed to remove benzene from air into an aqueous phase. For benzene treatment, the benzene gas is absorbed by liquid (absorbent). Absorption efficiency depends on the property of the liquid, contact area between the gas and the liquid, contact time between gas and liquid, and the absorption rate between the gas and the absorbent.

The efficiency, advantage, and disadvantage of these methods are shown in details in Table 2.1

Table 2.1 Technology for removal benzene

Device Inlet	Inlet Conc. PPMV	Efficiency	Advantages	Disadvantages
Absorption	250 1,000 5,000	90% 95% 98%	- Especially good for inorganic acid gasses	- Limited applicability
Adsorption	200 1,000 5,000	50% 90-95% 98%	- Low capital investment good for solvent recovery	- Selective applicability moisture and temperature constraints
Thermal incineration	20 100	95% 99%	- High destruction efficiency - Wide applicability can recover heat energy	- No organics can be recovered - Capital intensive
Catalytic incineration	50	90%	- High destruction efficiency	- No organics can be recovered
Flares	100	>95% >98%	- Can be less expensive than thermal - High destruction efficiency	- Technical limitations that can poison - No organics can be recovered - Large emissions only

In this work, the absorption method is chosen to controlling benzene emission. The absorption techniques are often used to remove benzene from gaseous stream, since they provide high performances in benzene treatment process.

2.3 Absorption process

Absorption is a mass transfer operation in which a gas stream is contacted with a liquid for the purpose of dissolving one or more components of the gas stream and to provide a solution of them in the solvent liquid. Mass transfer is directly proportional to the magnitude of the concentration gradient between the two phases.

2.3.1 Absorption mechanism

The absorption system, in case of removal gaseous pollutant, the contaminant gas stream must be contact with a liquid. There are three steps in the absorption process. The first step, the pollutant diffuses from the bulk area of the gas phase to the gas-liquid interface. The second step, gaseous pollutants transfer across the interface to the liquid phase. The third step, the pollutants diffuse into

the bulk area of the liquid, making room for additional gas molecules to be absorbed.

The most efficient system can be designed by knowing variables that control the process. It is assumed that the first and second steps occur simultaneously. The second step does not need to be considered when deriving absorption efficiency equations because it is extremely rapid. The absorption rate is dependent upon the diffusion rate in either the gas phase or the liquid phase.

Both gas phase controlled absorption and liquid phase controlled absorption are used to describe mass transfer rates. Each mechanism depends on the diffusion rate in both phases and upon the solubility of the pollutant in the liquid phase. The gas phase controlled systems absorb pollutants more readily than do the liquid phase controlled systems. Thus, absorption systems for air pollution control are basically designed to be gas phase controlled.

2.3.2 Gas solubility in liquid phase

Solubility of gaseous contaminant is an important factor affecting the amount of a contaminant that can be absorbed. Solubility is a function of both the pressure and temperature of the system. If the pressure of system increases, the amount of gas absorbed by the liquid also increases. If temperature increases, the amount absorbed decreases. At a constant temperature, the amount of a gas that dissolves in liquid is directly proportional to the partial pressure of that gas in equilibrium with that liquid as shown in Henry's law equation below:

$$p^* = Hx \quad (2.1)$$

where p^* = Partial pressure of solute at equilibrium (units of pressure)

H = Henry's law constant (pressure/mole fraction)

x = Mole fraction of solute in the liquid

If the partial pressure is low, the component has very little potential to leave the liquid phase, thus the component is high solubility. Henry's law is generally used to predict solubility of component in the low concentration range. The Henry's law constant is the slope of the calibration curve between partial pressure and

concentration. Henry's law can predict only for the permanent gases which do not change molecular form upon being dissolved.

High Henry's law coefficients compounds are the compounds that have high vapor pressures and low solubility. If Henry's law coefficient of compounds above 0.01 (milligrams per liter over milligrams per liter), they are considered as volatile compounds. If Henry's law coefficient is between 0.0001 and 0.01, the compounds are considered semi-volatile. If Henry's law coefficient is below 0.0001, the compound is considered nonvolatile from the aqueous phase. Table 2.2 provides the Henry's law coefficients for some compounds.

Table 2.2 Henry's law coefficients of some common compounds.

Compound	Gas-phase concentration [ppm/(mg/L)]
Octane	33,900
Oxygen	22,600
Hydrogen sulfide	255
Benzene	71
PCBs	2.96
Ammonia	0.78
Ethanol	0.66

2.3.3 Equipment description for absorption process

Absorption equipment is designed to increase the potential for absorption to occur by increasing the sufficient contact time and contact surface area between two phases. Mass transfer rate depends on the contact area between air and liquid. Absorption equipment includes:

Tray (Plate) columns/towers

Plate column includes of a vertical cylindrical vessel in which gas is injected into the tower from the bottom of the tower, rising gas and falling liquid on each tray. Bubble-cap or valve-cap trays are the vapor and liquid contact devices used in plate columns. To design an absorption process, the number of bubble-cap tray required in the process should be determined. Example of plate column is shown in Figure 2.1

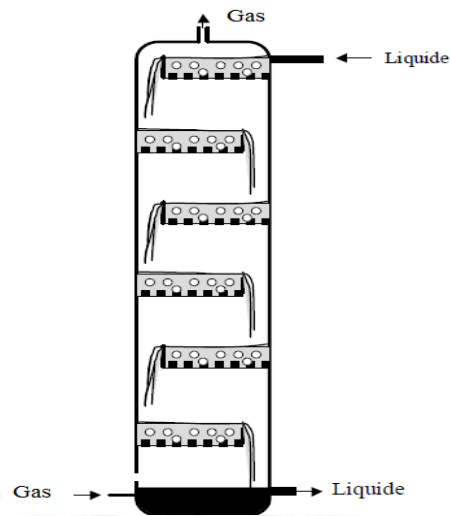


Figure 2.1 Pate column

Packed bed towers/columns

Packed bed tower is the most common gas absorption device. Packed bed tower consists of a vessel containing a packing material inside in order to provide a large surface area contact between air and liquid. Packed column are classified according to the relative direction of gas-to-liquid flow. The most common packed tower is the countercurrent flow tower, which flow of liquid and gas streams in opposite directions as shown in Figure 2.2. The gas stream enters the bottom of the tower and flows rising over the packing material. Liquid is sprayed at the top of the packing and flows downward over the packing material.

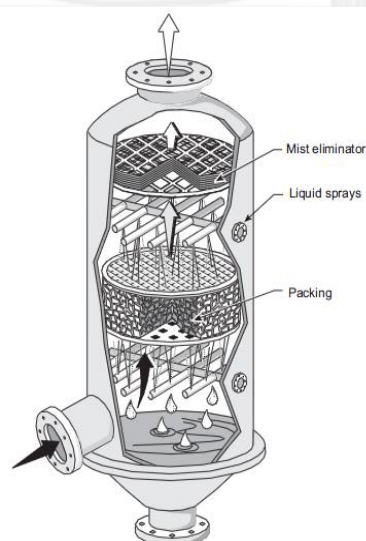


Figure 2.2 Packed towers

Spray towers/chambers

Spray towers or spray chambers consist of vacant vertical vessels containing nozzles that spray liquid into the vessels. The contaminated gas stream typically enters the bottom of the vessels and moves upward, while liquid is sprayed downward from one or more levels, thus it is countercurrent flow. The smaller liquid droplets provide a large surface area for absorbing gas. However, the liquid droplets must be large enough to not be carried out of the scrubber by the scrubbed outlet gas stream. The spray towers can be used for gas absorption, but they are not as effective as tray tower and packed column. Example is shown in Figure 2.3



Figure 2.3 Spray towers

Bubble columns

Bubble column reactor is widely used as gas-liquid absorption process. Bubble columns are basically a cylindrical vessel with a gas distributor at the bottom as show in Figure 2.4. The gas is sparged in the form of bubbles into a liquid phase. The bubble column can achieve high efficiency for benzene removal.

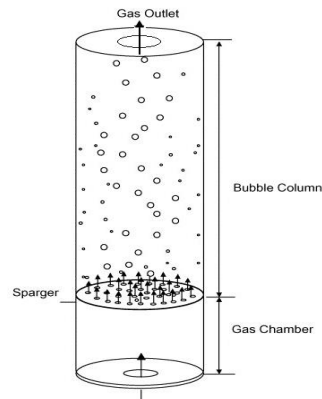


Figure 2.4 Bubble columns

The performance and efficiency of a bubble column is generally upon these factors:

- 1) Mass transfer parameters such as overall mass-transfer coefficients and liquid side mass transfer coefficients.
- 2) Hydrodynamic parameters such as bubble diameter, terminal rising bubble velocity, and bubble formation frequency.

Centrifugal contactors

Centrifugal contactors or annular centrifugal contactor, as shown in Figure 2.5, consist of a stationary ringed housing, intermeshed with a ringed rotating section. The liquid phase enters to the column and flow outward by centrifugal force. The gas flows inward by a pressure driving force. Very high mass transfer rates can be achieved with only moderately high rotation rates. This contactor is frequently used when tray tower or packed column is not available or when a short residence time is desired.

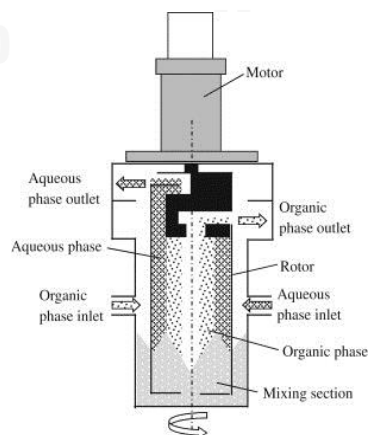


Figure 2.5 Centrifugal contactors

The different reactor types provide different gas-liquid interfacial area, which is an important parameter for absorption process. The bubble column reactor offers a number of advantages over the others such as simple construction, well mixed, high thermal stability, low energy requirements; thus low operation costs. Moreover, this reactor generates high amount of small bubble sizes, thus increase the residence time of the gas phase in liquid phase even under relatively high gas velocities, thereby improving mass transfer. Therefore, the bubble column reactor was chosen for controlling benzene in this work. The effect of various parameters on hydrodynamic and mass transfer of benzene is necessary to investigate for well understanding of the mechanism in order to increase benzene absorption in bubble column.

2.4 Mass transfer theory

Mass transfer is the net movement of a component from one location to another to minimize the concentration differences within the system. The theory has been always used as model for describe the transport of mass at gas-liquid interfacial area. Mass transfer occurs in many processes, such as absorption, evaporation, adsorption, and distillation. In a multi-phase system which called interphase mass transfer, a mass is transferred due to the chemical potential difference of each species. In a single phase system where temperature and pressure are uniform, the difference in chemical potential is due to the variation in concentration of each species. Van Winkle presented the two types of mass transfer mechanisms as follows:

- 1) Molecular diffusion: the diffusion from the random molecular motion
- 2) Eddy (turbulent) diffusion or convection: the diffusion from the random, macroscopic fluid motion

Molecular diffusion moves mass from regions of higher concentration to regions of lower concentration, and if left to continue indefinitely, it would result in equal concentrations on both sides of the system.

Mass transfer of a benzene gas which is absorbed in the solution is the mass transfer between phases and the convective mass transfer. Mass transfer between

the fluid and air depends on the movement properties and the dynamics. The equation of the convective mass transfer can be written according to Newton's law:

$$N_A = k_C \Delta C_A \quad (2.2)$$

In this equation, N_A is molar flux of specie A with respect to coordinates that are fixed in space, k_C is the convective mass transfer coefficient, and ΔC_A is the difference between the concentration at the phase boundary and the concentration at some arbitrarily defined point in the fluid medium.

Mass-transfer operations frequently involve the transfer of material between two contacting phases. In this section, we shall consider the mechanism of steady-state mass transfer between two phases.

2.4.1 Two - resistance theory

Interphase mass transfer involves three transfer steps, these three steps are: the mass transfer from the bulk condition of one phase to the interfacial surface, the transfer of mass across the interface to another phase, and the mass transfer from the interfacial surface to the bulk condition of second phase. A two-resistance theory was originally proposed by Whitman (1962), has been shown to be appropriate for many interphase mass transfer problems. The general theory has two principal assumptions which are:

1) The rate of mass transfer between the phases is controlled by the rates of diffusion through the phases on each side of the interface.

2) The rate of diffusion component across the interface is instantaneous. Therefore, equilibrium at the interface is maintained at all times.

Figure 2.6 shows the transfer of component A from the gas phase to the liquid phase with partial pressure gradient from the bulk gas composition ($p_{A,G}$), to the interfacial gas composition ($p_{A,i}$), and a concentration gradient in the liquid from ($c_{A,i}$), at the interface to the bulk liquid concentration ($c_{A,L}$). The distance between the interface and the location of component in the gas phase which the concentration of contaminant equals the bulk gas concentration, is the gas phase film thickness (δ_G), while the similar distance for the component in the liquid phase is referred to as the liquid phase film thickness (δ_L). If no resistance to mass transfer exists at the

interfacial surface, $p_{A,i}$ and $c_{A,i}$ are equilibrium concentrations. The concentrations $p_{A,i}$ and $c_{A,i}$ are related by thermodynamic relations. The $p_{A,i}$ can be less than, equal to, or greater than $c_{A,i}$ according to the equilibrium conditions at a certain fixed temperature and pressure of the system. Since transport is occurring from the $c_{A,L}$ will be greater than $c_{A,i}$ and similarly $p_{A,i}$ will be greater than $p_{A,G}$.

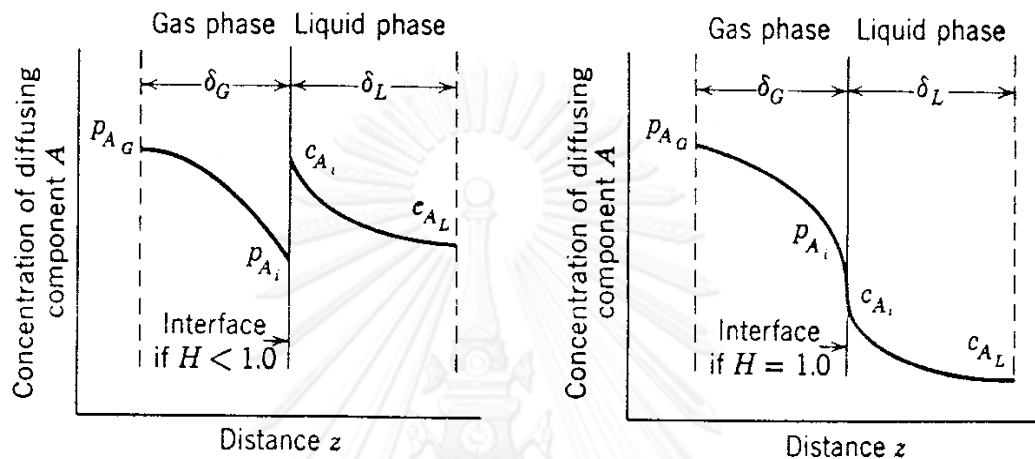


Figure 2.6 Concentration gradients between two contacting phases.

2.4.2 Overall mass transfer coefficient in liquid phase ($K_L a$)

The overall mass transfer coefficient is used in order to analyse the absorption process and the $K_L a$ determination procedure can be described as follows;

- Measuring the variation of outlet gas concentration with time until the saturated condition, for this small bubble column, the mass balance equation can be applied:

$$Q_g C_{g,in} = Q_g C_{g,out}(t) + V_L \frac{dC(t)}{dt} \quad (2.3)$$

In this equation, Q_g is the flow rate and V_L is the absorbent volume, $C_{g,in}$ and $C_{g,out}$ are the inlet and outlet concentration of benzene in the gas phase, respectively.

- Then, the concentration of VOCs in the liquid phase $C(t)$ can be expressed by:

$$C_L(t) = \frac{Q_g}{V_L} [C_{g,in}(t) - \int C_{g,out}(t) dt] \quad (2.4)$$

From this equation, the variation of the benzene concentration in the liquid phase with the time and also the saturated benzene concentration C^* can be obtained.

Based on the Non-stationary or dynamic method (Deckwer, 1992), the overall mass transfer coefficient in liquid phase ($K_L a$) is given by the following equation:

$$\frac{dC}{dt} = K_L a (C^* - C) \quad (2.5)$$

or in its integral form by:

$$\ln [C^* - C] = \ln C^* - k_L a(t) \quad (2.6)$$

where C and C^* are the concentration of contaminant and the saturation concentration of contaminant in the liquid phase, respectively.

2.4.3 Liquid-side mass transfer coefficient (K_L)

The overall volumetric mass transfer coefficient ($K_L a$) is the product of the liquid-side mass transfer coefficient (K_L) and the interfacial area (a). The liquid-side mass transfer coefficient is determined by Painmanakul *et al.* (2005) as:

$$K_L = \frac{K_L a}{a} \quad (2.7)$$

where

- K_L = Liquid-film mass transfer coefficient (m/min)
- $K_L a$ = Overall mass transfer coefficient in liquid phase (min^{-1})
- a = specific interfacial area (m^{-1})

The value of liquid-side mass transfer coefficient (K_L) and saturation concentration of contaminant in the liquid phase (C^*) depends on liquid surfactant, which involved the relevant physical and chemical properties of liquid phase.

Other than mass transfer parameters, the bubble performance and efficiency of a bubble column also depend on bubble hydrodynamic parameters, which are including bubble diameter (D_B), bubble formation frequency (f_B) and terminal rising bubble velocity (U_B).

2.5 Bubble hydrodynamic

This part will describe the determination method based on bubble hydrodynamic parameters in order to understand their effect on VOCs bubble characteristics on absorption mechanism and also to calculate the associated interfacial area. Bubble diameters (D_B), bubble formation frequency (f_B), and terminal rising bubble velocities are determined by image analysis.

2.5.1 Bubble diameter (D_B)

Normally, 60-100 bubbles obtained with any gas flow rate were captured and analyzed to be a good statistical representative. The average bubble diameter (d_{avg}) can be calculated from equation:

$$d_{avg} = \frac{\sum_{i=1}^N d_i}{N} \quad (2.8)$$

In this work, the Sauter mean bubble diameter (d_{32}) is used for present the bubble size. It refers to the diameter of a sphere with the same volume-to-surface ratio as the gas bubble and for a distribution of bubble sizes, is calculated from equation:

$$d_{32} = \frac{\sum_{i=1}^N d_i^3}{\sum_{i=1}^N d_i^2} \quad (2.9)$$

where N is the frequency of occurrence of bubbles, and d_i is bubble diameter

The gas bubbles size depends upon the gas flow rate through the orifices, the orifice diameter, the fluid properties, and the extent of turbulence prevailing in the liquid. What follows is for cases where turbulence in the liquid is solely that generated by the rising bubbles and when orifices are horizontal and sufficiently separated to prevent bubbles from adjacent orifices from interfering with each other.

- **Very slow gas flow rate:** For water-like liquids, the diameter can be calculated by equating the buoyant force on the immersed bubble, which tends to lift the bubble away from orifice, to the force due to surface tension, which tends to retain the bubble at the orifice. This provides the correlation as:

$$d_B = \left(\frac{6d_0\sigma g_c}{g\Delta\rho} \right)^{1/3} \quad (2.10)$$

- **Intermediate gas flow rates:** The bubbles generated in this zone are larger than those described above, although still fairly uniform, they form in chains rather than separately.

For air-water,

$$d_B = 0.0287d_0^{1/2}Re^{1/3} \quad (2.11)$$

For gases and liquids,

$$d_B = \left(\frac{72\rho_L}{\pi^2 g \Delta\rho} \right)^{1/4} Q_{G0}^{0.4} \quad (2.12)$$

- **Large gas flow rates:** The bubbles are smaller than those described above and non-uniform in size. For air-water orifice diameters 0.4 to 1.6 m:

$$d_B = 0.0071Re^{-0.05} \quad (2.13)$$

For the transition range ($Re = 2,100$ to $10,000$) there is no correlation of data. It is suggested that d_B for air-water can be approximated by the straight line on log-log coordinates between the points given by d_B at $Re = 2,100$ and $Re = 10,000$.

2.5.2 Terminal rising bubble velocity

In steady-state, the rising velocity of single gas bubbles, which occurs when the buoyant force equals the drag force on the bubbles, varies with the bubble diameter as show in Figure 2.7

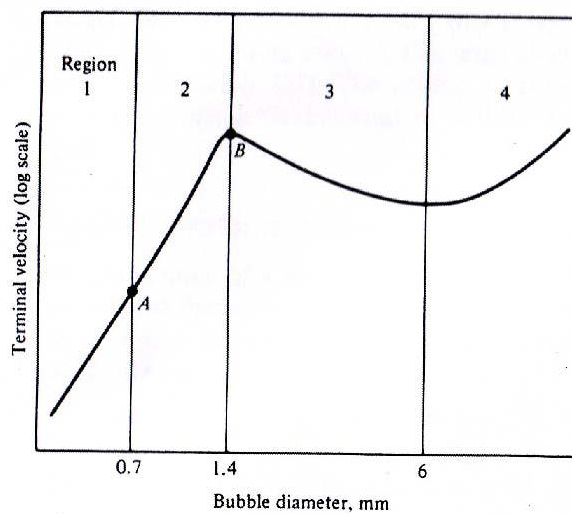


Figure 2.7 Terminal rising bubble velocity of single gas bubbles.

• **Region 1, $D_B < 0.7$ mm:** The bubbles are spherical, and they behave like rigid spheres, for which the terminal rising bubble velocity is given by Stokes' law:

$$U_B = \frac{gD_B^2\Delta\rho}{18\mu_L} \quad (2.14)$$

• **Region 2, 0.7 mm $< D_B < 1.4$ mm:** The gas within the bubble circulates, so that the surface velocity is not zero. Consequently the bubble rises faster than rigid spheres of the same diameter. There is no correlation of data; it is suggested that U_B may be estimated as following the straight line on Figure 2.7 drawn between points A and B.

• **Regions 3, (1.4 mm $< D_B < 6$ mm) and 4 ($D_B > 6$ mm):** The bubbles are no longer spherical and in rising follow a zigzag or helical path. For region 4 the bubbles have a spherically shaped cap. In both these regions the terminal velocity is

$$U_B = \sqrt{\frac{2\sigma g}{D_B\rho_L} + \frac{gD_B}{2}} \quad (2.15)$$

However the rising velocity of large numbers of bubbles crowded together may be different from that of isolated bubbles by liquid turbulence, which causes bubble coalescence and break-up. From Painmanakul *et al.* (2005) bubble rising velocity are determined by image analysis by estimating its distance between two frames at any time frame (t_{frame}) as shown in the equation below

$$U_B = \frac{\Delta D}{t_{\text{frame}}} \quad (2.16)$$

where U_B = bubble rising velocity (cm/s)
 ΔD = distance between two frames (cm)
 t_{frame} = time frame (s)

2.5.3 Bubble formation frequency (f_B)

Bubble formation frequency is the amount of bubble generated per one second. From Painmanakul *et al.* (2005), it can be calculated from the gas flow rate divided by bubble volume as shown in following equation:

$$f_B = \frac{Q_g}{V_B} \quad (2.17)$$

where f_B = Bubble formation frequency (s^{-1})
 Q_g = Gas flow rate (m^3/s)
 V_B = Bubble volume (m^3)

Airlift reactor is a modified bubble column, which is often applied in absorption processing because of their various advantages over the normal bubble column. The airlift reactor is characterized as a well-mixed reactor.

Media which generally used in packed column has been added to bubble column in order to improve contact between liquid-gas phases in a chemical process. The purpose of a media is typically to improve absorption efficiency and reduce pressure drop.

Therefore, this research approach combines advantages of airlift reactors and media. An internal-loop airlift reactor with different media which are packing media, suspended media, and the combine of packing media and suspended media, were used in this study for design the high benzene removal system.

2.5.4 Specific interfacial area (a)

Interfacial area (a) is the ratio of interfacial area of bubble and capacity of reactor at a certain time. It is a function of the bubble formation frequency, the terminal rising bubble velocity and the generated bubble diameter. It can be expressed as (Painmanakul *et al.*, 2005):

$$N_B = f_B \times \frac{H_L}{U_B} \quad (2.18)$$

$$a = N_B \times \frac{S_B}{V_{\text{total}}} = f_B \times \frac{H_L}{U_B} \times \frac{\pi D_B^2}{A H_L + N_B V_B} \quad (2.19)$$

where	a	=	Interfacial area (m^{-1})
	N_B	=	Number of bubbles generated
	S_B	=	Total bubble surface (m^2)
	V_{total}	=	Total volume in reactor (m^3)
	f_B	=	Bubble formation frequency (s^{-1})
	H_L	=	Liquid height (m)
	U_B	=	Bubble rising velocity (m/s)
	D_B	=	Bubble diameter (m)
	A	=	Cross-sectional area of reactor (m^2)
	V_B	=	Bubble volume (m^3)

Note that the value of S_B is calculated by multiplying the product of number of bubbles with bubble surface.

From the equation 2.19, the value of interfacial area depends on a very large number of parameters, including mixing condition and bubble generation, which are involved the capacity of reactor.

2.6 Airlift reactor

2.6.1 General concepts

Airlift reactor contains a liquid vessels divided into two zones which only one zone is sparged by gas. It improves circulation, gas transfer, and equalizes shear forces in the reactor. The different gas hold-up in the gassed and ungassed zone results in different bulk densities of the fluid in these regions which causes circulation of the fluid in the reactor by an airlift action. The major patterns of liquid circulation are determined by the design of the reactor, which has a channel for gas-liquid up flow and another channel for down flow. All airlift reactors include of four distinct sections with different flow characteristics as follow:

- **Riser:** The gas is injected at the bottom of column, and gas and liquid flow is predominantly upward.
- **Down-comer:** The down-comer section is parallel to the riser. It is connected to the riser at the top and at the bottom. The flow of gas and liquid is predominantly downward. The driving force for recirculation is the density difference between the down-comer and the riser.
- **Base:** In the majority of airlift reactor designs, the bottom connection zone between the riser and down-comer is very simple. It is usually believed that the base does not significantly affect the overall behavior of the reactor, but the design of this section can influence gas hold-up, liquid velocity, and solid phase flow.
- **Gas separator:** This section at the top of the reactor connects the riser to the down-comer, facilitating liquid recirculation and gas disengagement.

2.6.2 Classification

Airlift reactors can be divided into two basic classes of reactors on the basis of their structure: (1) the internal-loop (or baffled) vessels where what would otherwise be a simple bubble column has been split into a riser and a down-comer by an internal baffle, and (2) the external-loop or (outer-loop) vessel where the riser

and the down-comer are two quite separate tubes connected by horizontal section near the top and the bottom. The designs of both structures can be modified further, leading to variations in the fluid dynamics, in the extent of bubble disengagement from the fluid, and in the flow rates of the various phases. The different types of airlift reactor are shown in Figure 2.8.

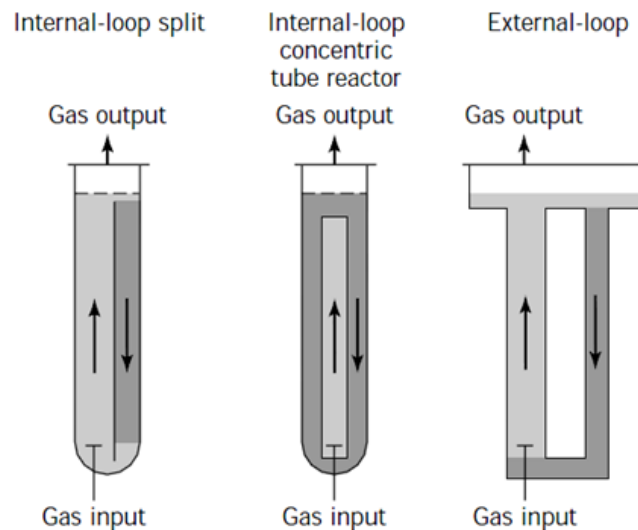


Figure 2.8 Different types of airlift reactors

2.6.3 Gas hold-up

Gas hold-up is the volumetric fraction of the gas in the total volume of a gas-liquid dispersion. The overall gas hold-up in the reactor is defined as:

$$\varepsilon = \frac{V_G}{V_L + V_G} \quad (2.20)$$

where V_G is gas volume in the reactor, and $V_G + V_L$ is the mixed volume of both phases. In airlift reactors, the individual riser gas hold-up (ε_r) and down-comer (ε_d) are related to the overall gas hold-up as

$$\varepsilon = \frac{A_r \varepsilon_r + A_d \varepsilon_d}{A_r + A_d} \quad (2.21)$$

This equation is exact for internal-loop airlifts and is able to use for external-loops when the dispersion heights in the riser and the down-comer are nearly equal.

2.6.4 Liquid circulation

In airlift reactor, the liquid circulates along a well path, which up flow in riser and down flow in down-comer. It depends on difference of gas hold-up between the

riser and down-comer zones of an airlift reactor. A mean circulation velocity (U_{Lc}) is defined by Blenke (1979), which calculated using the following equation:

$$U_{Lc} = \frac{x_c}{t_c} \quad (2.22)$$

where x_c is the circulation path length and t_c is the average time for one complete recirculation.

By mass balance, the superficial velocity in the down-comer (U_{Ld}) and the superficial velocity in the riser (U_{Lr}) are related as follow:

$$U_{Lr}A_r = U_{Ld}A_d \quad (2.23)$$

where A_r and A_d are the cross-sectional area of riser and down-comer respectively.

The superficial velocity must be distinguished from the true linear liquid velocity, also known as the interstitial velocity (V_L). The interstitial velocity is related to the superficial velocity as follows:

$$V_{Lr} = \frac{U_{Lr}}{1 - \epsilon_r} \quad (2.24)$$

and

$$V_{Ld} = \frac{U_{Ld}}{1 - \epsilon_d} \quad (2.25)$$

In this research work, different small plastic media particles are added in the reactors in order to enhance surface contact between gas and liquid phases, which related to an increase in overall mass transfer coefficient in the reactors.

2.7 Plastic media

Media play an important role on the performance of packed bed column. They are used to provide the consistent surface for mass transfer operations. The tower packing typically made from metal, ceramic, and thermoplastic such as polyethylene and polypropylene (PP), high density polyethylene (HDPE), and polyvinyl chloride (PVC).

Media elements may be arranged in an absorber in one of two ways: random or structured designs. The following factors provide a general guide for selecting packing.

- **Cost:** The packing is normally specified in the lowest cost material of manufacture that will satisfy temperature and corrosion requirements. Plastic packing are generally less expensive than metal and ceramic packing.

- **Low pressure drop:** Pressure drop is a function of the volume of void space in a tower when filled with packing. Normally, the larger packing size for a given bed size, the smaller the pressure drop becomes. This is important because a high pressure drop would mean that more energy is required to drive the gas up the distillation column.

- **Corrosion resistance:** Ceramic packing is basically used for high temperature and corrosion chemicals.

- **Large specific area:** Packing is used for maximize the specific surface area. Increasing the surface area per unit volume maximizes the vapor-liquid contact area, which provides high removal efficiency. Efficiency normally increases as the random packing size is decreased.

- **Structural strength:** Packing must be strong enough to resist normal loads during installation, service, physical handling, and thermal fluctuations.

- **Weight:** Heavy packing may require additional support materials or heavier tower construction. Plastics packing have an advantage in this area because they are lighter than either ceramic or metal packing.

- **Design flexibility:** Packing must be able to handle the process changes without substantially affecting removal efficiency.

In this work the small plastic media particle will added in to the reactors instead of the large-size packing media. The advantages of small plastic media over the large size of random packing element are:

- Small plastic media particles are well suspended into the liquid phase; thus, the contaminant particles in tap water cannot be clogged in the porous of media as normally occur in pack bed.
- Cost of small plastic media particles is lower than those of the packing media.

Since benzene is a relatively insoluble contaminant, the only pure water cannot be a good absorbent for achieve the required removal efficiency. Other kinds of substance are required for used as absorbent or add to water.

2.8 Surfactant

A surfactant is a compound that reduces the surface tension of a liquid, the interfacial tension between two liquids, or that between a liquid and a solid. There are a wide variety of these compounds that work with oil, water, and an assortment of other liquids. At the molecular level, a surfactant consists of at least one lyophilic (“solvent-loving”) and one lyophobic (“solvent-fearing”) group in the molecule. If the surfactant is used with water or an aqueous solution, the respective terms are hydrophilic and hydrophobic. A surfactant can be classified by the presence of formally charged groups in its head as shown in Figure 2.9.

A non-ionic surfactant has no charge groups in its head. The head of an ionic surfactant carries a net charge. If the head carries a net negative charge, the surfactant is more specifically called anionic; if the charge is positive, it is called cationic. If a surfactant contains a head with two oppositely charged groups, it is termed zwitterionic. Some of surfactant types include:

- **Cationic surfactant** is the surfactant that the surface-active part is cation. It is usually salt of quaternary ammonium hydroxide, which its hydrogen of the ammonium ion have been replaced with alkyl groups.
- **Anionic surfactant** is the surfactant that ionizes to yield a positive charge, free ion and a negative charge which localizes at the interface.
- **Non-ionic surfactant** is the surfactant that does not ionize and have to depend on groups in the molecule to make it soluble. The groups are usually polymers of ethylene oxide (C_2H_4O).
- **Amphoteric surfactant** is the surfactant that contains both positive and negative surface-active part.

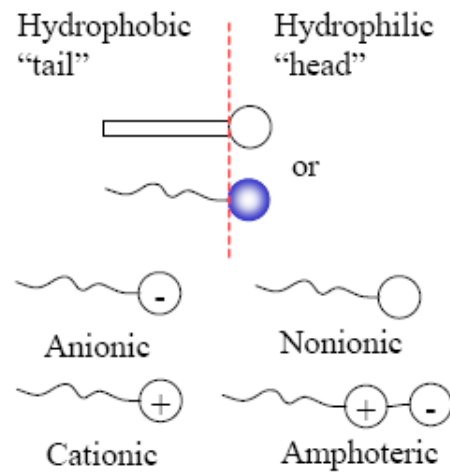


Figure 2.9 Symbols of surface active agent

2.9 Activated carbon

Adsorption is a process where a solid is used for removing a soluble substance from the water. In this process active carbon is the solid. Activated carbon (also called activated charcoal, activated coal, or carbo activates) is a form of carbon processed to be riddled with small, low-volume pores that increase the surface area available for adsorption or chemical reactions. Their very big internal surface is in range between 500 - 1500 m²/g.

Physical adsorption is the primary means by which activated carbon works to remove contaminants from water. Their highly porous nature provides a large surface area for contaminants to collect. In simple terms, physical adsorption occurs because all molecules exert attractive forces, especially molecules at the surface of a solid (pore walls of carbon), and these surface molecules seek other molecules to adhere to. The large internal surface area of carbon has many attractive forces that work to attract other molecules. Thus, contaminants in water are adsorbed to the surface of carbon by surface attractive forces similar to gravitational forces. Adsorption from solution occurs as a result of differences in adsorbate concentration in the solution and in the carbon pores. The adsorbate migrates from the solution through the pore channels to reach the area where the strongest attractive forces are.

Besides physical adsorption, chemical reactions can occur on a carbon surface. Water contaminants were adsorbed because the attraction of the carbon

surface for them is stronger than the attractive forces that keep them dissolved in solution (Deithorn and Mazzoni, 2014).

Active carbon comes in many variations base on their physical characteristics:

- Powder Activated Carbon (PAC)
- Granular Activated Carbon (GAC)
- Extruded activated carbon (EAC)
- Bead activated carbon (BAC)
- Impregnated carbon
- Polymer coated carbon

The GAC version, mostly used in water treatment, is used in this research work. It has a relatively larger particle size compared to powdered activated carbon; therefore, it presents a smaller external surface. Diffusion of the adsorbate is thus an important factor. The GACs are preferred for all absorption of gases and vapors as their rate of diffusion are faster. Granulated carbons have been used for water treatment, deodorization and separation of components of flow system and are also used in rapid mix basins. GAC can be either in granular or extruded form. GAC is designated by sizes such as 8×20, 20×40, or 8×30 for liquid phase applications and 4×6, 4×8 or 4×10 for vapor phase applications. The most popular aqueous phase carbons are the 12×40 and 8×30 sizes because they have a good balance of size, surface area, and head loss characteristics.

2.10 Literature reviews

2.10.1 VOC absorption in bubble column

Peevaa *et al.* (2001) have studied the absorption of n-decane in water-silicone oil emulsions in a laboratory-scale bubble column at different gas flow rates for the whole range of emulsion compositions. They found that the volumetric mass transfer coefficient ($K_L a$) to the emulsions in the bubble column reactor is independent of the emulsions composition. Since the solubility of decane in silicone oil is high, the rate of absorption is an approximately 70% of the incoming decane in a single pass through a relatively small apparatus. The experiments indicate that the

rate of VOC absorption into emulsions of silicone oil can reach high values using a small fraction of oil. This bubble column system provided a high VOC absorption capacity.

2.10.2 Airlift reactor

Airlift reactor has been investigated for absorbing oxygen, which is a relatively insoluble gas in water as same as benzene. Freitas and José (2001) determined oxygen mass transfer coefficient (K_La) in a high solids loading three-phase internal-loop airlift reactor. They studied the effect of the airflow rate, solids loading, solids density and the liquid-phase properties on K_La . They reported that the increased airflow rate and the introduction of ethanol increased the K_La in the reactor. The progressive introduction of solids and a small increase on solids density caused the increase mass transfer rate. Moreover, the investigators determined correlations for the K_La with the riser superficial gas velocity and solids loading.

2.10.3 The hydrodynamics and mass transfer characteristics in airlift reactor with packed bed

There are many researches combined airlift reactor with packed bed and fluidized beds in order to study the effect of these packing on hydrodynamics and mass transfer characteristics. All of the researches showed that the elements enhanced the overall gas-liquid volumetric mass transfer coefficient (K_La).

Chisti *et al.* (1990) studied the influence of motionless mixers on the K_La value in an external-loop type airlift bioreactor. This study used aqueous salt solution and pseudoplastic solution of carboxymethyl cellulose as liquid phase. The presence of SMV-12 static mixers increased K_La by 30-500%, depending on the fluid thickness. The increased K_La involved the increased gas hold-up and gas-liquid interfacial area, which depend on bubble breakup accomplished by the static mixing elements.

Han *et al.* (2000) designed a gas-liquid-solid inverse fluidization airlift bioreactor, which combining advantages of external-loop airlift reactors and inverse fluidized beds. They investigated the gas hold-up in the riser, the particle loading in the down-comer and the liquid circulation velocity in the loop. The results showed that the gas hold-up in the riser increased with the increase in the superficial gas

velocity and particle loading, and the two-phase drift model of Zuber and Findlay satisfactorily fitted the gas hold-up in the GLS-IFAB. The liquid circulation velocity decreased with the increase in the particle loading whereas it increased with the gas velocity. It was found that the Richardson and Zaki model fitted experimental data of bed expansion of liquid-solid inverse fluidization in the down-comer well. Based on an energy balance, two hydrodynamic models were proposed to predict the liquid circulation velocity in the present bioreactor.

Meng *et al.* (2002) combined the packed bed bioreactor (PB) and an external loop airlift bioreactor (ELAB) design strategies into one vessel for studied the hydrodynamics behavior of the combined system. A woven nylon packing used as a packing installed in the riser section of the airlift bioreactor. This study showed that the gas hold-up continuously increased by increasing the packing height and packing porosity up to 0.99, but at a porosity of 1.0 (no packing), the gas hold-up dropped. Moreover, increased amounts of packing in the riser of the bioreactor, whether in the form of packing height or packing density, the liquid circulation rate was decreased caused by the increased frictional resistance and tortuosity. Bubbles that passing through the packed bed were more uniform and had smaller size while the Bodenstein number was decreased that indicated greater axial dispersion and enhanced mixing. The authors concluded that the highest gas hold-up improved mass transfer. It prepared large void spaces and reduced plugging and liquid frictional losses.

Nikakhtari and Hill (2005) investigated gas hold-up and mass transfer rates of three volatile organic chemicals (VOCs) in an external loop airlift bioreactor (ELAB), with and without packing. They used a stainless steel mesh packing with 99.0% porosity as a packed bed in the riser section of ELAB. The results show that the packing enhanced the overall volumetric mass transfer coefficient ($K_L a$) by an average of 65.1% and 33.4% for toluene and benzene, respectively, in comparison with unpacked bed. Moreover, the packing increased gas hold-up and decreased bubble size in the reactor, which increase the mass transfer rates. Desorption of VOCs was slower than absorption, which was explained by the change in gas bubble sizes in the presence of VOCs. A full, mechanistic mathematical model was

developed to predict the transient concentration distribution in the ELAB and was shown to be an accurate method to determining $K_L a$ for VOC absorption in ELABs with low liquid circulation rate, as compared to models assuming well-mixed conditions.

Moraveji *et al.* (2012) studied the effects of various surface active agents (SDS, HCTBr and Tween 40) with different concentrations (0-5 ppm) added to pure water on the hydrodynamic and mass transfer characteristics of oxygen in a spilt-cylinder airlift bioreactor both with and without packed bed. They reported that the surfactant solutions decrease surface tension of the liquid and produce smaller bubbles compared with pure water. The surfactants increased mixing time and overall gas hold-up (ϵ) although the liquid circulation velocity (U_{Lc}) and volumetric mass transfer coefficient ($K_L a$) decreased. Moreover, the packed bed reactor increased the $K_L a$ in comparison with unpacked bed reactor. They decreased bubbles size and U_{Lc} , which the decrease in U_{Lc} caused higher gas-hold up.

2.10.4 Solubility of benzene in different solutions

The solubility of benzene in various surfactants was studied in order to design of gas absorption operations. Erto and Lancia (2012) studied the solubility of benzene in amphiphilic block copolymers (ABC). The four ABC used in this work included: two thermosensitive ABC containing poly-ethylene oxide and poly-propylene oxide blocks - Pluronic[®] L62 and Pluronic[®] P123, one non-thermosensitive ABC - poly(vinyl pyrrolidone) - polystyrene (PVP-PS), and one non-ionic surfactant - polyoxyethylene sorbitol monooleate (Tween 80[®]). Each copolymer aqueous solution, benzene Henry's constant (H) is calculated. Moreover, the investigators studied the effects of temperature (4–90 °C) and copolymer concentration (4–20%). The results showed that, at 20 °C and 4% copolymer concentration, the H values are in the 50 -280 atm, with a ranking PVP-PS < P123 < Tween 80 < L62. Due to the formation of a higher number of micelles, and increase in copolymer concentration results in an increase in benzene solubility. All the copolymers were slightly increased in benzene Henry's constant with temperature except P123. The investigators concluded that the P123 aqueous solution is the most promising liquid for benzene recovery among those

investigated, being effective for both operations of gas absorption (at low temperature) and solvent regeneration by thermal stripping (at high temperature).

2.11 Research focuses

These literature reviews suggest that even though a wide variety of experiments have been performed on bubble column and airlift reactor with media, the knowledge of many factors inside this reactor can be further enhanced. The literature reviews also illustrate that there is still a lack of some information on bubble hydrodynamic behaviors and mass transfer mechanisms of bubble column and airlift reactor with small plastic media particles. For this propose, a bubble column and an internal loop lift reactor with small plastic media are required for determine and associate both important parameters for well understanding the mechanism in order to enhance the absorption of hydrophobic VOCs (benzene in this study).

This research work is mainly focused on the study of benzene absorption in a bubble column and an internal loop airlift reactor with small plastic media particles in order to designed an effectively benzene controlled system. The effects of different types and concentration of small plastic media particles on oxygen mass transfer and bubble hydrodynamic characteristics in a bubble column are studied in order to find the appropriate condition for mass transfer efficiency of hydrophobic substance. The bubble hydrodynamic behaviors and mass transfer characteristics of oxygen and benzene in the reactor are studied.

CHAPTER III METHODOLOGY

3.1 Research overview

The purpose of this study was to determine the impact of plastic media on oxygen mass transfer and bubble hydrodynamic parameters at a variety of gas flow rate in a bubble column (BC) and an internal loop airlift reactor (ILALR). The different types and amount of small size plastic particles were added into the reactors, overall mass transfer coefficients and bubbles diameter were investigated. These experimental results can be applied for designing a high-efficiency benzene absorption system. Research flow chart can be demonstrated in Figure 3.1

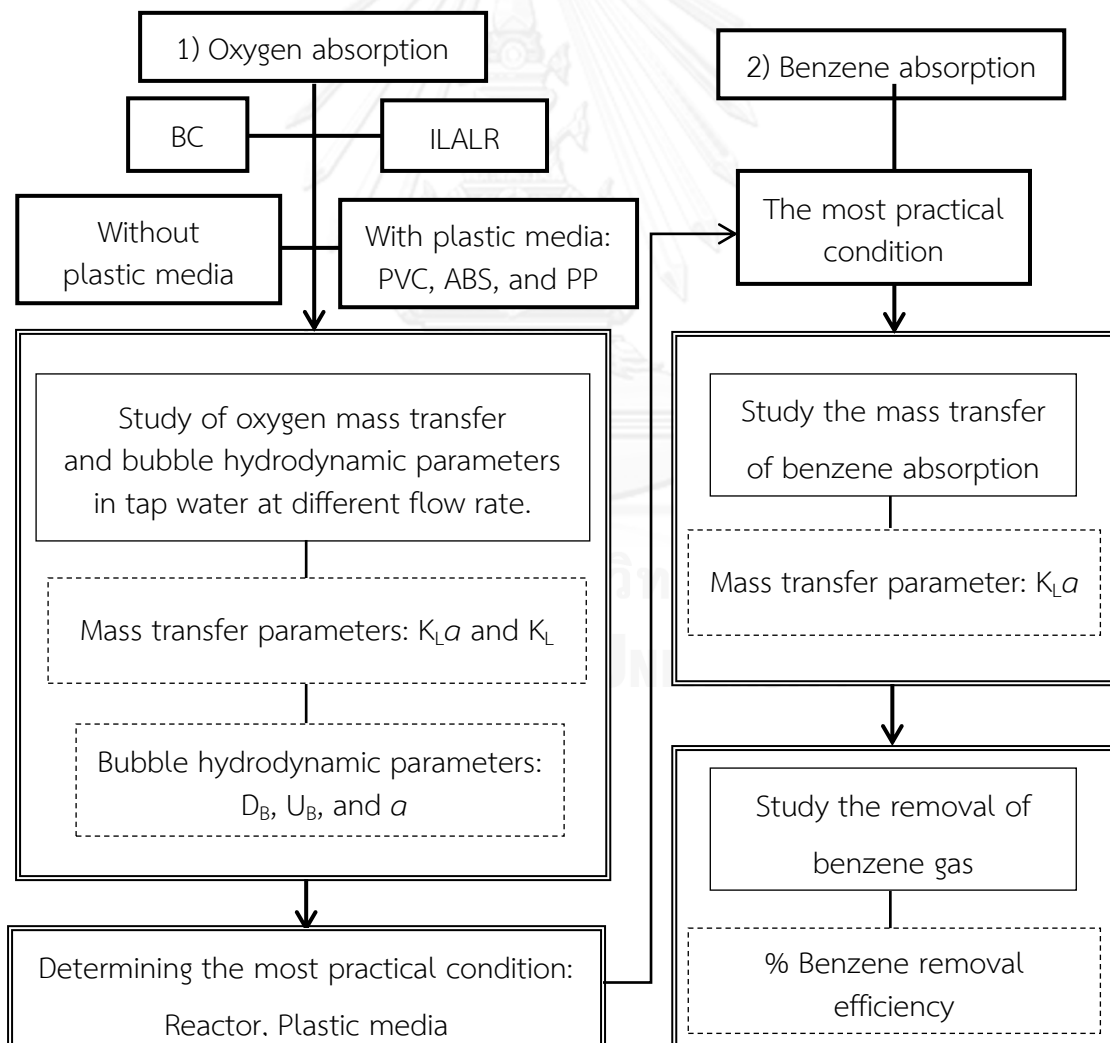


Figure 3.1 Experimental framework

3.2 Experimental set-up

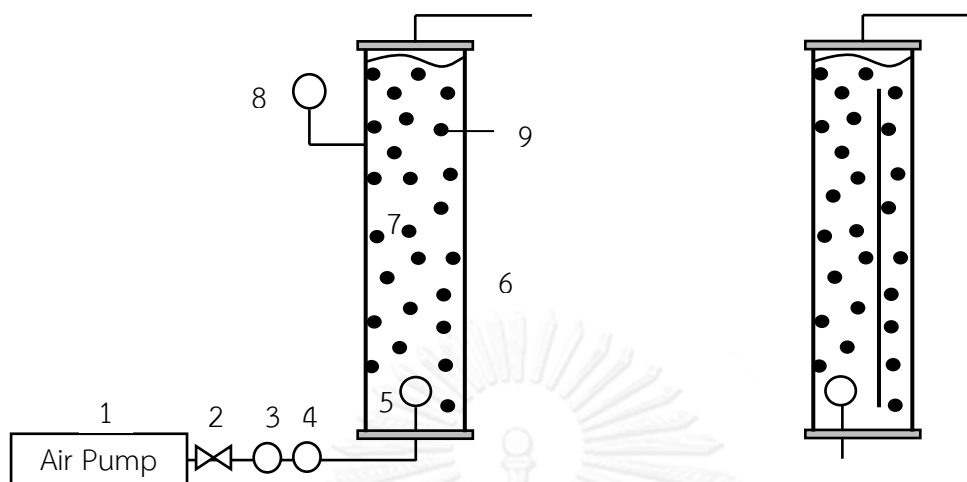


Figure 3.2 Bubble column (BC)

Figure 3.3 Internal loop airlift reactor (ILALR)

The schematic diagrams of experimental set-up for this research work were shown in Figures 3.2 and 3.3. The equipment used in this study contains:

- | | |
|-------------------------------|-------------------------------|
| 1) Air pump | 2) Ball valve |
| 3) Pressure gage | 4) Gas flow meter |
| 5) Rigid orifice gas diffuser | 6) Reactor |
| 7) Liquid phase | 8) Dissolved oxygen electrode |
| 9) Plastic media | |

The BC was made of Plexiglas with 14 cm in diameter and 100 cm in height. For ILALR system, the rectangular Plexiglas baffle (with 13 cm width, 80 cm height, and 0.5 cm thickness) was installed within the BC in order to divide the cross section into a riser zone and a down-comer zone. The gas diffuser was injected at the bottom of reactors: in the middle and in the riser zone for BC and ILALR, respectively. The gas diffuser used in this work was rigid orifice with 5 cm in diameter as shown in the Figure 3.4



Figure 3.4 Rigid orifice gas diffuser

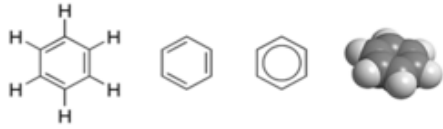
3.3 Materials and methods

3.3.1 Chemical agents

In this study, sodium sulfite (Na_2SO_3 , Analytical grade, 99.99 %) was purchased from Ajax Finechem Australiz Company. Benzene (C_6H_6 , analytical grade, 99%) was purchased from Roongsub Chemical Company.

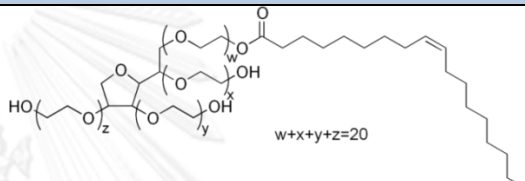
Benzene is an organic chemical compound and is very volatile and readily partitions into the atmosphere. Its molecule is composed of a ring of six carbon atoms joined with six hydrogen atoms. Benzene is a clear, colorless liquid that has an aromatic odor and is highly flammable. Benzene is toxic, has mutagenic properties and can cause cancer in humans. Short term exposure to low levels can be irritating to eyes, cause drowsiness, dizziness, rapid heart rate, headaches, tremors, confusion and in some cases unconsciousness. Exposure to high concentrations can result in death (EPA, 2009). The physical and chemical properties of benzene are shown in details in Table 3.1.

Table 3.1 Physical and chemical properties of benzene

Property	Characteristic
Structure	
Chemical formula	C_6H_6
Molecular weight	78.11 g/mol
Color	Clear, colorless liquid
Melting point	5.5 °C
Boiling point	80.1 °C
Density at 15 °C, g/cm^3	0.8787
Odor	Aromatic
Solubility: Water at 25 °C Organic solvent	w/w:0.188% Alcohol, chloroform, ether, carbon disulfide, oils, acetone, carbon, tetrachloride, glacial acetic acid
Partition coefficients: Log K_{ow} Log K_{oc}	2.13 1.8-1.0
Vapor pressure at 20 °C	75 mm Hg
Henry's law constant at 25 °C	$5.5 \times 10^{-3} \text{ atm}\cdot\text{m}^3/\text{mol}$
Autoignition temperature	498 °C
Flashpoint	-11 °C (closed cup)
Flammability limits in air	1.2% (lower limit); 7.8% (upper limit)
Conversion factors	1 ppm = 3.24 mg/m^3 at 20°C and 1 atm pressure; 1 mg/m^3 = 0.31 ppm
Explosive limits	1.4% (lower limit); 8% (upper limit)

Tween 80 (Polyoxyethylene (20) sorbitan monooleate) is used in this work as a surfactant for benzene absorption. It is a nonionic surfactant and emulsifier derived from polyethoxylated sorbitan and oleic acid. The Tween 80 is a viscous, water-soluble yellow liquid. The hydrophilic groups in this compound are polyoxyethylene groups which are polymers of ethylene oxide. The Tween 80 is often used in food and other products as an emulsifier. Its physical and chemical properties are shown in Table 3.2

Table 3.2 Physical and chemical properties of Tween 80

Property	Characteristic
Structure	
Chemical formula	$C_{64}H_{124}O_{26}$
Molecular weight	1310 g/mol
Appearance	Amber colored viscous liquid
Detergent Class	Nonionic
Critical Micelle Concentration (CMC)	0.012 mM (0.0016%, w/v)
Density	1.06 – 1.09 g/mL, oily liquid
Boiling point	> 100°C
Solubility in water	Very soluble
Solubility in other solvents	Soluble in ethanol, cottonseed oil, corn oil, ethyl acetate, methanol, toluene
Main hazards	Irritant
Flash point	113 °C, 235 °F, 386 K

3.3.2 Plastic media

The three different plastic media particles with different concentration (2-15 (%v/v)) were used in this work contain:

- Polyvinyl Chloride (PVC)
- Acrylonitrile Butadiene Styrene (ABS)
- Polypropylene (PP)

The properties of these three small plastic media particles were shown in details in the Table 3.3

Table 3.3 Types and properties of plastic media

Media types	Polyvinyl Chloride (PVC)	Acrylonitrile Butadiene Styrene (ABS)	Polypropylene (PP)
			
Density	1380 kg/m ³	1050 kg/m ³	946 kg/m ³
Average size	0.425 mm	0.305 mm	0.349 mm
Specific surface area	0.018 m ² /m ³	0.014 m ² /m ³	0.028 m ² /m ³

3.3.3 Benzene generator

For generating benzene gas in this study, 100 mL of pure benzene was added in a closed Erlenmeyer flask. Then, air was injected into the flask in order to generating benzene gas stream from their volatilization. The schematic diagram of experimental set-up for benzene generation is show in Figure 3.5

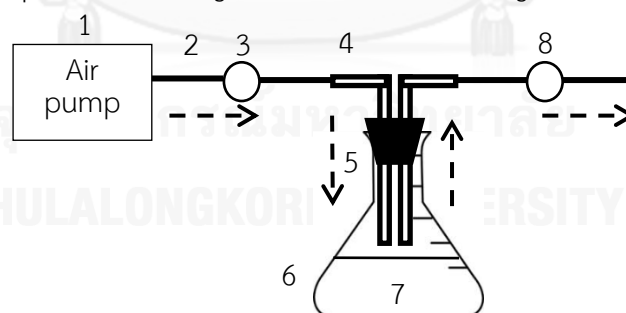


Figure 3.5 Benzene generator

The equipment used for benzene generator contains:

- | | |
|-------------------|-----------------------|
| 1) Air pump | 2) Gas tube |
| 3) Ball valve | 4) Glass tube L shape |
| 5) Rubber stopper | 6) Erlenmeyer flask |
| 7) Pure benzene | 8) Gas flow meter. |

3.4 Analytical methods

3.4.1 Mass transfer parameters

- **The overall mass transfer coefficient ($K_L a$)**

The overall mass transfer coefficient ($K_L a$) is used in order to analyse the absorption process. According to the Non-stationary or dynamic method (Deckwer, 1992), the $K_L a$ is given by the following equation:

$$\frac{dc}{dt} = K_L a (C^* - C) \quad (3.1)$$

or in its integral form by:

$$\frac{\ln [C^* - c]}{\ln C^*} = - K_L a (t) \quad (3.2)$$

where C and C^* are the concentration of contaminant and the saturated concentration of contaminant in the liquid phase, respectively. The slope of this equation gives $- K_L a$

- **Liquid film mass transfer coefficient (K_L)**

The liquid film mass transfer coefficient (K_L) was the proportions of the overall mass transfer coefficient and interfacial area (a) obtained experimentally in this study. Therefore, the value of K_L can be determined by Sardeing *et al.* (2006):

$$K_L = \frac{K_L a}{a} \quad (3.3)$$

3.4.2 Bubble hydrodynamic parameters

- **Bubbles diameter (D_B)**

The bubble hydrodynamic parameters were determined with photographic technique by using a Basler high speed camera (350 images/second) as shown in Figure 3.6. The 60-150 moving bubbles were randomly chosen in twenty pictures which captured at the middle of the reactor (0.6 m above the bottom). Then, bubbles diameter was measured by PylonViewer vision software. The Sauter mean bubble diameter (d_{32}), which refers to the diameter of a sphere with the same volume to surface ratio as the gas bubble and for a distribution of bubble sizes, is calculated from equation (Kracht *et al.*, 2008):

$$D_B = d_{32} = \frac{\sum_{i=1} d_i^3}{\sum_{i=1} d_i^2} \quad (3.4)$$



Figure 3.6 High speed camera

- Specific interfacial area (a)

For BC and the riser zone of ILALR, the specific interfacial area (a) is the ratio of bubble surface (S_B) and the total volume of reactor (V_T). It can be calculated using Garcia Maldonado equation (Painmanakul *et al.*, 2005):

$$a = N_B \times \frac{S_B}{V_{total}} = f_B \times \frac{H_L}{U_B} \times \frac{\pi D_B^2}{A H_L + N_B V_B} \quad (3.5)$$

where	a	=	Interfacial area (m^{-1})
	N_B	=	Number of bubbles generated
	S_B	=	Total bubble surface (m^2)
	V_{total}	=	Total volume in reactor (m^3)
	f_B	=	Bubble formation frequency (s^{-1})
	H_L	=	Liquid height (m)
	U_B	=	Bubble rising velocity (m/s)
	D_B	=	Bubble diameter (m)
	A	=	Cross-sectional area of reactor (m^2)
	V_B	=	Bubble volume (m^3)

The bubble formation frequency can be calculated by the following equation

$$f_B = \frac{Q_G}{V_B} \quad (3.6)$$

where	f_B	=	Bubble formation frequency (s^{-1})
	Q_G	=	Gas flow rate (m^3/s)
	V_B	=	Bubble volume (m^3)

For the down-comer zone of ILALR, the specific interfacial area is the proportions of the overall mass transfer coefficient and the liquid film mass transfer coefficient as show in the following equation:

$$a = \frac{K_L a}{K_L} \quad (3.7)$$

- **Terminal rising bubble velocity (U_B)**

The bubble rising velocity were calculated by taking picture of bubble in reactor to analyze its distance at any time frame, thus, the bubble rising velocity were calculated from equation (Painmanakul and Hébrard, 2008):

$$U_B = \frac{\Delta D}{t_{\text{frame}}} \quad (3.8)$$

where U_B = Terminal rising bubble velocity
 ΔD = Distance between two frames
 t_{frame} = Time frame

3.4.3 Gas flow rate: Down-comer zone (Q_G)

From the equation 3.5, and 3.6, the Q_G : Down-comer (Q_G) can be determined by the equation below:

$$Q_G = f_B \times V_B = a \times \frac{U_B}{H_L} \times \frac{A_{H_L} + N_B V_B}{\pi D_B^2} \times V_B \quad (3.9)$$

3.4.4 Benzene removal efficiency (%Eff)

The benzene removal efficiency (%Eff) indicated the performance of the absorption process occurred in the reactor. It was defined as the ratio between the amounts of benzene gas transferred and injected to the liquid phase. Note that the area under curve obtained with gas chromatography was used as the benzene concentration. The %Eff can be determined by the following equation:

$$\%Eff = \frac{C_{\text{inlet}} - C_{\text{outlet}}}{C_{\text{inlet}}} \times 100 = \frac{\text{Area}_{\text{inlet}} - \text{Area}_{\text{outlet}}}{\text{Area}_{\text{inlet}}} \times 100 \quad (3.10)$$

3.4.5 Oxygen concentration

The oxygen concentrations in liquid phase were measured by dissolved oxygen electrode (DO electrode). The DO electrode was positioned within the reactors at depth of 0.45 m from the surface of the gas-free liquid. Moreover, the DO

electrode was inserted at the middle of the BC, and the both side (Riser zone and down-comer zone) of the ILALR.

3.4.6 Benzene concentration

In this work, the overall mass transfer coefficients ($K_L a$) of benzene absorption were calculated by plot the equation 3.2. The concentrations of benzene in liquid phase will be measured with time by UV-Visible spectroscopy technique. The values of absorbent observed referred to the concentration of benzene in liquid phase. Moreover, the sample (liquid phase) were collected at 1-25 minutes.

For study the benzene removal efficiency, the benzene gas inlet and outlet of the reactor were collected into air bag at 5.0-5.5 minutes. The benzene gas concentrations were measured by the Agilent Technologies gas chromatograph (GC) 6890N equipped with flame ionization detector. A fused-silica, HP-1 column (100% dimethyl-polysiloxane; 30 m x 0.32 mm i.d., 0.2 μ m film thickness), supplied by J&W Scientific, USA was employed, with helium (purity 99.995%) as carrier gas at flow rate of 2.1 mL.min⁻¹. The column temperature was programmed as follows: 40 °C for 5 min, then post run to 200 °C and holding time for 1 min. The injection port and detector were operated at 100-250 °C, respectively. The area under curve of benzene gas obtained with gas chromatography was applied to calculate the benzene removal efficiency.

3.5 Experimental procedure

The scope of this work is as follows:

1. Effect of plastic media on overall mass transfer coefficient in BC.
2. Effect of plastic media on bubble hydrodynamic parameter in BC.
3. Study the oxygen mass transfer and bubble hydrodynamic parameters in ILALR.
4. Effect of plastic media on oxygen mass transfer and bubble hydrodynamic parameters in ILALR.
5. Comparison the effect of best plastic media condition on mass transfer and bubble hydrodynamic parameters in BC and ILALR.
6. Application for benzene gas absorption.

1. Effect of plastic media on overall mass transfer coefficient in BC.

The objective of this study was to evaluate the oxygen mass transfer characteristics in BC with the different applied gas flow rates. The outline of this part was presented in Figure 3.7, and the summary variables concerning to this study can be presented in Table 3.4.

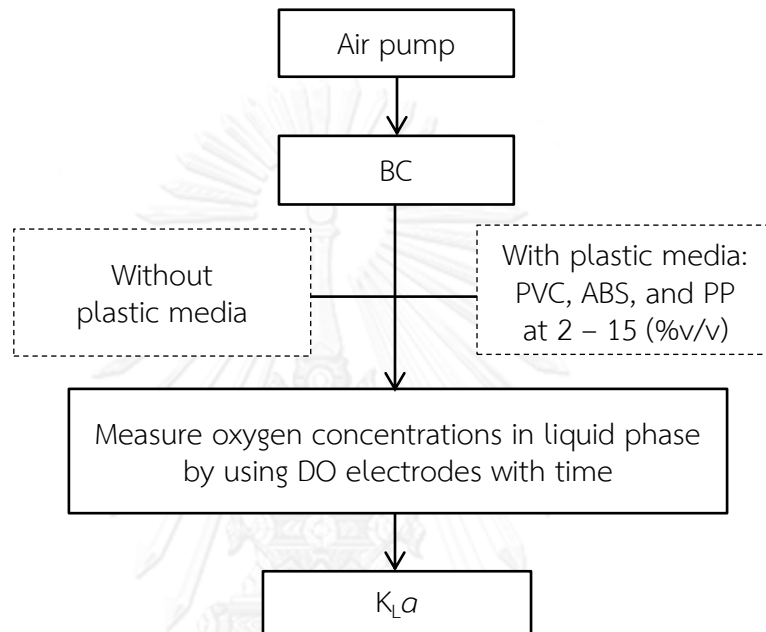


Figure 3.7 Flow diagram for studying effect of plastic media on overall mass transfer coefficient in BC.

Table 3.4 Variable of studying effect of plastic media on $K_L a$ coefficient in BC.

Fixed Variable	Parameter
Reactor	Bubble column
Gas phase (absorbate)	Oxygen
Liquid phase (absorbent)	Tap water
Independent Variable	Parameter
Gas flow rate	2.5, 5, 10, 15, and 20 L/min
Media type	PVC, ABS, PP
Media concentration	2, 5, 10, 15 (%v/v)
Dependent Variable	Parameter
Mass transfer parameters	$K_L a$

2. Effect of plastic media on bubble hydrodynamic parameter in BC.

The aim of this part was to evaluate the bubble hydrodynamic in BC at different gas flow rates. The outline of this part was presented in Figure 3.8, and the summary variables concerning to this study can be presented in Table 3.5.

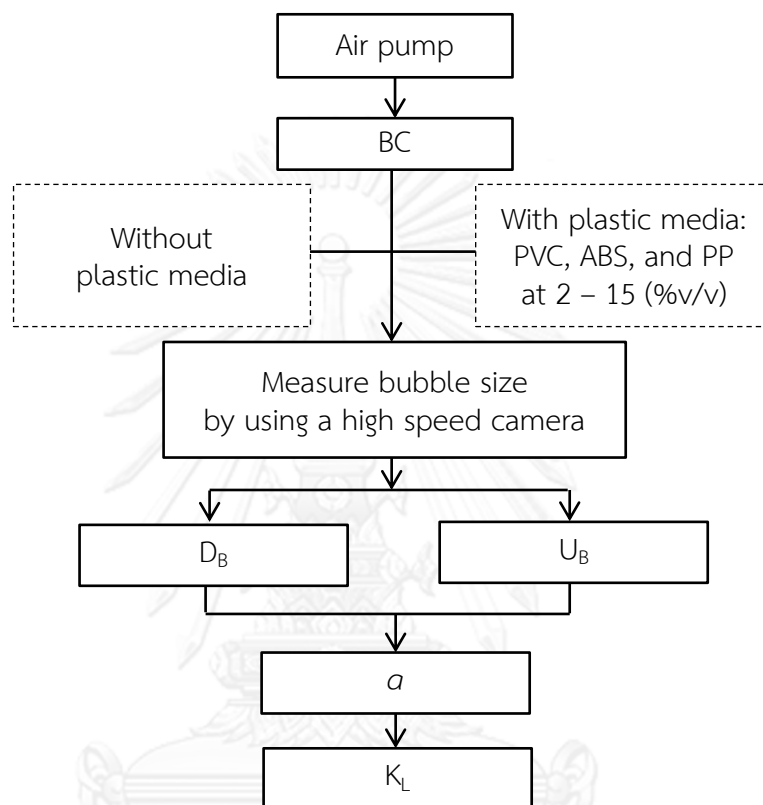


Figure 3.8 Flow diagram for studying effect of plastic media on bubble hydrodynamic parameter in BC.

Table 3.5 Variable of studying effect of plastic media on bubble hydrodynamic parameter in BC.

Fixed Variable	Parameter
Reactor	Bubble column
Gas phase (absorbate)	Oxygen
Liquid phase (absorbent)	Tap water
Independent Variable	Parameter
Gas flow rate	2.5, 5, 10, 15, and 20 L/min
Media type	PVC, ABS, PP
Media concentration	2, 5, 10, 15 (%v/v)
Dependent Variable	Parameter
Mass transfer parameters	K_L
Bubble hydrodynamic parameters	U_B , D_B , and a

3. Study the oxygen mass transfer and bubble hydrodynamic parameters in ILALR.

The objective of this part is to study the oxygen mass transfer and bubble hydrodynamic characteristics in ILALR with a variety of gas flow rates. The outline of this study was presented in Figure 3.9 and the summary variables concerning to this study can be presented in Table 3.6.

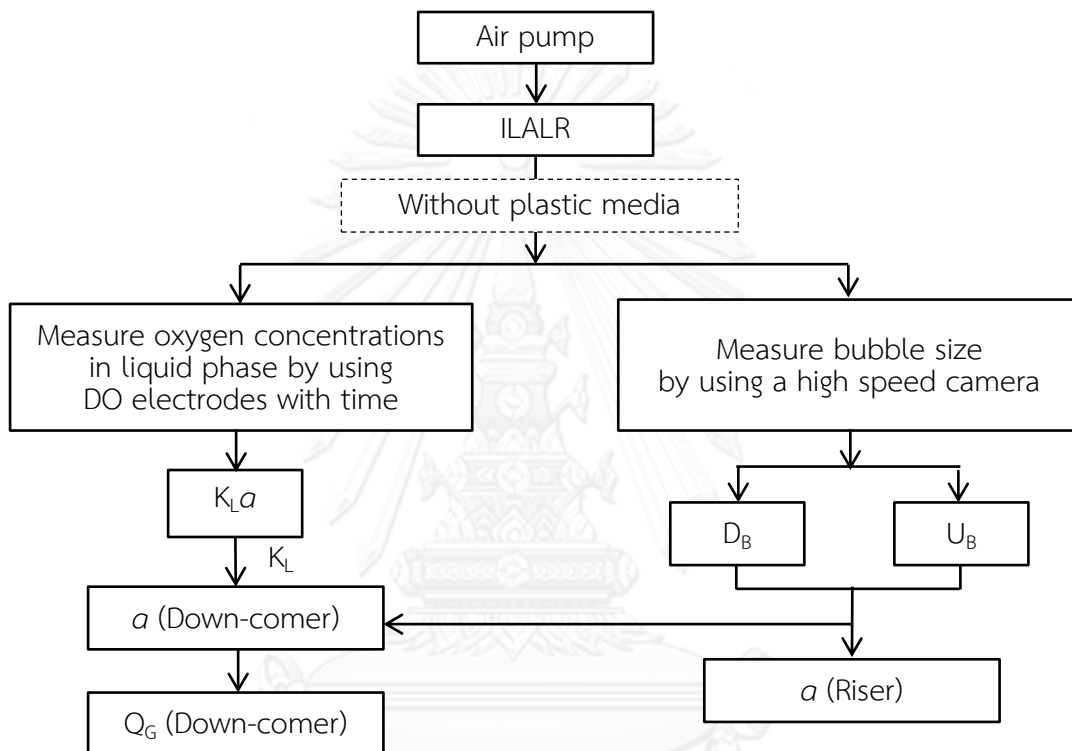


Figure 3.9 Flow diagram for studying the oxygen mass transfer and bubble hydrodynamic parameters in ILALR.

Table 3.6 Variable of studying the oxygen mass transfer and bubble hydrodynamic parameters in ILALR.

Fixed Variable	Parameter
Reactor	Internal loop airlift reactor
Gas phase (absorbate)	Oxygen
Liquid phase (absorbent)	Tap water
Independent Variable	Parameter
Gas flow rate	2.5, 5, 7, 10, 12, 15, and 20 L/min
Media type	PVC, ABS, PP
Dependent Variable	Parameter
Mass transfer parameters	$K_L a$ (Riser and down-comer zone)
Bubble hydrodynamic parameters	U_B , D_B , and a (Riser and down-comer zone)

4. Effect of plastic media on oxygen mass transfer and bubble hydrodynamic parameters in ILALR.

The aim of this study is to evaluate the effect of plastic media on hydrodynamic and oxygen mass transfer characteristics in ILALR with a variety of gas flow rates. The outline of this study was presented in Figure 3.10 and the summary variables concerning to this study can be presented in Table 3.7.

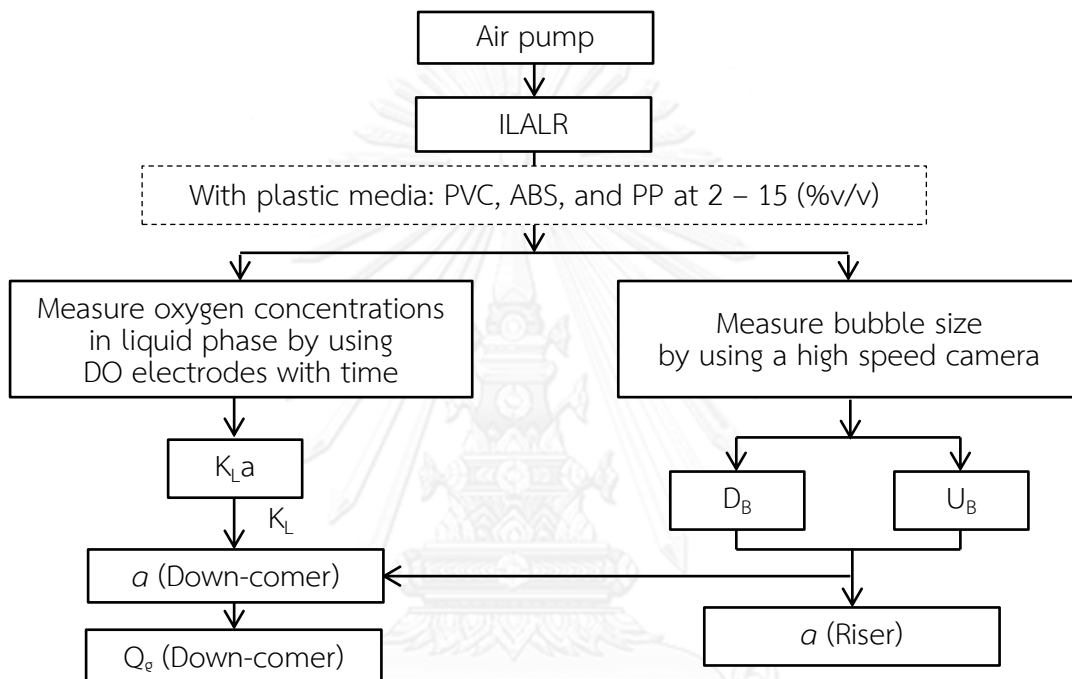


Figure 3.10 Flow diagram for studying the effect of plastic media on oxygen mass transfer and bubble hydrodynamic parameters in ILALR.

Table 3.7 Variable of studying the effect of plastic media on oxygen mass transfer and bubble hydrodynamic parameters in ILALR.

Fixed Variable	Parameter
Reactor	Internal loop airlift reactor
Gas phase (absorbate)	Oxygen
Liquid phase (absorbent)	Tap water
Independent Variable	Parameter
Gas flow rate	2.5, 5, 10, 15, and 20 L/min
Media type	PVC, ABS, PP
Media concentration	2, 5, 10, 15 (%v/v)
Dependent Variable	Parameter
Mass transfer parameters	$K_L a$ (Riser and down-comer zone)
Bubble hydrodynamic parameters	U_B , D_B , and a (Riser and down-comer zone)

5. Comparison the effect of best plastic media condition on mass transfer and bubble hydrodynamic parameters in BC and ILALR.

The aim of this study is to comparing the effect of best plastic media condition on mass transfer and bubble hydrodynamic parameters in BC and ILALR. The best reactor used was determined. The parameters compared were presented in Table 3.8.

Table 3.8 Variable of studying the oxygen mass transfer and bubble hydrodynamic parameters in BC and ILALR.

Fixed Variable	Parameter
Reactor	BC and ILALR
Gas phase (absorbate)	Oxygen
Liquid phase (absorbent)	Tap water
Gas flow rate	2.5, 5, 10, 15, and 20 L/min
Independent Variable	Parameter
Media addition	Most practical type and concentration of media (15% of PP media)
Dependent Variable	Parameter
Mass transfer parameters	$K_L a$, K_L (Riser and down-comer zone)
Bubble hydrodynamic parameters	D_B , and a (Riser and down-comer zone)

6. Application for benzene gas absorption.

The objective of this study is to apply the most practical condition obtained with oxygen absorption part for enhance benzene gas absorption. The outline of this study was shown in Figure 3.11 and the summary variables concerning to this study can be presented in Table 3.9.

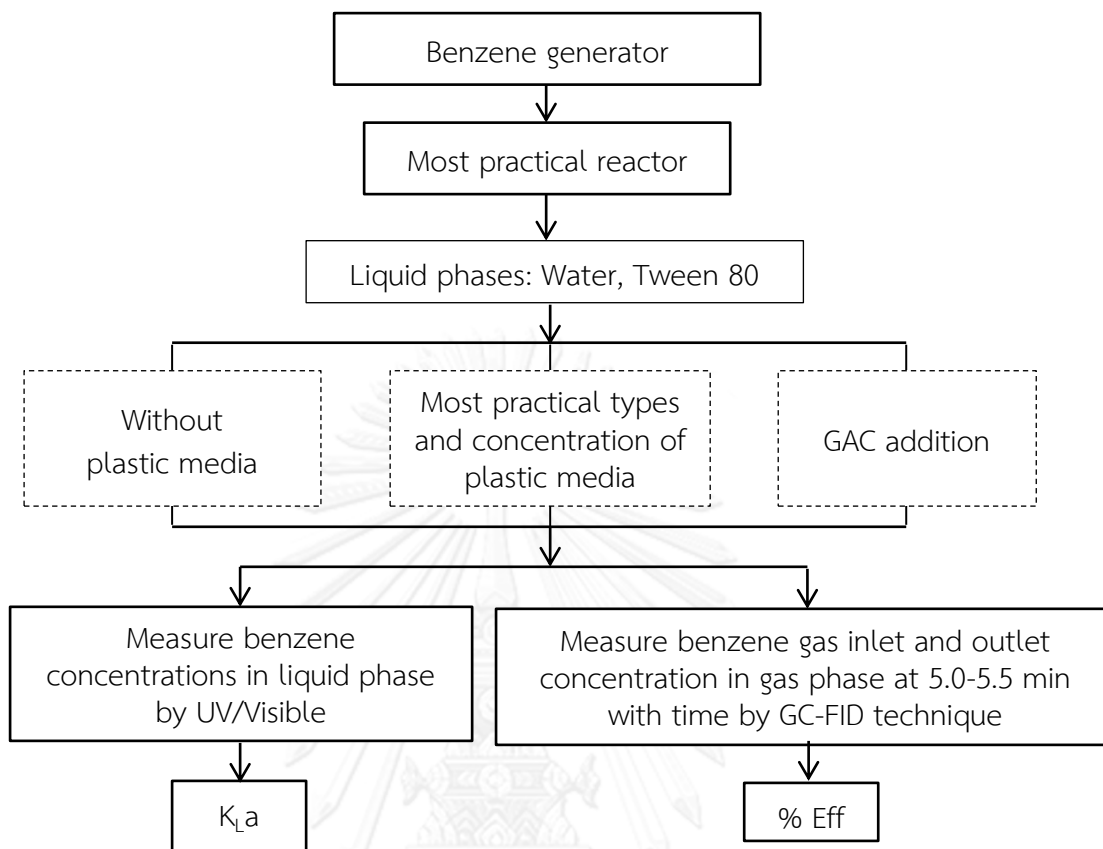


Figure 3.11 Flow diagram for studying application for benzene gas absorption.

Table 3.9 Variable of studying application for benzene gas absorption.

Fixed Variable	Parameter
Reactor	Most practical reactor (ILALR)
Gas phase (absorbate)	Benzene
Liquid phase (absorbent)	Tap water, Tween 80 (0.1 and 1.0 CMC)
Gas flow rate	10 L/min
Pure benzene liquid (For generate benzene gas)	100 mL
Independent Variable	Parameter
Media addition	Most practical type and concentration of media (15% of PP media)
Granular activated carbon (GAC)	195 g
Dependent Variable	Parameter
Mass transfer parameters	$K_L a$ (Riser zone)
Benzene gas removal efficiency	% Eff

CHAPTER IV

RESULTS AND DISCUSSIONS

The effect of plastic media on oxygen mass transfer and bubble hydrodynamic parameters at a variety of gas flow rate in a bubble column (BC) and an internal loop airlift reactor (ILALR) will be discussed in this chapter. Moreover, the application of the best condition was applied to removal benzene gas from the gas stream. The results were consists of 5 parts as follow:

1. Effect of plastic media on overall mass transfer coefficient in BC.
2. Effect of plastic media on bubble hydrodynamic parameter in BC.
3. Study the oxygen mass transfer and bubble hydrodynamic parameters in ILALR.
4. Effect of plastic media on oxygen mass transfer and bubble hydrodynamic parameters in ILALR.
5. Comparison the effect of best plastic media condition on mass transfer and bubble hydrodynamic parameters in BC and ILALR.
6. Application for benzene gas absorption.

4.1 Effect of plastic media on overall mass transfer coefficient in BC.

The aim of this study was to determine the impact of plastic media with different density on overall mass transfer coefficient ($K_L a$) at a variety of gas flow rate in the BC. For analyzed the $K_L a$ values, the oxygen concentrations in the liquid phase were measured with time using dissolved oxygen electrode, and calculated as previously described in equation 3.2. Different types and amounts of plastic media were added into the BC in order to study the overall mass transfer coefficients.

- **No plastic media**

Figure 4.1 presents the variation of overall mass transfer coefficient with gas flow rates obtained in the BC.

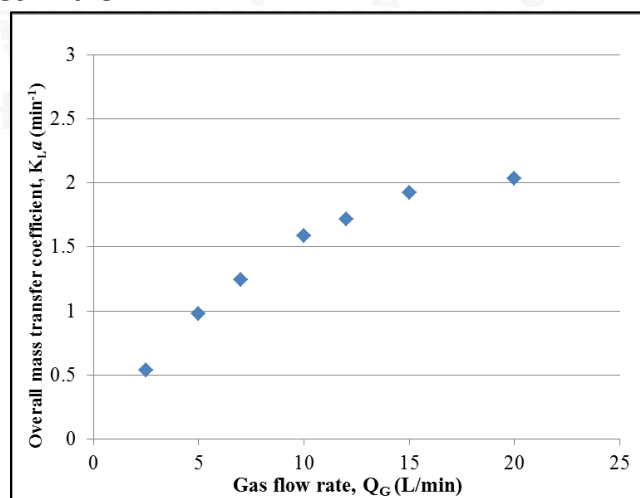


Figure 4.1 Overall mass transfer coefficient versus gas flow rate in BC

As shown in Figure 4.1, it can be seen that the values of $K_L a$ obtained with BC varied between 0.53 and 2.03 min^{-1} for gas flow rates changing between 2.5 and 20 L/min. The $K_L a$ values increased with the gas flow rate. It also observed that the slow increase of $K_L a$ values at a high flow rate. This result was due to the bubble coalescence phenomena at high gas flow rate, and thus affected the specific interfacial area and the $K_L a$ coefficient. This was similar to the observation that was reported by others (Gourich *et al.*, 2006; Pjontek *et al.*, 2014).

- **Polyvinyl Chloride (PVC)**

Figure 4.2 presents the variation of overall mass transfer coefficient with gas flow rates obtained in the BC for different amount of PVC.

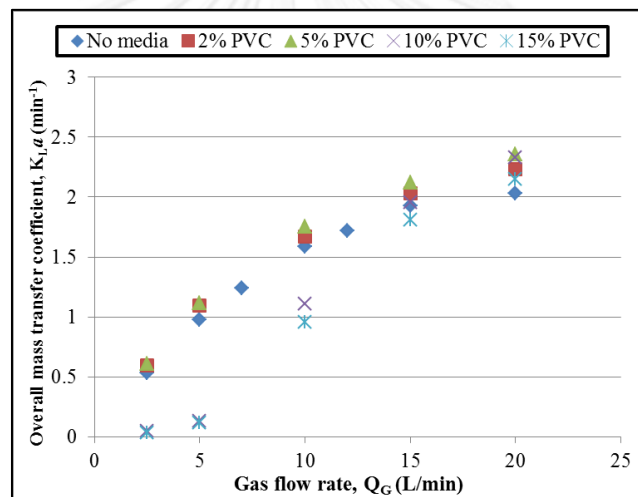


Figure 4.2 Overall mass transfer coefficient versus gas flow rate in BC for different amount of PVC

According to Figure 4.2, it was shown that the $K_L a$ values varied between 0.04 to 2.36 min^{-1} when gas flow rates augmented between 2.5 and 20 L/min. The $K_L a$ values increased with the gas flow rate. The addition of PVC media can modify the $K_L a$ coefficient; therefore, the positive effect can be found in the case of 2–5% of PVC addition. However, it can be stated that the large amount of PVC loadings in the BC (more than 10% of PVC media loadings) can cause the adversely effect on the $K_L a$ values. The highest and lowest $K_L a$ values were observed with the 5% and 15% PVC addition, respectively. This was due to high density of PVC particles, which settled down and located at the bottom of the reactor, blocking or modifying the bubble generation from the diffuser.

- Acrylonitrile Butadiene Styrene (ABS)

Figure 4.3 presents the variation of overall mass transfer coefficient with gas flow rates obtained in the BC for different amount of ABS.

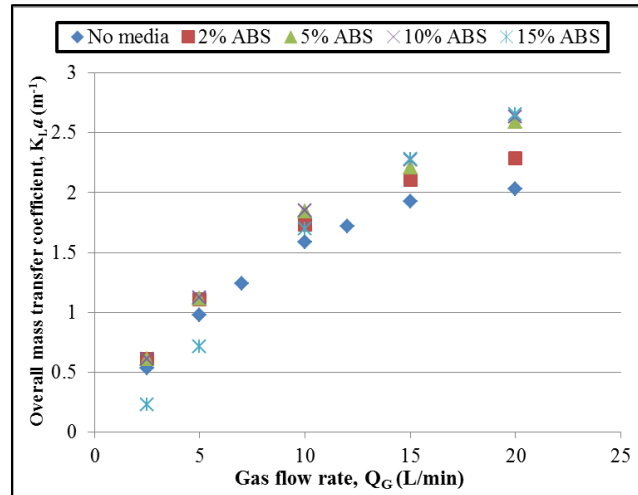


Figure 4.3 Overall mass transfer coefficient versus gas flow rate in BC for different amount of ABS

According to Figure 4.3, the K_La values obtained with BC rose with the gas flow rates. The values of K_La were in range of 0.23 – 2.63 min^{-1} when the gas flow rate varied between 2.5 – 20 L/min. Similar to the case of PVC media, the high ABS loading (15% media loadings) can decrease the values of K_La values. However, the adversely effect of ABS media presence was insignificantly observed in this work compare to the case of PVC media loading. In this regard, the difference of media density ($\rho_{\text{ABS}} = 1050 \text{ kg/m}^3$ and $\rho_{\text{PVC}} = 1380 \text{ kg/m}^3$) and of suspension phenomena occurred in the reactor should be responsible for these results. That is to say fewer amounts of ABS media located at the bottom of the reactor.

In conclusion, the positive effect of ABS and PVC addition (high density media) was not clearly observed in this study. Therefore, the effect of PP media which its density lower than water ($\rho_{\text{PP}} = 946 \text{ kg/m}^3$) will be analyzed in the following section.

- Polypropylene (PP)

Figure 4.4 presents the variation of overall mass transfer coefficient with gas flow rates obtained in the BC for different amount of PP.

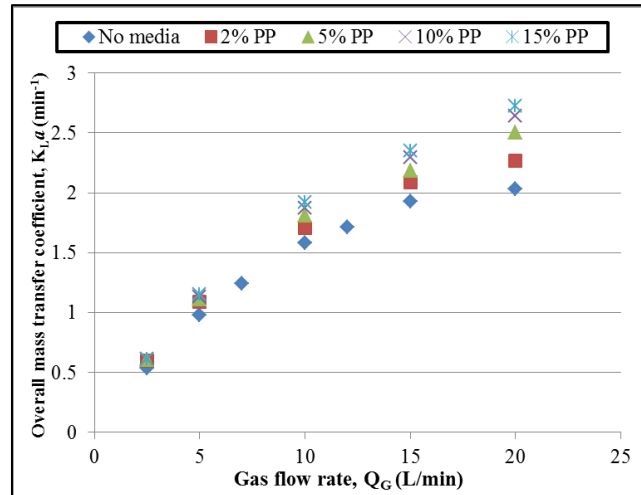


Figure 4.4 Overall mass transfer coefficient versus gas flow rate in BC for different amount of PP

From the Figure 4.4, the $K_L a$ values obtained in BC increased with the gas flow rate. The $K_L a$ values varied between 0.59 to 2.72 min⁻¹ when gas flow rate ranged between 2.5 - 20 L/min. The PP media can be well suspended within the reactor, the enhancement of $K_L a$ coefficients can be thus obtained, in this part, and possibly due to the increase of contact surface between gas and liquid phases.

By considering the effect of PP loading, it can be noted that the increase of PP media presence in the liquid phase can augment the $K_L a$ values obtained in this study. In this regard, the highest $K_L a$ values were found at 15%PP (34% increased). Moreover, the undesirable outcome from the media settled at the bottom of reactor was not observed. As the $K_L a$ coefficient related with the liquid-side mass transfer coefficient (K_L) and the specific interfacial area (a); the bubble size (D_B) and the terminal rising bubble velocity (U_B) are the important factors governing the previous mass transfer parameters. Therefore, it is interesting to continue analyzing on the bubble size and U_B value obtained with different types of media and operating conditions in the next section in order to provide a better understanding on mass transfer mechanism occurred within the reactor.

4.2 Effect of plastic media on bubble hydrodynamic parameter in BC.

Propose of this part was study the effect of plastic media on bubble hydrodynamic parameter in the BC. Bubble diameter (D_B) and terminal rising bubble velocity (U_B) in the BC were analyzed for different types and concentrations of small plastic media particles.

4.2.1 Effect of plastic media on the bubble size in BC.

In this section, the variation of the bubble diameter (D_B) with different plastic media addition (type and amount) and operating conditions (gas flow rates) were studied in the BC. The values of bubble diameter can be obtained by using the Image Treatment Techniques by using the high speed camera (350 images/second). Moreover, the sampling point was located at the middle of the reactor (0.6 m above the bottom). Notably, in order to obtain statistically significant distribution, the average bubble diameter (D_B), presented in this study, was deduced from the measurement of 60-150 bubbles. The Sauter mean bubble diameter (d_{32}) from equation 3.4 was used as the bubble diameter (D_B) in this work.

- **No plastic media**

Figure 4.5 presents the variation of bubble diameter with gas flow rates obtained in the BC.

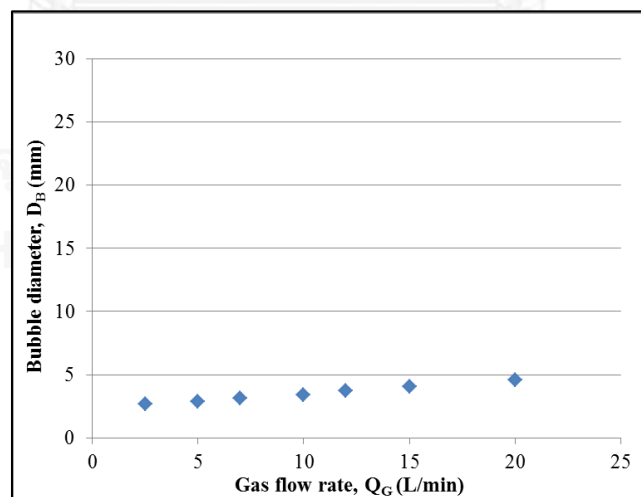


Figure 4.5 Bubble diameter versus gas flow rate in BC

According to Figure 4.5, the bubble diameter obtained in BC were in range from 2.65 to 4.57 mm when gas flow rates changing between 2.5 and 20 L/min. The bubble sizes were slightly increased with the gas flow rate due to the coalescence phenomena of many small bubbles suspended in the reactor. The photographs of bubbles in BC at different gas flow rate were shown in the Figure 4.6.

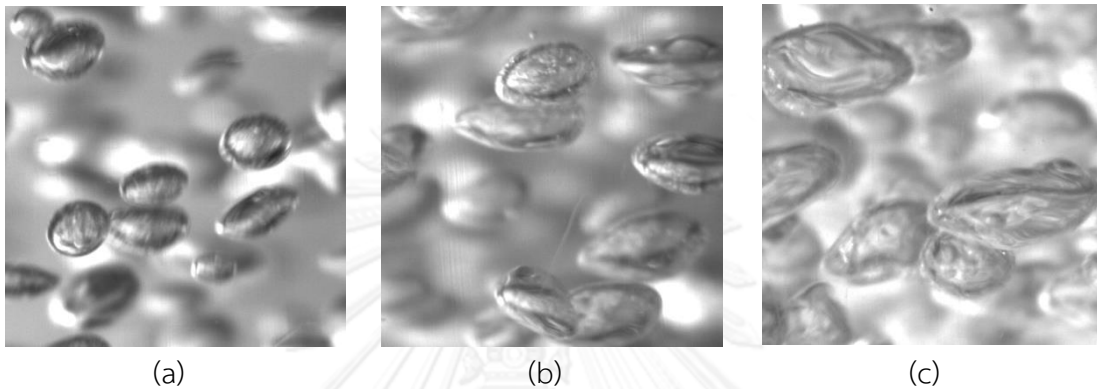


Figure 4.6 Bubble formation photographs in BC at gas flow rate:
(a) 2.5 L/min (b) 5 L/min, and (c) 20 L/min

The bubble size distributions for different gas flow rates were illustrated in the Figure 4.7. It can be seen that equilibrium shapes were observed for all three gas flow rates. Moreover, the peaks obtained at high gas flow rates were wider than those obtained at low gas flow rates. Coalescence and break-up of bubbles play a role for this result. This was similar to the observation reported by others (Hasanen *et al.*, 2006; Polli *et al.*, 2002).

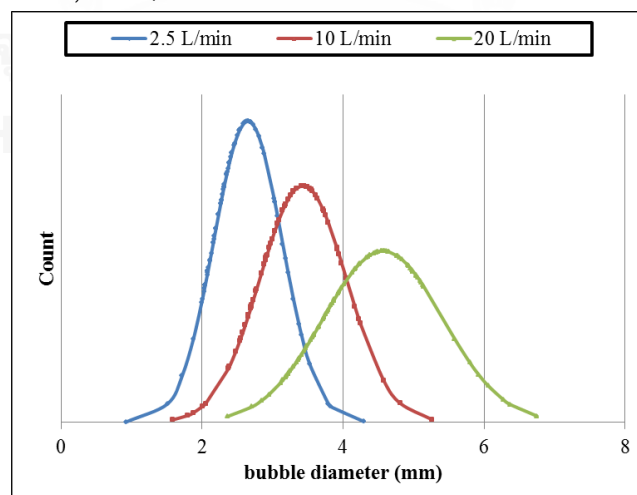


Figure 4.7 Bubble size distribution measured in the BC at different gas flow rate

- Polyvinyl Chloride (PVC)

Figure 4.8 presents the variation of bubble diameter with gas flow rates obtained in the BC for different amount of PVC.

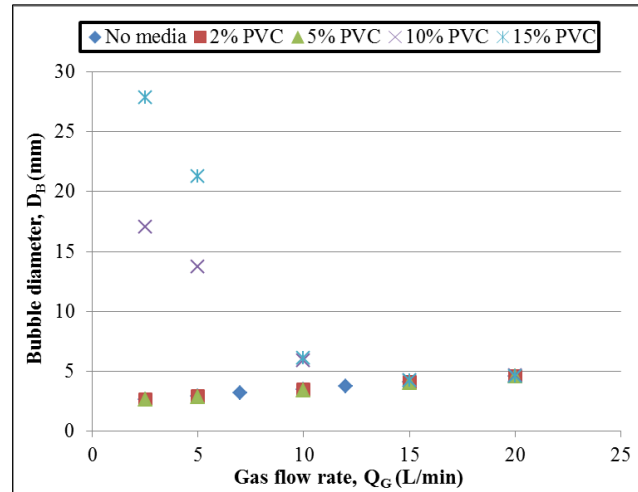


Figure 4.8 Bubble diameter versus gas flow rate in BC for different amount of PVC

According to Figure 4.8, for PVC media loading in the BC, it can be shown that the bubble diameters were obtained at range of 2.64-27.89 mm for gas flow rate changing between 2.5 and 20 L/min. Furthermore, it can be noted that the bubble sizes gained at low media concentration (2-5% PVC loadings) were not significantly changed. Whereas, at high concentration of media (10-15% PVC loadings), the increase of bubble size can be observed. The accumulated of PVC media at the bottom of the reactor can possibly perform as the gas diffuser with large orifice size for generating the bubble as shown in Figure 4.9. It can be observed that the orifice size has been verified by various studies as one of the most factors controlling the bubble size.

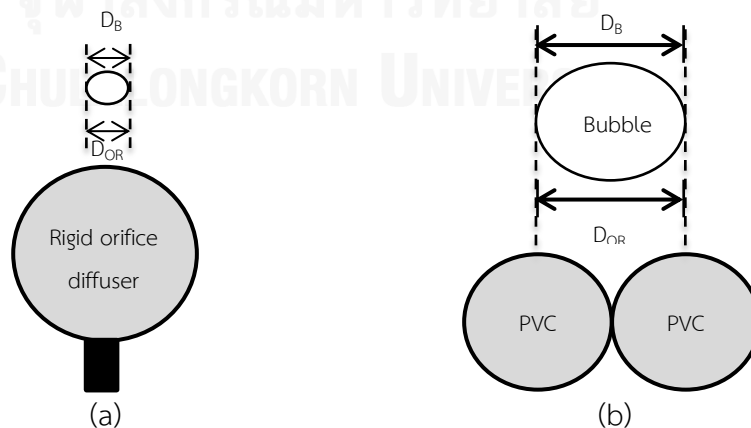


Figure 4.9 Bubble size and bubble generator for:

(a) No media (b) large PVC loadings

- Acrylonitrile Butadiene Styrene (ABS)

Figure 4.10 presents the variation of bubble diameter with gas flow rates obtained in the BC for different amount of ABS.

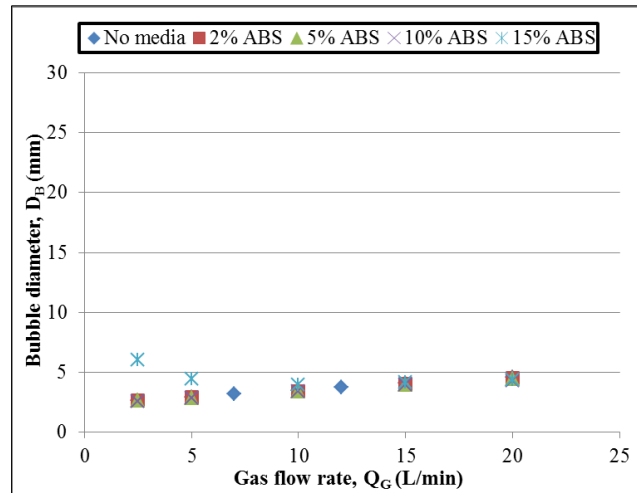


Figure 4.10 Bubble diameter versus gas flow rate in BC for different amount of ABS

As shown in Figure 4.10, the bubble diameter in BC increased from 2.58 to 6.03 mm when gas flow rates augmented between 2.5 and 20 L/min. By considering this Figure, at low ABS media loading in the BC, the values of D_B were closed to those of no media. However, same as case of PVC media loading, at high concentration of media (15% ABS loadings), the increase in bubble size can be observed. As discussed previously, the ABS media can be suspended in tap water, as well as, submerged at the bottom of reactor. Thus, the high amount of ABS loading provides smaller adversely effect on the bubble size compare to the case of PVC media loading. The occurrence of bubbles and plastic media particles (PVC and ABS) in BC was shown in Figure 4.11.

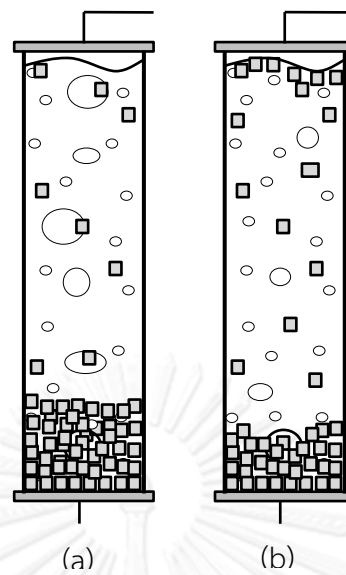


Figure 4.11 Occurrence of bubbles and plastic media particles in BC for:
(a) PVC, and (b) ABS

- **Polypropylene (PP)**

Figure 4.12 presents the variation of bubble diameter with gas flow rates obtained in the BC for different amount of PP.

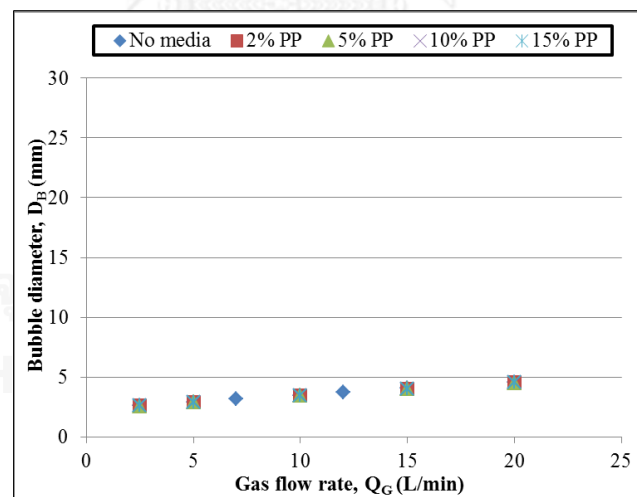


Figure 4.12 Bubble diameter versus gas flow rate in BC for different amount of PP

As shown in Figure 4.12, it can be shown that the bubble diameter obtained with BC for 2-15% PP loading varied between 2.56 and 4.56 mm for gas flow rates changing between 2.5 and 20 L/min. The bubble diameter increased continuously with the gas flow rate. Moreover, it can be observed that the bubble size was not significantly changed compare to those of no media. Simulation of bubbles and PP

media particles occur in the BC shown in the Figure 4.13. It can be noted that the PP media particles were well suspended in liquid phase; therefore, the negative effect from the plastic media located at the bottom of the BC was not observed.

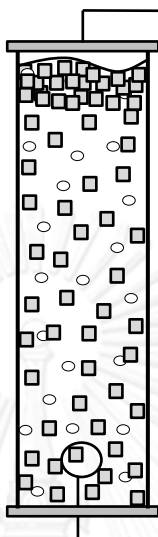


Figure 4.13 Occurrence of bubbles and plastic media particles in BC for PP

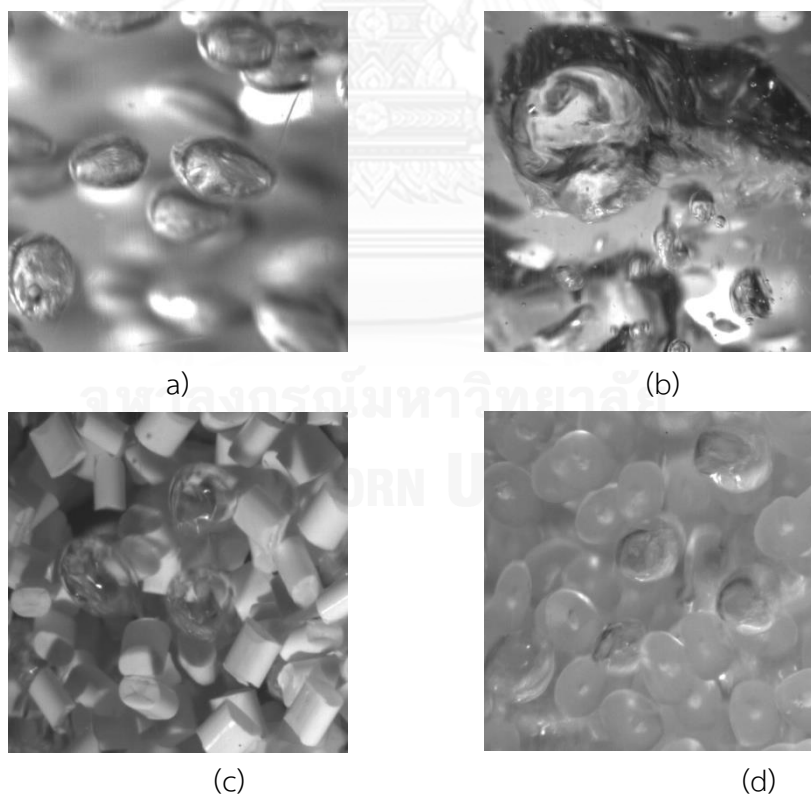


Figure 4.14 Bubble formation photographs in BC at gas flow rate 5 L/min for:

- (a) No plastic media
- (b) 15% PVC loading
- (c) 15% ABS loading, and
- (d) 15% PP loading

In conclusion, for plastic media addition in the BC, the PP media addition did not provide an increase in bubble size as obtained with the case of high amount of PVC and ABS loading. This result can be stated that, due to their lower density than water, the PP particles not accumulate at the bottom of the BC; thus, they did not perform as the large orifice size diffuser. Therefore, the bubble diameter obtained with PP addition was similar to those obtained with no media. The photographs of bubbles for the 15% of plastic media addition in the BC at 5 L/min were showed in Figure 4.14. From the Figure, it proved that the bubble size obtained with 15% of PP media addition was similar to those observed for no media. Furthermore, the largest bubble size was detected in 15% of PVC media loading.

By considering the results from part 4.1 (Figure 4.4), the $K_L a$ values significantly increased with increasing the amount of PP media in the BC. Whereas, from part 4.2 (Figure 4.12), the addition of the PP media not significantly effect on the bubble sizes. Therefore, the increase in $K_L a$ value must due to the change in other parameter. The terminal rising bubble velocity (U_B) is an important parameter that deducted to the specific interfacial area (a), and also to the $K_L a$ values. The decreased in U_B value was due to the increased in specific interfacial area and $K_L a$ values. Therefore, the next section, effect of the three plastic media on U_B values in the BC will be studied.

4.2.2 Effect of plastic media on terminal rising bubble velocity (U_B) in BC.

In this section, the variation of the terminal rising bubble velocity (U_B) with different types (PVC, ABS, PP) and amount of plastic media particles (2, 5, 10, 15 (%v/v)) were studied at different gas flow rate (2.5, 5, 10, 15, 20 L/min) in the BC. As same as the measuring of bubble diameter, the U_B values can be obtained by using the Image Treatment Techniques by using the high speed camera (350 frames/second). The sampling point was located at the middle of the reactor (0.6 m above the bottom of the BC). The 10 rising bubbles were measured. The U_B values were calculated from equation 3.8.

- No plastic media

Figure 4.15 presents the variation of terminal rising bubble velocity with gas flow rates obtained in the BC.

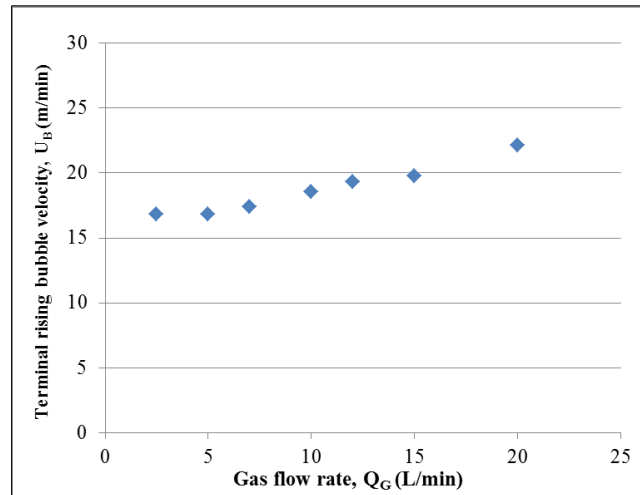


Figure 4.15 Terminal rising bubble velocity versus gas flow rate in BC

Concerning to Figure 4.15, the U_B values obtained in BC for no plastic media addition varied between 16.80 and 22.17 m/min for gas flow rates varying between 2.5 and 20 L/min. From the Figure, it can be noted that the U_B values linearly increased with the gas flow rate.

- Polyvinyl Chloride (PVC)

Figure 4.16 presents the variation of terminal rising bubble velocity with gas flow rates obtained in the BC for different amount of PVC.

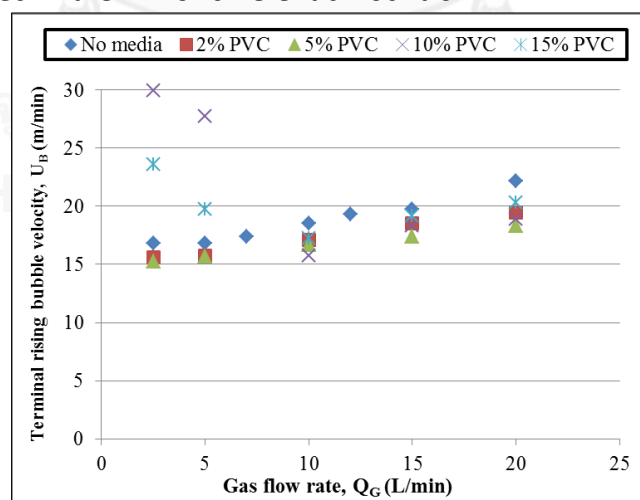


Figure 4.16 Terminal rising bubble velocity versus gas flow rate in BC for different amount of PVC

According to Figure 4.16, the values of U_B obtained experimentally varied between 15.27-29.94 m/min while gas flow rates change between 2.5 - 20 L/min. The lowest and highest U_B values were observed at 5% and 15% of PVC media loading, respectively. Moreover, the results have shown that, at low PVC addition (2-5% of media loading), the U_B values were lower than those obtained with no media. However, for high PVC media loading (10-15% of media loading), at low gas flow rate (2.5-5 L/min), the U_B values were greater than those of no media. These results can be explained that, the suspended PVC particles within the liquid phase decreased the U_B value; however, the increase in bubble size caused an increase in the U_B value.

By considering to the low media addition, the suspended media momentarily hindered the rising-up of bubble as well as increased the flow-path distance of bubble in the reactor, which consequently decreased the vertically rising-bubble distance observed for a time period, caused the decreased in U_B value.

- **Acrylonitrile Butadiene Styrene (ABS)**

Figure 4.17 presents the variation of terminal rising bubble velocity with gas flow rates obtained in the BC for different amount of ABS.

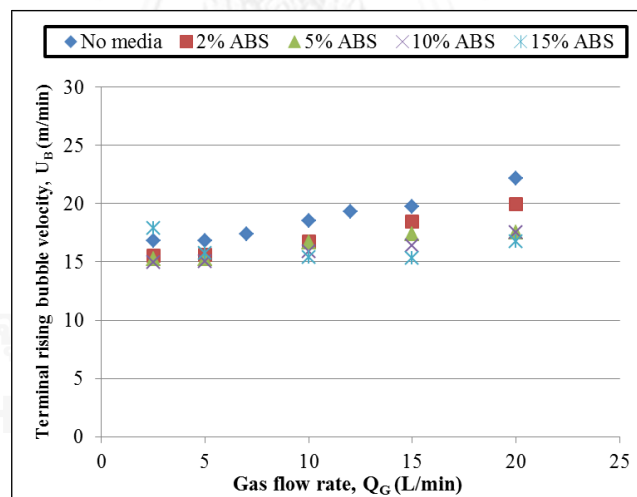


Figure 4.17 Terminal rising bubble velocity versus gas flow rate in BC for different amount of ABS

From the Figure 4.17, the increase of the U_B values were obtained with gas flow rate. The values of the U_B varied between 14.98–17.90 m/min for gas flow rates varying between 2.5 and 20 L/min. From the Figure, it was observed that the addition of low media loading (2-10% of ABS loading) caused the decreased in the U_B values. Whereas for 15% of ABS loading, at low gas flow rate (2.5 L/min), the U_B values were

higher than those obtained with no media: the large size of the bubble obtained at this gas flow rate should be responsible for this result. It can be stated that the U_B values obtained with 15% of ABS loading were lower than those obtained with 15% PVC loading due to the smaller bubble size. Moreover, as the previously describe, it was noticed that the decrease in U_B value is due to the presence of suspended plastic media; therefore, the U_B value obtained with ABS addition was lower than those obtained with PVC addition.

- **Polypropylene (PP)**

Figure 4.18 presents the variation of terminal rising bubble velocity with gas flow rates obtained in the BC for different amount of PP.

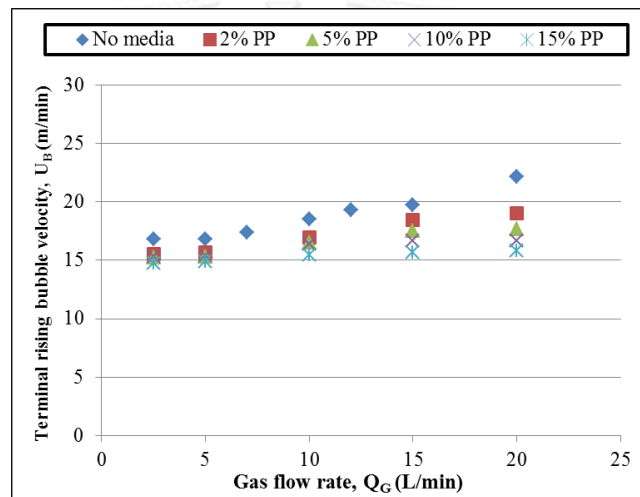


Figure 4.18 Terminal rising bubble velocity versus gas flow rate in BC for different amount of PP

Form the results in Figure 4.18, the U_B values obtained with the BC for 2-15% of PP loading varied between 14.75 and 19.00 m/min for gas flow rates changing between 2.5 and 20 L/min. It may be seen from the Figure that U_B values slightly increase with increasing gas flow rate. Furthermore, the increased in PP media loading decreasing the U_B values especially at high gas flow rate. Therefore, it can conclusion that the addition of PP media provided the decreased in U_B values, which related to the increased in the specific interfacial area and also the $K_L a$ values.

In conclusion, the addition of media in the BC were significantly reduced the values of terminal rising bubble velocity (U_B), which deducted to an increase in values of specific inter facial area (a). Therefore, the next section, the effect of plastic media on the specific interfacial area obtained in the BC was investigated.

4.2.3 Effect of plastic media on the specific interfacial area (a) in BC.

In this section, the interfacial area, which calculated from the bubble size, bubble formation frequency and their rising velocity as previously described in equation 3.5, were presented.

- **No plastic media**

Figure 4.19 presents the variation of specific interfacial area with gas flow rates obtained in the BC.

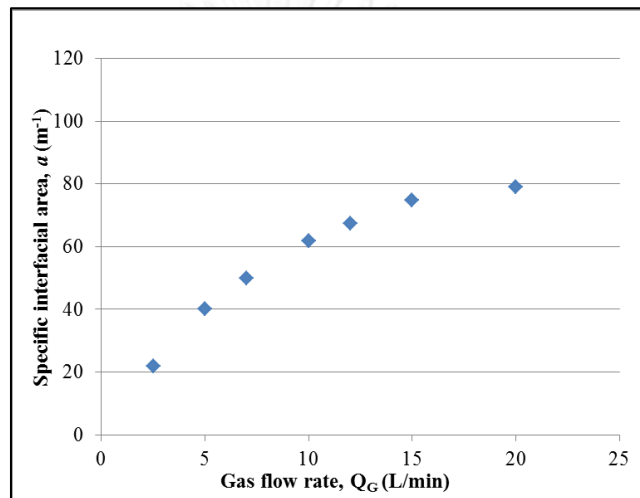


Figure 4.19 Specific interfacial area versus gas flow rate in BC

From Figure 4.19, the specific interfacial area increase with the gas flow rates. These values varied between 21.90 and 79.09 m^{-1} for gas flow rates varying between 2.5 and 20 mL/s: the specific interfacial area obtained with high gas flow rate was greater than low gas flow rate. Moreover, it can be note that the slow increase of the specific interfacial area was observed at high gas flow rate due to the bubble coalescence phenomena in the reactor.

- **Polyvinyl Chloride (PVC)**

Figure 4.20 presents the variation of specific interfacial area with gas flow rates obtained in the BC for different amount of PVC.

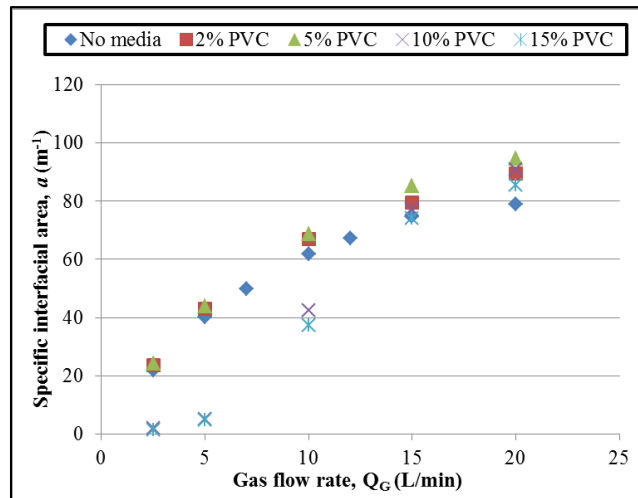


Figure 4.20 Specific interfacial area versus gas flow rate in BC for different amount of PVC

By considering the Figure 4.20, it can be shown that the specific interfacial area values were increased with the gas flow rate. The specific interfacial area obtained in the BC varied between 1.49-94.8 m^{-1} for the gas flow rate varied between 2.5 to 20 L/min. The addition of low amount of PVC media (2-5 % of plastic media) enhanced the specific interfacial area. Whereas, for high amount of PVC media (more than 10% of plastic media), the values of specific interfacial area were decreased especially at the low gas flow rate (2.5-5 L/min). The large bubble diameters obtained should be responsible for these results.

- **Acrylonitrile Butadiene Styrene (ABS)**

Figure 4.21 presents the variation of specific interfacial area with gas flow rates obtained in the BC for different amount of ABS.

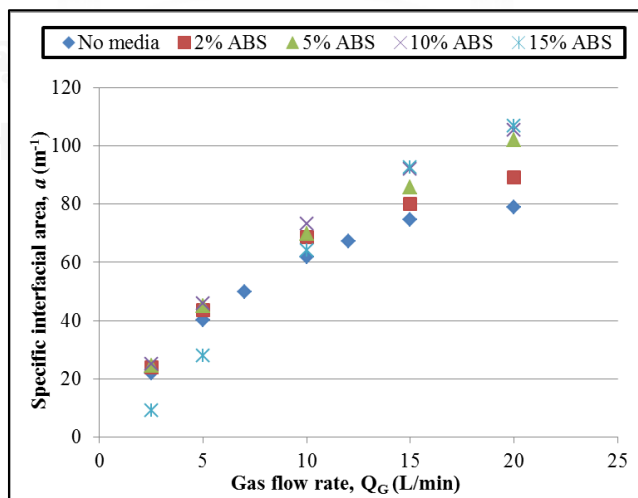


Figure 4.21 Specific interfacial area versus gas flow rate in BC for different amount of ABS

Form the results in Figure 4.21, the specific interfacial area values obtained with the BC for 2-15% of ABS loading varied between 9.04 and 107.07 m^{-1} for gas flow rates changing between 2.5 and 20 L/min. It may be seen from the Figure that the specific interfacial area increased with increasing gas flow rate. Considering the 15% ABS loading at low gas flow rate (2.5-5 L/min), the values of specific interfacial area were lower than those obtained with no media due to the bubble size.

- **Polypropylene (PP)**

Figure 4.22 presents the variation of specific interfacial area with gas flow rates obtained in the BC for different amount of PP.

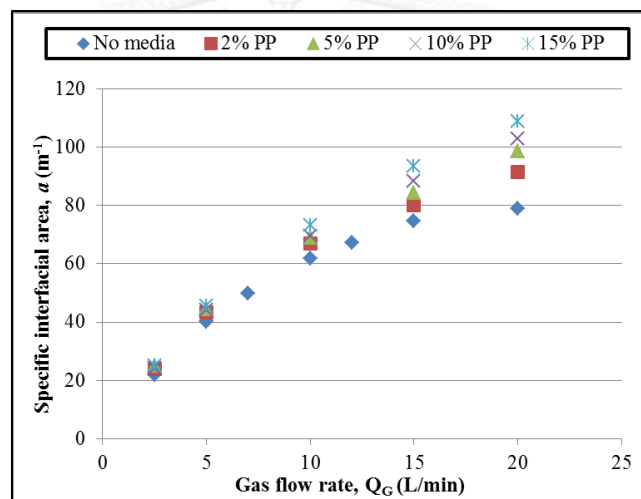


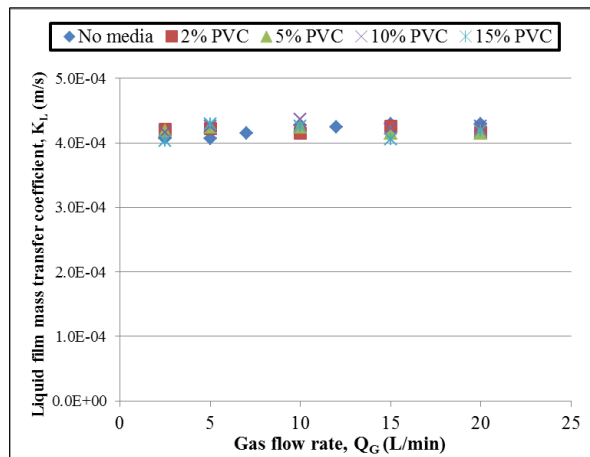
Figure 4.22 Specific interfacial area versus gas flow rate in BC for different amount of PP

From the Figure 4.22, the specific interfacial area obtained in the BC increased with the gas flow rate. The specific interfacial area values varied between 23.78 to 108.96 m^{-1} when gas flow rate ranged between 2.5 - 20 L/min. As discussed previously, the PP media can be well suspended within the reactor and reduced the U_B values in the reactor, therefore; the enhancement of specific interfacial area can be thus obtained.

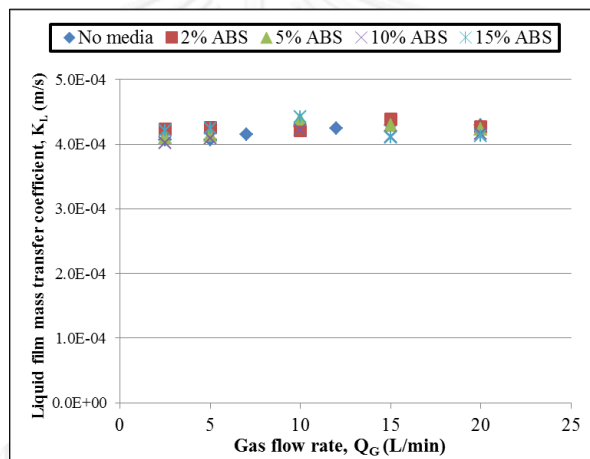
4.2.4 Study the liquid film mass transfer coefficient (K_L) in tap water.

The liquid film mass transfer coefficient or K_L is a mass transfer parameter. It was calculated from the values of $K_L a$ divided by the specific interfacial area as shown in the equation 3.3.

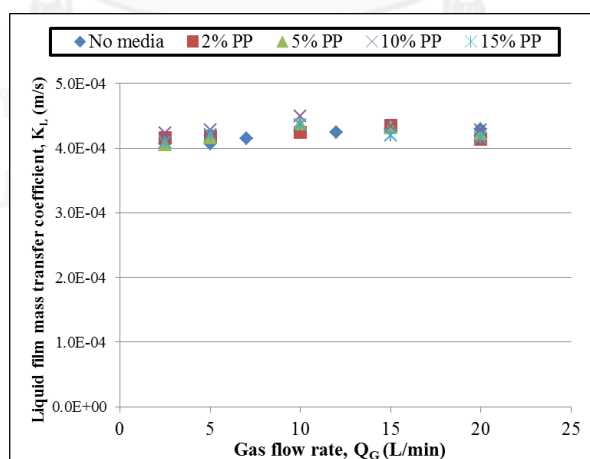
Figure 4.23 presents the variation of liquid film mass transfer coefficient with gas flow rates obtained in the BC for different amount of plastic media.



(a)



(b)



(c)

Figure 4.23 Liquid film mass transfer coefficient versus gas flow rate in BC for different types of plastic media: (a) PVC, (b) ABS, and (c) PP

From the results in Figure 4.23, whatever the gas flow rate applied in this work, the values of K_L were not significantly changed. Moreover, it can be stated that the K_L coefficients were in range of 4.02×10^{-4} to 4.49×10^{-4} in the BC. This is coincided with results obtained by Sardeing *et al.* (2006). The literature has shown that the K_L values obtained with Higbie's equation were close to those obtained with tap water (90%) at bubble diameters for $D_B < 6$ mm. The appropriate model for predicted the K_L values should be proposed.

$$K_L = 2 \sqrt{\frac{D_{O_2} U_B}{\pi D_B}}$$

For the same liquid phase, the increase on $K_L a$ must be primarily conformed to an increase in specific interfacial area, which related to the decrease in the U_B values as shown in previously studied.

From the part 4.1 and 4.2, it can be conclusion that the addition of plastic media can provide the increase in mass transfer rate in the BC. However, the adversely affect due to the high concentration of plastic particles located, and modifying the bubble size from the diffuser was observed. An internal loop airlift reactor (ILALR) was an interested reactor to increase the $K_L a$ values due to the increase in liquid-gas contact time. Moreover, the liquid and gas recirculation in the reactor may be able to increase the suspension of plastic media and also reduce their accumulation at the bottom of the reactor. Therefore, the effect of plastic media on oxygen mass transfer and bubble hydrodynamic parameters in an ILALR will be analyzed in the next part.

4.3 Study the oxygen mass transfer and bubble hydrodynamic parameters in ILALR.

The aim of this part was study the oxygen mass transfer and bubble hydrodynamic parameters in ILALR. The overall mass transfer coefficient, bubble diameter, and terminal rising bubble velocity were observed at different gas flow rates. The methods for analyzed the values of these parameters were the same as in the BC.

4.3.1 Overall mass transfer coefficient ($K_L a$) in ILALR.

Figure 4.24 presents the variation of overall mass transfer coefficient with gas flow rates obtained in the BC (No media, and best type and concentration of plastic media) and ILALR.

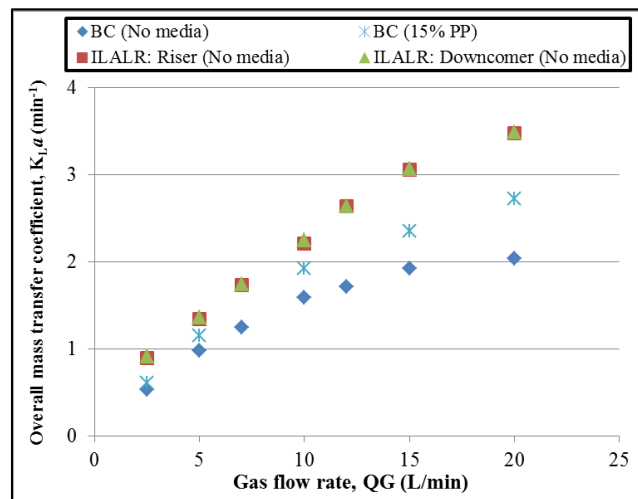


Figure 4.24 Overall mass transfer coefficient versus gas flow rate in BC and ILALR

From Figure 4.24, for all causes, it can be noted that the $K_L a$ values were increased with the gas flow rate. Concerning to the ILALR, the $K_L a$ values obtained in the riser zone were closed to those obtained in the down-comer zone: the variation of the $K_L a$ values varied between $0.89\text{-}3.47 \text{ min}^{-1}$ and $0.91\text{-}3.48 \text{ min}^{-1}$ for the riser zone and the down-comer zone, respectively. Furthermore, the highest $K_L a$ values obtained with ILALR were found at gas flow rate 20 L/min: 71% and 37% increased compare to the BC (No media), and the best type and concentration of plastic media in the BC (15% PP), respectively. The liquid and bubble recirculation in ILALR should be responsible for these results. Thus, the increase in the $K_L a$ values may be due to the increase in bubble-liquid contact time. The bubbles recirculation in BC and ILALR were shown in Figure 4.25.

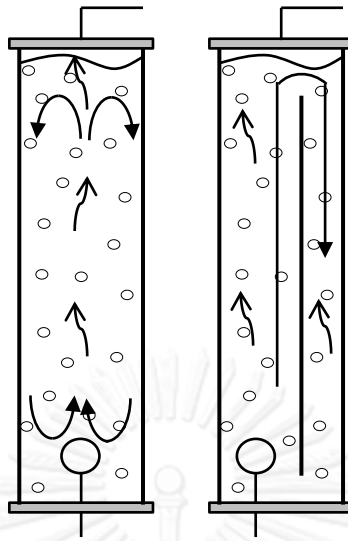


Figure 4.25 Liquid and bubbles recirculation in BC and ILALR

For the next section, the bubble sizes obtained in the riser zone and the down-comer zone of the ILALR were determined at different gas flow rates for providing a better understanding on mass transfer mechanism.

4.3.2 Bubble size in ILALR.

Figure 4.26 presents the variation of bubble diameter with gas flow rates obtained in the BC and ILALR.

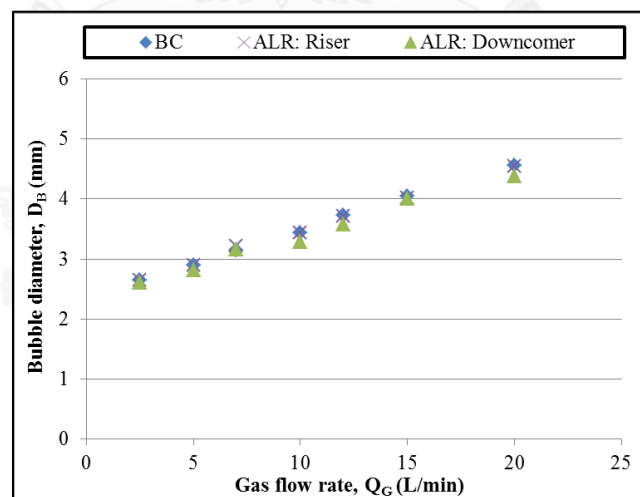


Figure 4.26 Bubble diameter versus gas flow rate in BC and ILALR

According to Figure 4.26, the bubble diameter in the BC increased from 2.65 to 4.57 mm when gas flow rates augmented between 2.5 and 20 L/min. For ILALR, at the same range of the gas flow rates, it can be found that the range of bubble sizes

are 2.62 - 4.39 mm for the riser zone, and 2.66 - 2.48 mm for the down-comer zone. Moreover, the bubble sizes from both reactors were closed and linearly increased with the gas flow rate. The photographs of bubbles in ILALR at different gas flow rate were shown in the Figure 4.27. The similar diffuser used in this work should control the average bubble size. This result proved that the difference of $K_L a$ values obtained with BC and ILALR not depended on the change in bubble size. Therefore, the next section, the terminal rising bubble velocities were analyzed in both side of the ILALR for different gas flow rates.

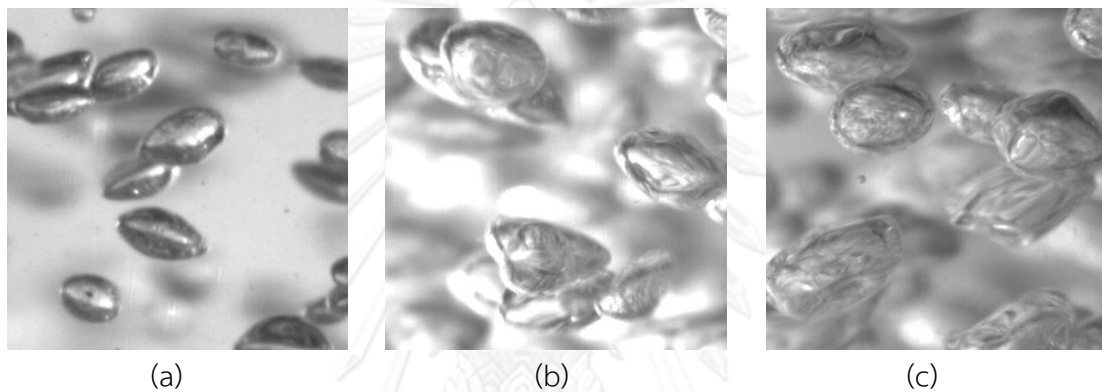


Figure 4.27 Bubble formation photographs in ILALR at gas flow rate:
(a) 2.5 L/min (b) 5 L/min, and (c) 20 L/min

4.3.3 Terminal rising bubble velocity (U_B) in ILALR.

Figure 4.28 presents the variation of terminal rising bubble velocity with gas flow rates obtained in the BC and ILALR.

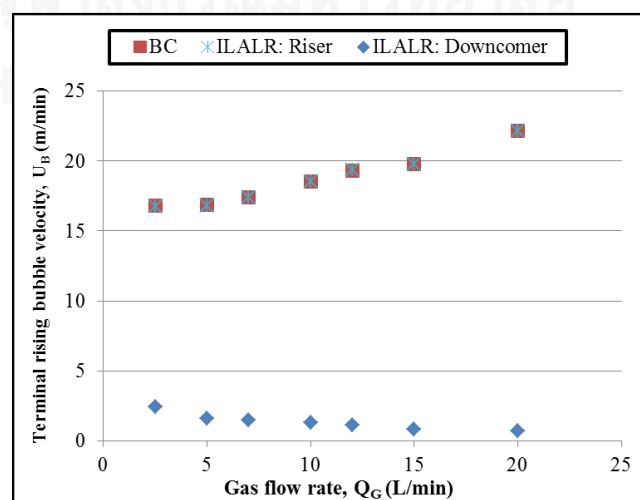


Figure 4.28 Terminal rising bubble velocity versus gas flow rate in ILALR

According to Figure 4.28, for the riser zone, it was shown that the U_B values varied between 16.75 to 22.18 m/min for riser zone, whereas, for the down-comer zone, the U_B values varied between 2.42 to 0.70 m/min, when gas flow rates changing between 2.5 and 20 L/min. The U_B values obtained with the riser zone increased with the gas flow rate. Moreover, the U_B values obtain in the riser zone of ILALR were closed to those obtain in BC. For the down-comer zone of the reactor, the values of the U_B decreased with the gas flow rate. It can be noted that the liquid recirculated from the riser zone reduced the rising of bubble in the down-comer zone. The rising bubbles in down-comer zone of ILALR at different gas flow rates were shown in the Figure 4.29. Note that, the low values of the U_B in the down-comer zone caused an increase in the bubble-liquid contact time in the reactor.

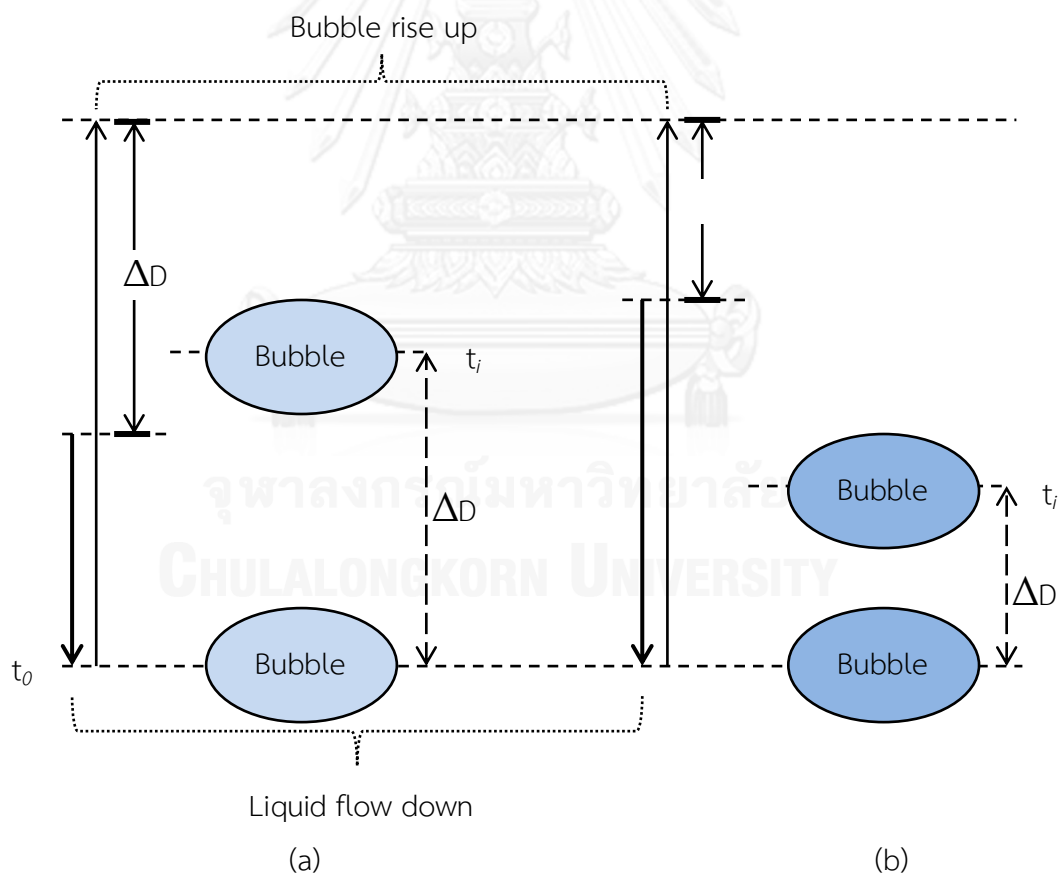


Figure 4.29 Rising bubble in down-comer zone of ILALR at:
(a) low gas flow rate (b) high gas flow rate

4.3.4 Specific interfacial area (a) in ILALR.

The specific interfacial area in the ILALR can divide into two parts: Riser zone and down-comer zone. For the riser zone, the specific interfacial area was calculated by equation 3.5, which was the same as case of BC. However, the cross-sectional area (A) of reactor was changed to the cross-sectional area of the riser zone. And for the down-comer zone, the specific interfacial area was calculated by the overall mass transfer coefficient divide by the liquid film mass transfer coefficient, which was shown in equation 3.7.

Figure 4.30 presents the specific interfacial area with gas flow rates obtained in the BC and ILALR.

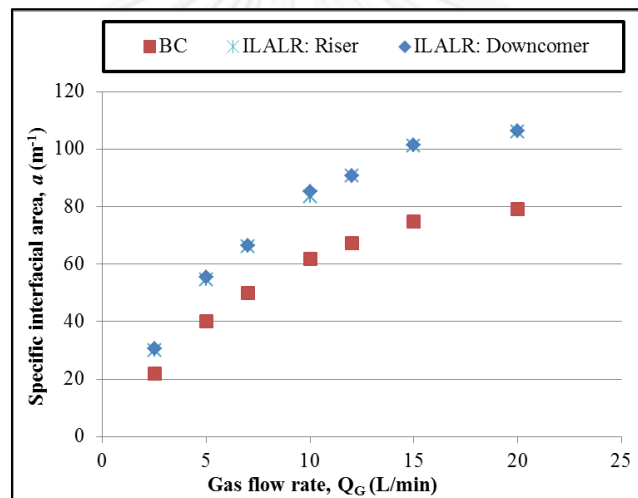


Figure 4.30 Specific interfacial area versus gas flow rate in BC and ILALR

As shown in Figure 4.30, it can be shown that the values of specific interfacial area obtained with BC and ILALR. For ILALR, at gas flow rates changing between 2.5 and 20 L/min, the specific interfacial area varied between 30.01-106.10 m^{-1} , and 33.78-128.89 m^{-1} obtained in the riser zone and the down-comer zone, respectively. The specific interfacial area increased with the gas flow rate. It should be observed that the slow increase of the specific interfacial area at a high flow rate. This result was due to the bubble coalescence phenomena at high gas flow rate, and thus affected the specific interfacial area.

From the Figure 4.29, it can be noted that the liquid flow from the riser zone into the down-comer zone affected to the U_B value. In the down-comer zone, the high liquid flow down can reduced the U_B value. Therefore, the gas flow rate in the down-comer zone was analyzed in the next section in order to prove this explanation.

4.3.5 Effect of plastic media on the gas flow rate in down-comer zone (Q_G) of ILALR

The gas flow rate in down-comer zone (Q_G) of the ILALR was calculated by the equation 3.9 as shown below. Note that the cross-sectional area (A) and the specific interfacial area (a) used are obtained with the down-comer zone of ILALR.

$$Q_G = f_B \times V_B = a \times \frac{U_B}{H_L} \times \frac{AH_L + N_B V_B}{\pi D_B^2} \times V_B$$

Figure 4.31 presents the variation of gas flow rate (Down-comer zone) with gas flow rates (Riser zone) obtained in the ILALR.

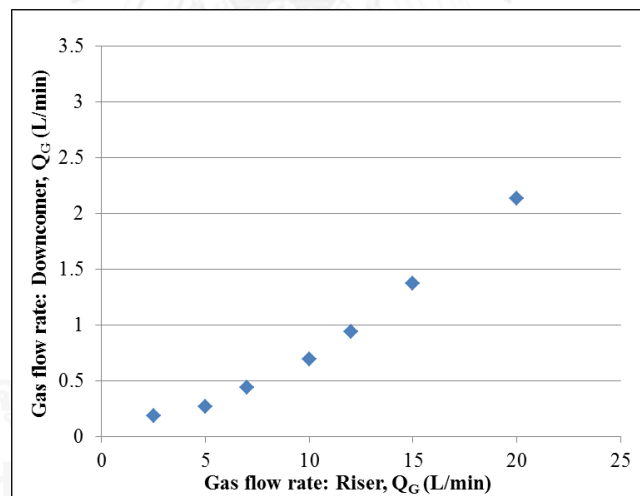


Figure 4.31 Gas flow rate (Down-comer zone) versus gas flow rate (Riser zone) in ILALR

From Figure 4.31, the gas flow rates obtained in the down-comer zone in ILALR were in range of 0.18-2.13 L/min while the gas flow rate applied to the riser zone of the reactor varying between 2.5 and 20 L/min. It can be seen that the gas flow rates (Down-comer zone) were continuously increased with the gas flow rate (Riser zone). Noted that the ratio of Q_G (Down-comer zone) to Q_G (Riser zone) were in

range of 0.054-1.01; it seems slowly increased with gas flow rate applied. It can be noted that, at high gas flow rate, the high amount of bubble and liquid circulated from the riser zone to the down-comer zone was significantly increased. The Figure 4.32 showed the gas flow rate (Down-comer zone and riser zone) of the ILALR.

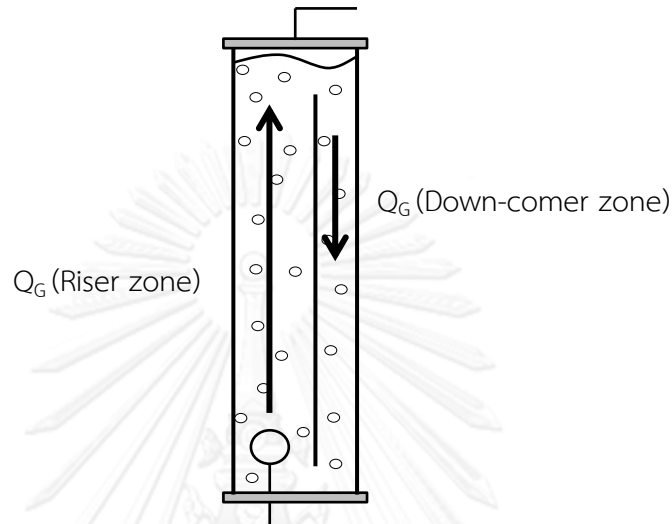


Figure 4.32 Gas flow rate (Down-comer zone and riser zone) of ILALR

For the next part, the plastic media were added into the ILALR in order to increase the bubble-liquid contact time between gas and liquid phases. The effect of plastic media on oxygen mass transfer and bubble hydrodynamic and mass transfer parameters will be explored in ILALR.

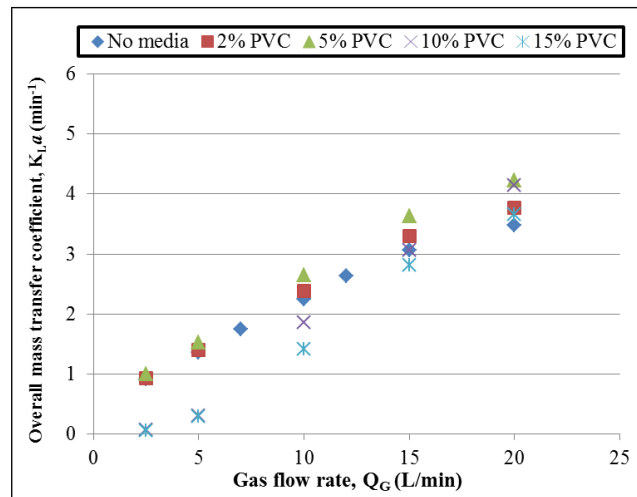
4.4 Effect of plastic media on oxygen mass transfer and bubble hydrodynamic parameters in ILALR.

The objective of this part was to study the impact of different types and amounts of plastic media on oxygen mass transfer and bubble hydrodynamic parameters in ILALR. The overall mass transfer coefficient, bubble diameter, and terminal rising bubble velocity were observed at different gas flow rates. The methods for analyzed the values of these three parameters were the same as in the BC.

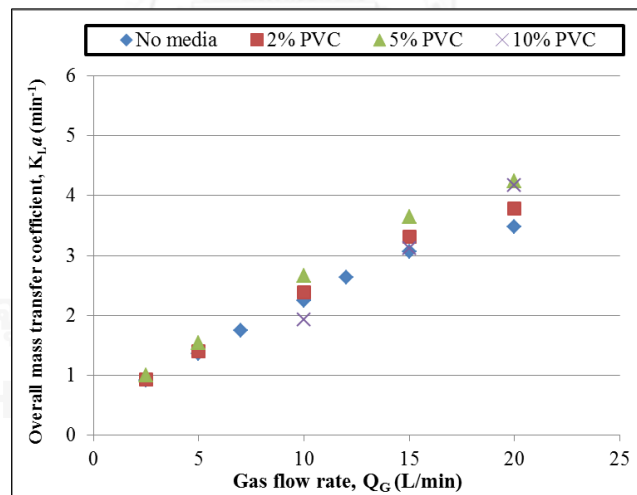
4.4.1 Effect of plastic media on the overall mass transfer coefficient ($K_L a$) in ILALR

- Polyvinyl Chloride (PVC)

Figure 4.33 presents the variation of overall mass transfer coefficient with gas flow rates obtained in the ILALR for different amount of PVC.



(a)



(b)

Figure 4.33 Overall mass transfer coefficient versus gas flow rate in ILALR for different amount of PVC: (a) Riser zone, (b) Down-comer zone

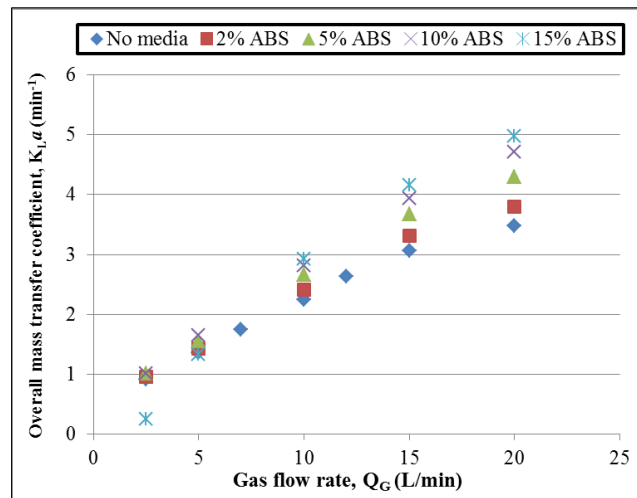
From the Figure 4.33, it can be shown that the K_La values observed in the riser zone (a) were close to those observed in the down-comer zone (b). The K_La values increased with the gas flow rate.

According to Figure riser zone, it was shown that the K_La values varied between 0.057 to 4.23 min^{-1} when gas flow rates augmented between 2.5 and 20 L/min. Same as the case of BC, the positive effect can be found in the case of 2–5% of PVC addition. Whereas, the addition of 10-15% PVC media provided the negative effect due to the accumulation of PVC particles at the bottom of the reactor, increased the bubble size in the reactor. It can be noted that the adverse effects obtained in ILALR were lower than those obtained in BC due to the liquid and bubble recirculation in the ILALR increased the suspension of PVC particles, and decrease the PVC particles at the bottom of the reactor.

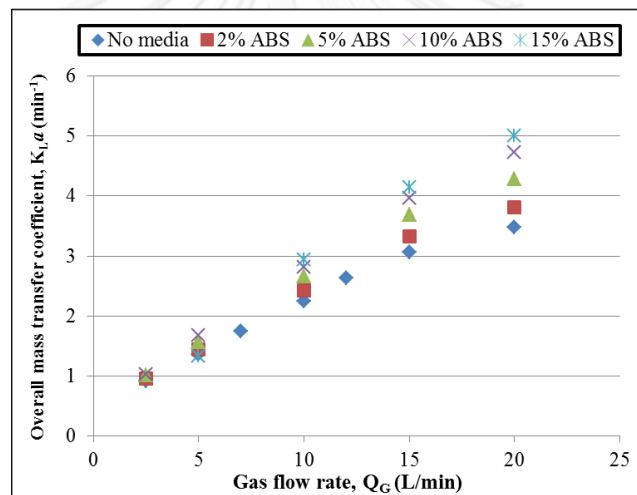
For the down-comer zone, the K_La values varied between 1.92 to 4.25 min^{-1} when gas flow rates changing between 2.5 and 20 L/min. However, for 15% of PVC addition, it can be noted that the K_La values at low gas flow rate (2-5 L/min) cannot be measured because the dissolve oxygen not continuously increased with time at the down-comer zone. This can be noted that the PVC particles at the bottom of the reactor hindrance of bubbles fluid.

- **Acrylonitrile Butadiene Styrene (ABS)**

Figure 4.34 presents the variation of overall mass transfer coefficient with gas flow rates obtained in the ILALR for different amount of ABS.



(a)



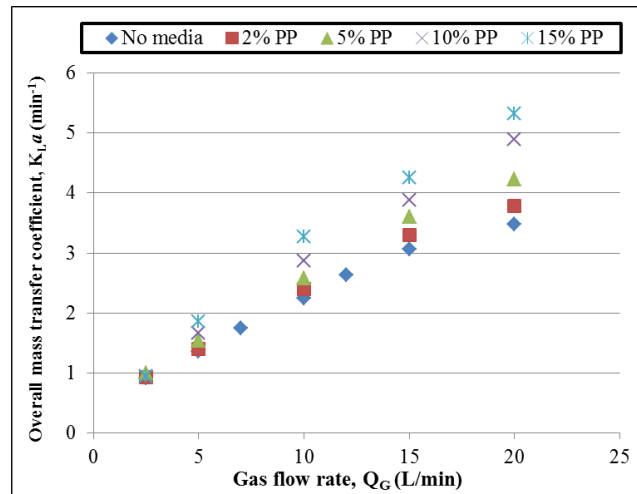
(b)

Figure 4.34 Overall mass transfer coefficient versus gas flow rate in ILALR for different amount of ABS: (a) Riser zone, (b) Down-comer zone

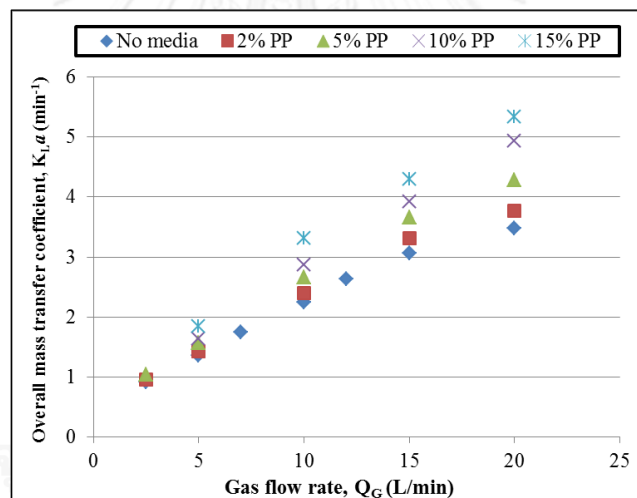
According to the Figure 4.34, the $K_L a$ coefficient obtained in both zone of the ILALR (Riser and down-comer zone) provided same trendline and increased with the gas flow rate. The variation of $K_L a$ coefficients obtained in the riser zone and down-comer zone of the reactor ranged between $0.24\text{--}4.98\text{ min}^{-1}$ and $0.96\text{--}5.01\text{ min}^{-1}$, respectively. Same as case of the BC, for 2-10% of ABS media addition, the positive effect can be found. Whereas, at low gas flow rate (2.5-5 L/min), the $K_L a$ coefficient obtained with 15% ABS loading were lower than those obtained with no media. Furthermore, for the Figure 4.31 (b), it can be shown that the $K_L a$ values at low gas flow rate (2.5 L/min) cannot be measured because the plastic particles at the bottom of the reactor hindrance of bubbles fluid.

- Polypropylene (PP)

Figure 4.35 presents the variation of overall mass transfer coefficient with gas flow rates obtained in the ILALR for different amount of PP.



(a)



(b)

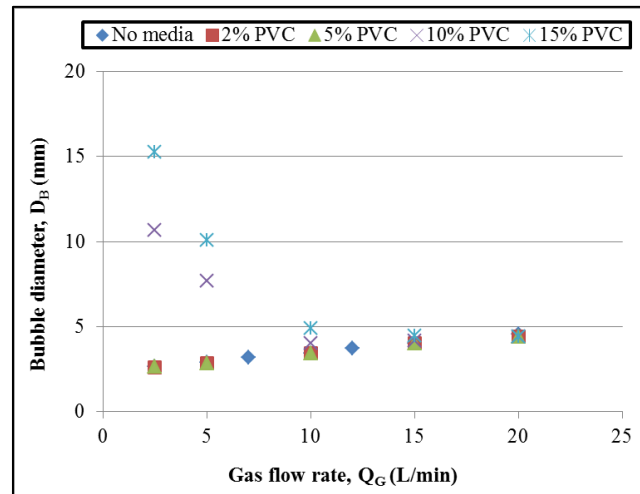
Figure 4.35 Overall mass transfer coefficient versus gas flow rate in ILALR for different amount of PP: (a) Riser zone, (b) Down-comer zone

According to Figure 4.35, the $K_L a$ values obtained with ILALR rose with the gas flow rates. When the gas flow rate varied between 2.5 – 20 L/min, the values of $K_L a$ coefficient were in range of 0.93 – 5.33 min^{-1} and 0.95-5.34 min^{-1} for the riser zone and the down-comer zone of the ILALR, respectively. The $K_L a$ coefficient obtained from both zones of the reactor were closed. The highest $K_L a$ value was obtained with 15% of plastic media loading (53% increased).

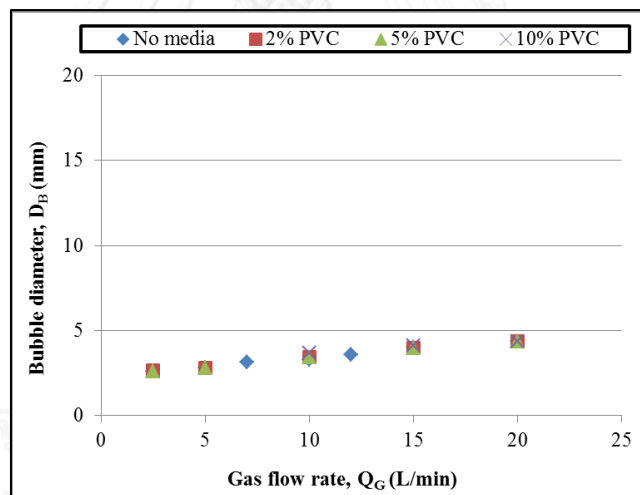
4.4.2 Effect of plastic media on bubble size parameter in ILALR.

- Polyvinyl Chloride (PVC)

Figure 4.36 presents the variation of bubble diameter with gas flow rates obtained in the ILALR for different amount of PVC.



(a)



(b)

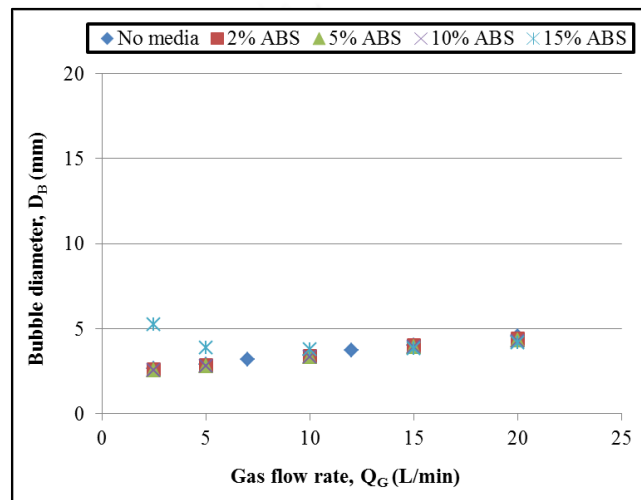
Figure 4.36 Bubble diameter versus gas flow rate in ILALR for different amount of PVC: (a) Riser zone, (b) Down-comer zone

Figure 4.36 (a) shows that the addition of low concentration of PVC (2-5% of plastic media loading) not has significant effect on the bubble size, whereas the high addition of PVC (10-15% of plastic media loading) caused an increase in bubble size. Same as the case of BC, the PVC particles which located at the bottom of the reactor caused an increase in bubble size. Moreover, the values of bubble size obtained with BC were larger than those obtained with ILALR.

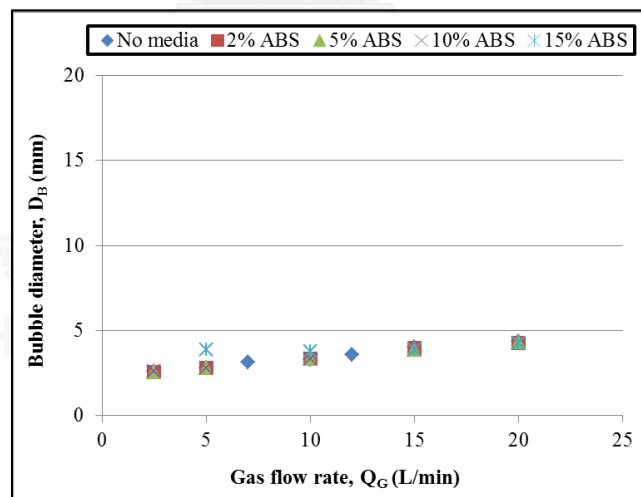
From the Figure 4.36 (b), for all cases, the bubble sizes were no significantly changed. Furthermore, it can be noted that, for 15% of PVC at low gas flow rates (2.5-7 L/min), the bubble cannot be observed. This result can be explained that the large size of bubble trend to not circulated from the riser zone to the down-comer zone.

- **Acrylonitrile Butadiene Styrene (ABS)**

Figure 4.37 presents the variation of bubble diameter with gas flow rates obtained in the ILALR for different amount of ABS.



(a)



(b)

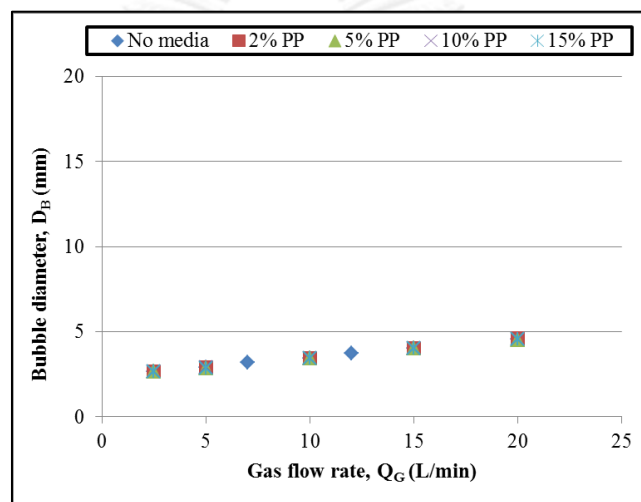
Figure 4.37 Bubble diameter versus gas flow rate in ILALR for different amount of ABS: (a) Riser zone, (b) Down-comer zone

According to Figure 4.37, for ABS media loading in the ILALR, it can be shown that the bubble diameters were obtained at range of 2.58-5.26 mm and 2.59-4.39

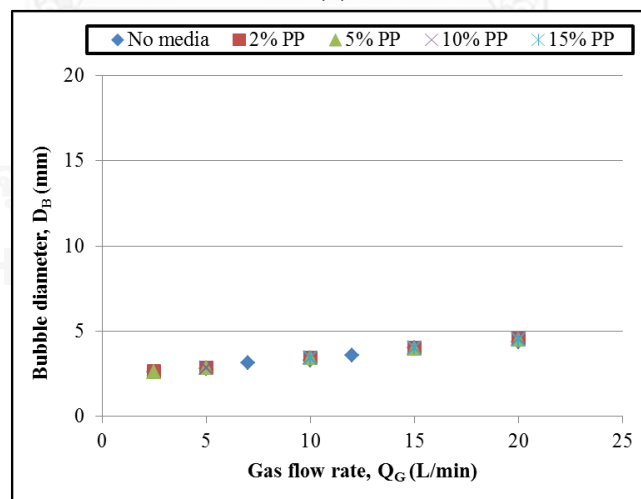
mm for the riser zone and the down-comer zone, respectively. Furthermore, it can be noted that the bubble sizes gained at low media concentration (2-10% ABS loadings) were not significantly changed. Whereas, at high concentration of media (15% ABS loadings), the increase of bubble size can be observed at low gas flow rate (2.5-10 L/min). However, the values of bubble size obtained with BC for 15% ABS loading were larger than those obtained with ILALR.

- Polypropylene (PP)

Figure 4.38 presents the variation of bubble diameter with gas flow rates obtained in the ILALR for different amount of PP.



(a)



(b)

Figure 4.38 Bubble diameter versus gas flow rate in ILALR for different amount of PP: (a) Riser zone, (b) Down-comer zone

According to the Figure 4.38, the bubble sizes obtained in the riser zone and the down-comer zone increased with the gas flow rate. The bubble diameters obtained at gas flow rate ranged between 2.5 - 20 L/min varied between 2.64-4.59 mm and 2.61-4.56 mm for the riser zone and the down-comer zone, respectively. The same trendline of the bubble sizes gained from both zone of the reactor were observed. However, for 15% of PP loading at low gas flow rate (2.5 L/min), the bubble cannot recirculate from the riser zone to the down-comer zone.

In conclusion, the addition of PP particles performed better than the addition of PVC and ABS. Due to their lower density than water, it can be noted that the PP particles not accumulate at the bottom of reactors; thus, they did not perform as the large orifice size diffuser. The photographs of bubbles for the plastic media loadings were showed in Figure 4.39. It demonstrated that for 15% PP loading was similar to those observed for no media. Meanwhile, the largest was detected in PVC loading.

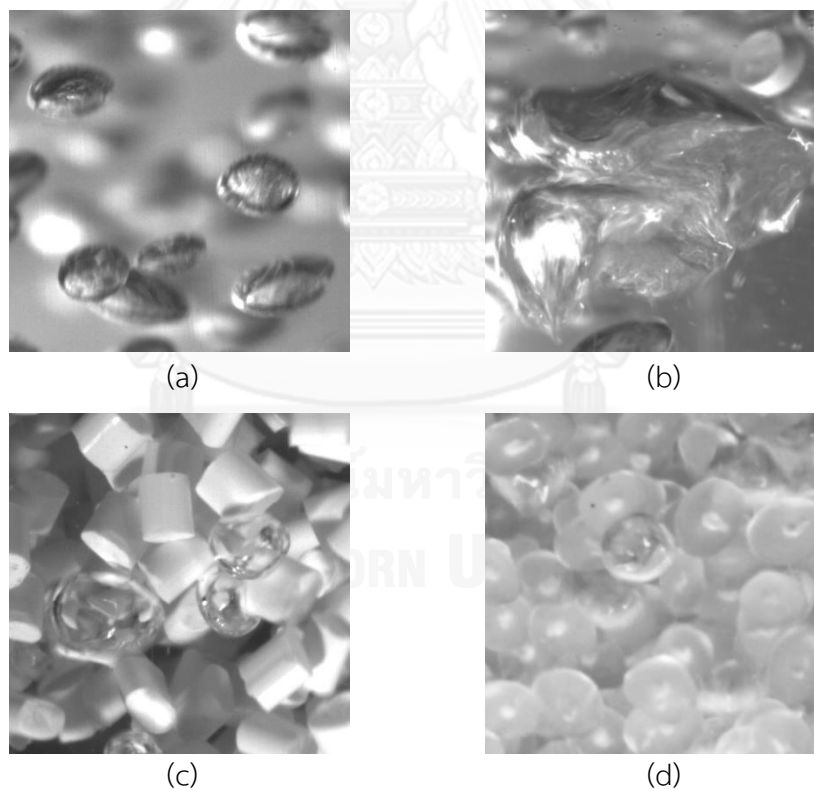
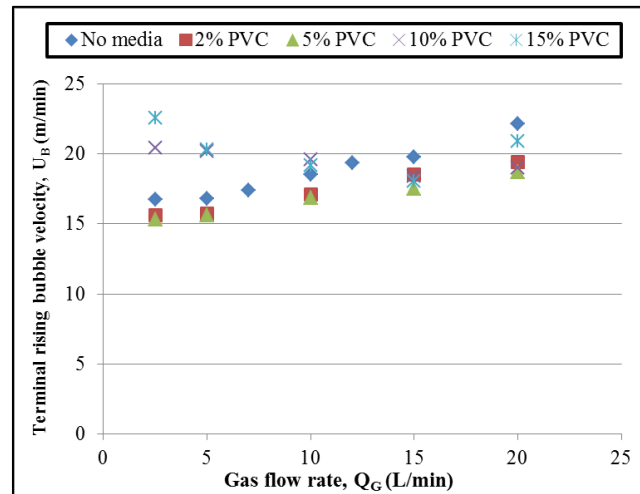


Figure 4.39 Bubble formation photographs in ILALR (Riser zone) at gas flow rate 5 L/min for: (a) No plastic media (b) 15% PVC loading (c) 15% ABS loading, and (d) 15% PP loading

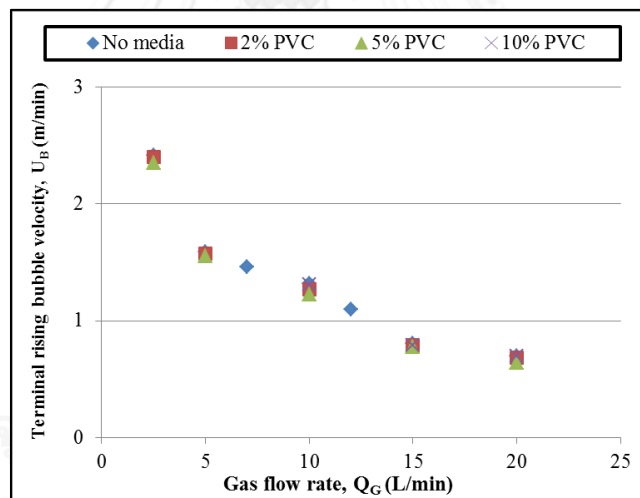
4.4.3 Effect of plastic media on terminal rising bubble velocity in ILALR

- Polyvinyl Chloride (PVC)

Figure 4.40 presents the variation of terminal rising bubble velocity with gas flow rates obtained in the ILALR for different amount of PVC.



(a)



(b)

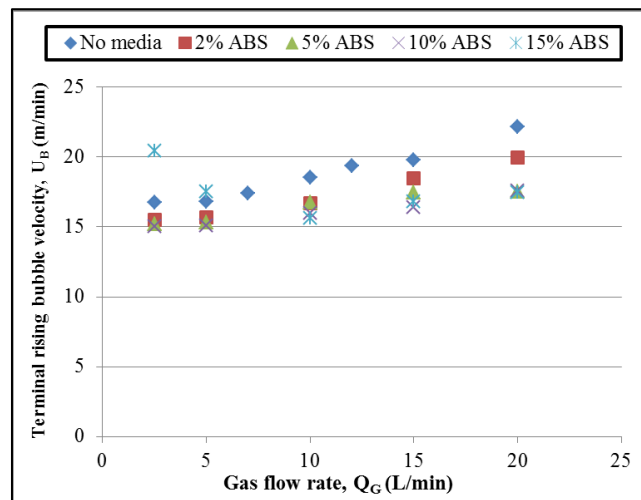
Figure 4.40 Terminal rising bubble velocity versus gas flow rate in ILALR for different amount of PVC: (a) Riser zone, (b) Down-comer zone

According to Figure 4.40 (a), the U_B values obtained experimentally varied between 15.31-22.56 m/min while gas flow rates change between 2.5 - 20 L/min. The U_B values increased with the gas flow rate. Same as the case of BC, the lowest and highest U_B values were observed at 5% and 15% of PVC media loading, respectively. Furthermore, at low PVC media loading (2-5% loading), the U_B values were lower than those obtained with no media. However, for high PVC media loading (10-15% loading), low gas flow rate (2.5-5 L/min), the U_B values were greater than those of no

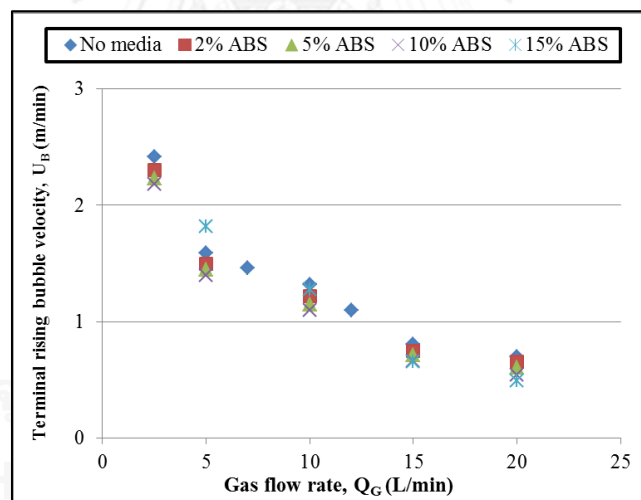
media. The large size of the bubble diameters obtain with the case of high PVC media should be responsible for these results.

- **Acrylonitrile Butadiene Styrene (ABS)**

Figure 4.41 presents the variation of terminal rising bubble velocity with gas flow rates obtained in the ILALR for different amount of ABS.



(a)



(b)

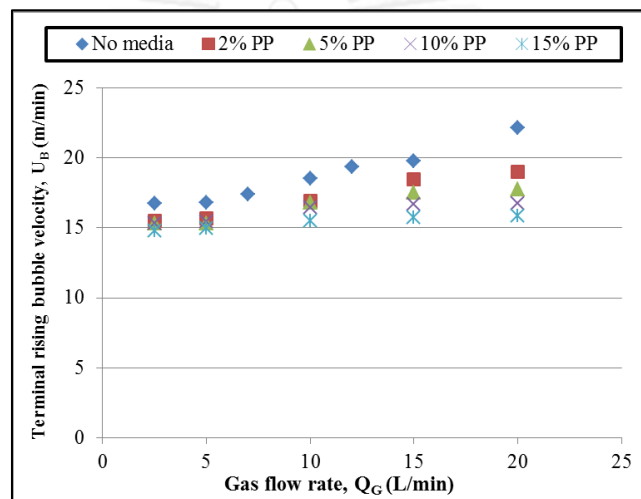
Figure 4.41 Terminal rising bubble velocity versus gas flow rate in ILALR for different amount of ABS: (a) Riser zone, (b) Down-comer zone

As shown in Figure 4.41 (a), the U_B in riser zone of the ILALR increased from 15.02 to 20.42 m/min when gas flow rates augmented between 2.5 and 20 L/min. By considering this Figure, at low ABS media loading (2-10% of media loading), the values of U_B were lower than those of no media. However, same as case of PVC media loading, at high concentration of media (15% ABS loadings), the increase in U_B can be observed due to the increase in bubble size. However, the values of U_B

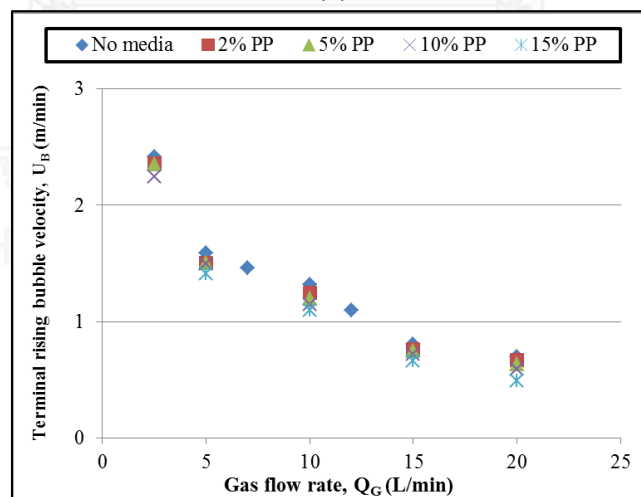
obtained with BC were higher than those obtained with the riser zone of ILALR: the difference of bubble size should be responsible for these results. For the down-comer zone of the ILALR, as shown in Figure 4.41 (b), the U_B decreased from 0.49 to 2.23 m/min when gas flow rates augmented between 2.5 and 20 L/min. It can be noted that an increase in gas flow rate of the riser zone caused the decrease in the U_B values in the down-comer zone. Moreover, the addition of ABS media caused the increase in the U_B values.

- **Polypropylene (PP)**

Figure 4.42 presents the variation of terminal rising bubble velocity with gas flow rates obtained in the ILALR for different amount of PP.



(a)



(b)

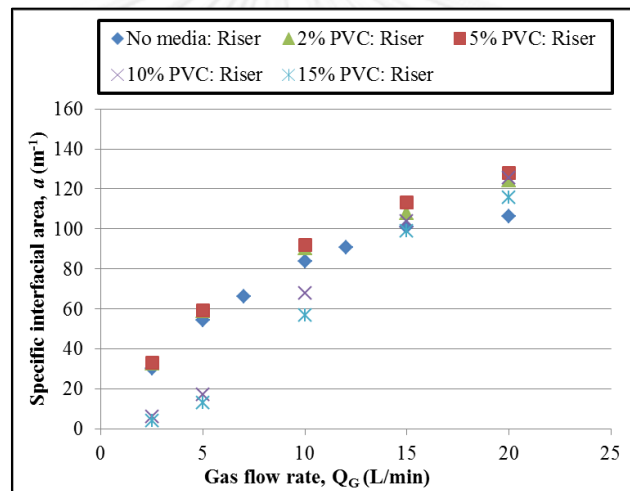
Figure 4.42 Terminal rising bubble velocity versus gas flow rate in ILALR for different amount of PP: (a) Riser zone, (b) Down-comer zone

Concerning to Figure 4.42, the variation of U_B obtained experimentally varied between 14.78-19.04 m/min for the riser zone and 0.49-2.36 m/min while gas flow rates can change between 2.5 - 20 L/min. The values of the U_B increased with gas flow rate in the riser zone, whereas, decreased with gas flow rate in the down-comer zone. It can be stated that the addition of PP media provided the lower of U_B values in the reactor. Moreover, the U_B values obtained with the riser zone of the ILALR were lower than those obtained with the BC. This result was due to the small bubble size obtained in the ILALR.

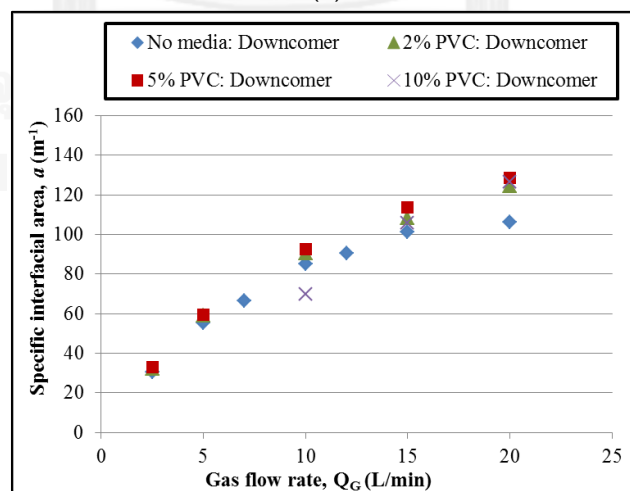
4.4.4 Effect of plastic media on the specific interfacial area (a) in ILALR

- Polyvinyl Chloride (PVC)

Figure 4.43 presents the variation of specific interfacial area with gas flow rates obtained in the ILALR for different amount of PVC.



(a)



(b)

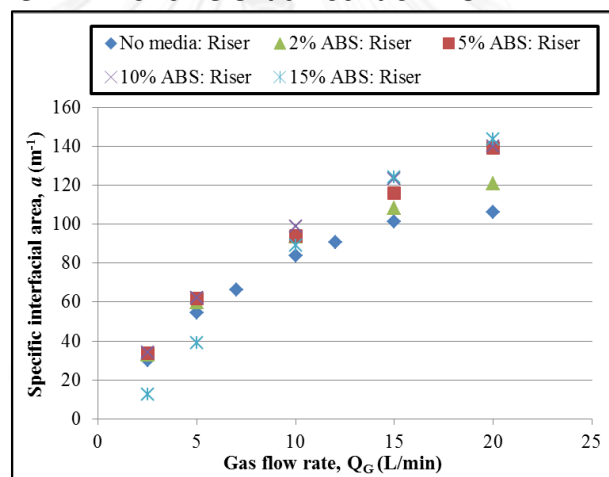
Figure 4.43 Specific interfacial area versus gas flow rate in ILALR for different amount of PVC: (a) Riser zone, (b) Down-comer zone

Figure 4.43 (a) shows that the addition of low concentration of PVC (2-5% of plastic media loading) not has significant effect on the specific interfacial area, whereas the high addition of PVC (10-15% of plastic media loading) caused the decrease in the specific interfacial area, especially at low gas flow rate. Same as the case of BC, the PVC particles which located at the bottom of the reactor caused the increase in bubble size and the decrease in the specific interfacial area. Moreover, the values of specific interfacial area obtained with BC were lower than those obtained with ILALR, which related to the $K_L a$ value.

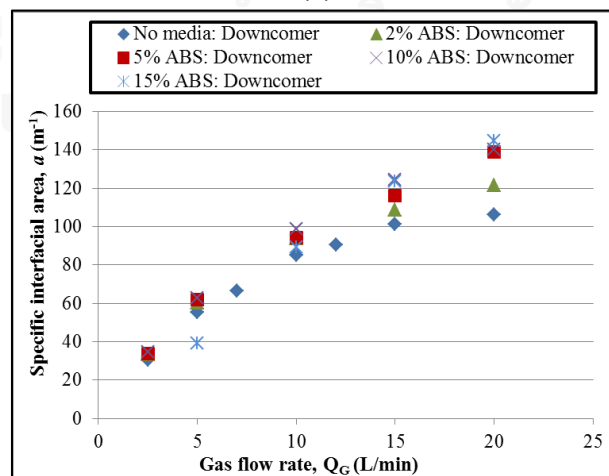
From the Figure 4.43 (b), for all cases, the specific interfacial area values were closed to those of the riser zone. Moreover, the specific interfacial area of 15% PVC cannot be calculated because the bubble generated in the riser zone not recirculated into the down-comer zone.

- **Acrylonitrile Butadiene Styrene (ABS)**

Figure 4.44 presents the variation of specific interfacial area with gas flow rates obtained in the ILALR for different amount of ABS.



(a)



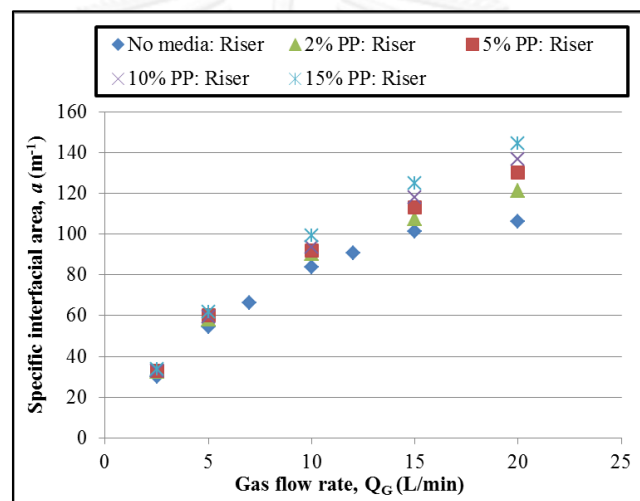
(b)

Figure 4.44 Specific interfacial area versus gas flow rate in ILALR for different amount of ABS: (a) Riser zone, (b) Down-comer zone

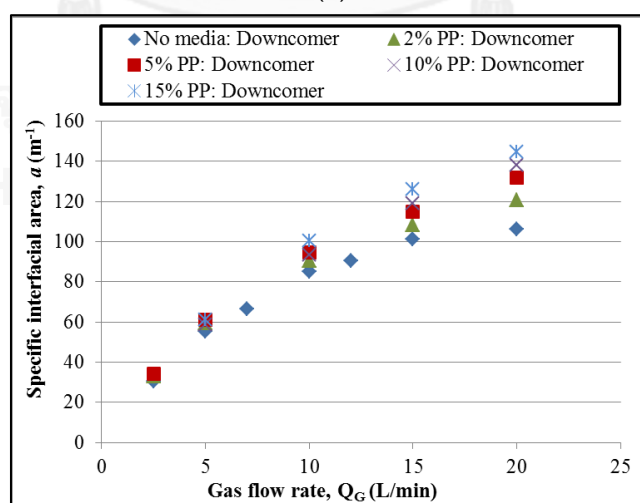
According to Figure 4.44, it was shown that the specific interfacial area varied between 12.41 to 143.77 m^{-1} for riser zone, whereas, for the down-comer zone, the specific interfacial area values varied between 33.46 to 144.64 m^{-1} , when gas flow rates changing between 2.5 and 20 L/min. For both side of the reactor, the values of specific interfacial area were closed and increased with the gas flow rate. Moreover, for the 15% ABS loading at low gas flow rate (2.5-5 L/min), the values of specific interfacial area were lower than those obtained with no media due to the large bubble size obtained.

- **Polypropylene (PP)**

Figure 4.45 presents the variation of specific interfacial area with gas flow rates obtained in the ILALR for different amount of PP.



(a)



(b)

Figure 4.45 Specific interfacial area versus gas flow rate in ILALR for different amount of PP: (a) Riser zone, (b) Down-comer zone

Considering the Figure 4.45, it was shown that the specific interfacial area varied between 32.48 to 144.25 m^{-1} for riser zone, and 33.11 to 144.57 m^{-1} for down-comer zone, when gas flow rates ranged between 2.5 and 20 L/min. The specific interfacial area in both zones were closed and continuously increased with the gas flow rate. The highest values obtained for both zone of the reactor were observed for 15% of PP particles at gas flow rate 15 L/min.

4.4.5 Effect of plastic media on the gas flow rate (Down-comer zone) in ILALR

- Polyvinyl Chloride (PVC)

Figure 4.46 presents the variation of gas flow rate (Down-comer zone) with gas flow rates (Riser zone) obtained in the ILALR for different amount of PVC.

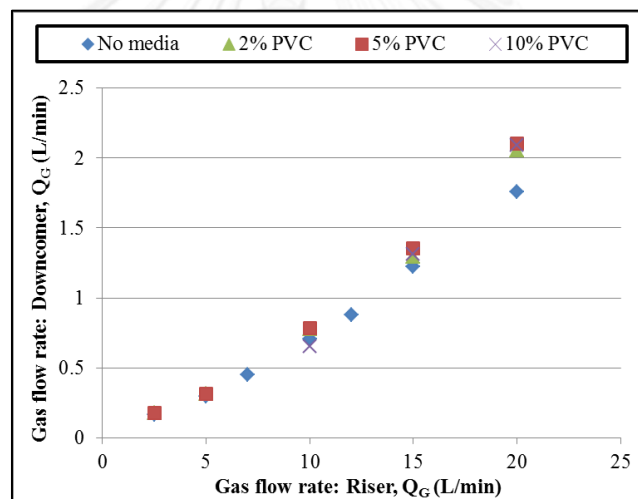


Figure 4.46 Gas flow rate (Down-comer zone) versus gas flow rate (Riser zone) in ILALR for different amount of PVC

From the Figure 4.46, it was shown that the gas flow rate obtained in down-comer zone varied between 0.18 to 2.10 L/min when gas flow rates applied into the riser zone changing between 2.5 and 20 L/min. Moreover, it can be noted that the gas flow rate (Down-comer zone) slowly increased with the gas flow rate (Riser zone). Due to none of bubble in the down-comer zone, the gas flow rate (Down-comer zone) for 15% PVC cannot be calculated.

- Acrylonitrile Butadiene Styrene (ABS)

Figure 4.47 presents the variation of gas flow rate (Down-comer zone) with gas flow rates (Riser zone) obtained in the ILALR for different amount of ABS.

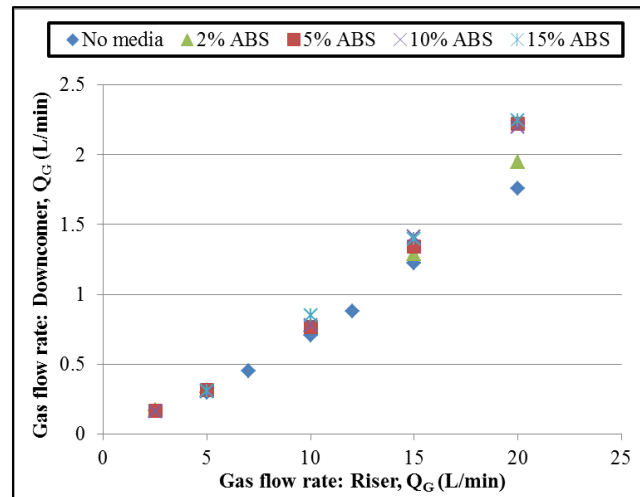


Figure 4.47 Gas flow rate (Down-comer zone) versus gas flow rate (Riser zone) in ILALR for different amount of ABS

According to the Figure 4.47, it was shown that the gas flow rate obtained in down-comer zone varied between 0.17 to 2.25 L/min when gas flow rates applied into the riser zone changing between 2.5 and 20 L/min. The increase in gas flow rate (Riser zone) caused an increase in the gas flow rate (Down-comer zone). Moreover, for 15% of ABS loading at gas flow rated applied into riser zone 2.5 L/min, the gas flow rate (Down-comer zone) cannot be calculated due to none of bubble in the down-comer zone.

- Polypropylene (PP)

Figure 4.48 presents the variation of gas flow rate (Down-comer zone) with gas flow rates (Riser zone) obtained in the ILALR for different amount of PP.

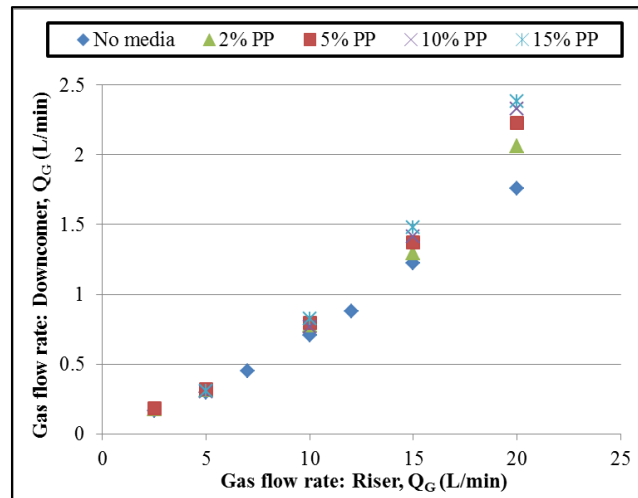


Figure 4.48 Gas flow rate (Down-comer zone) versus gas flow rate (Riser zone) in ILALR for different amount of PP

It can be shown from the Figure 4.48 that the gas flow rate obtained in down-comer zone varied between 0.18 to 2.38 L/min while the gas flow rates applied into the riser zone ranged between 2.5 and 20 L/min. The increase in gas flow rate (Riser zone) caused an increase in the gas flow rate (Down-comer zone). Moreover, the highest value of gas flow rate (Down-comer zone) was observed with 15% PP media addition at gas flow rate applied 20 L/min.

4.5 Comparison the effect of best plastic media condition on mass transfer and bubble hydrodynamic parameters in BC and ILALR.

By analyzed the best condition for oxygen absorption in this work, the impacts of 15%PP (best type and concentration of plastic media) obtained with the BC and ILALR on the $K_L a$, D_B , a , and K_L parameters were show in Figure 4.49-4.52.

- **Overall mass transfer coefficient ($K_L a$) in BC and ILALR**

Figure 4.49 presents the variation of overall mass transfer coefficient with gas flow rates obtained in the BC and ILALR for no media and 15% of PP.

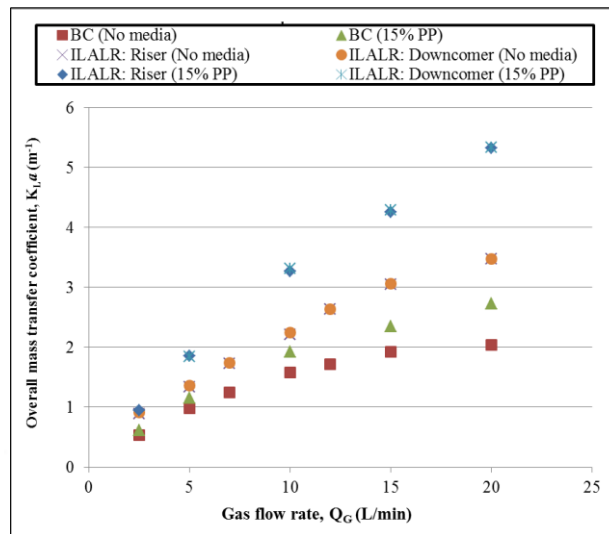


Figure 4.49 Overall mass transfer coefficient versus gas flow rate in BC and ILALR

According to the Figure 4.49, the K_La values obtained with ILALR were higher than those obtained with BC. Moreover, at 20 L/min, the addition of 15% PP provided an increase in the K_La values for 34% and 53% obtained with BC and ILALR, respectively. It can be noted that the higher increase in K_La values obtained with ILALR was due to the higher amount of suspended PP particles within the tap water. Therefore, the bubble and liquid recirculation in ILALR should be responsible for this result.

- **Bubble diameter (D_B) in BC and ILALR**

Figure 4.50 presents the variation of bubble diameter (D_B) with gas flow rates obtained in the BC and ILALR for no media and 15% of PP.

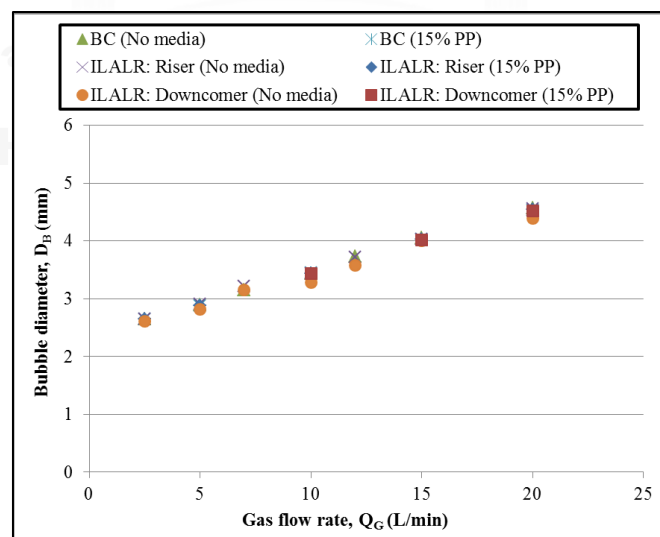


Figure 4.50 Bubble diameter versus gas flow rate in BC and ILALR

By considering to the Figure 4.50, the bubble diameters obtained with BC and ILALR (Riser and down-comer zone) were close. From the Figure, it can be stated that:

- For all gas flow rates, the bubble size obtained with BC and ILALR for no media and 15% PP addition were closed. The similar gas diffuser used in this work should be responsible for this result.
- The bubble size obtained for all cases depend only on the gas flow rates. The increased in gas flow rate provided an increase in bubble diameter. In this regard, the bubble coalescence phenomena should be responsible for this result.
- The addition of 15% PP media, and the different type of reactors not modified the bubble size.
- By considering the bubble diameter in the ILALR, for both no media and 15% of PP addition, the bubble diameters obtained with riser zone were closed to those of down-comer zone.

From these results, it can be again concluded that the change in specific interfacial area by adding PP media was not related to the change in bubble size.

- **Specific interfacial area (a) in BC and ILALR**

Figure 4.51 presents the variation of specific interfacial area (a) with gas flow rates obtained in the BC and ILALR for no media and 15% of PP.

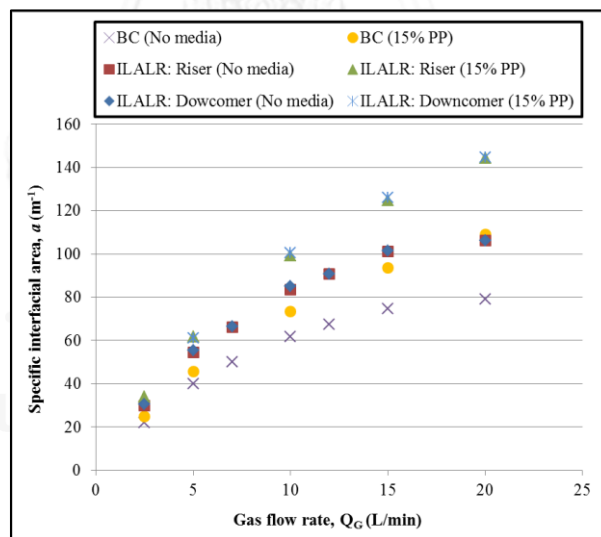


Figure 4.51 Specific interfacial area versus gas flow rate in BC and ILALR

From the Figure 4.51, the specific interfacial areas obtained with ILALR (Riser and down-comer zone) were higher than those of BC. Moreover, at 20 L/min, the 15% of PP media loading caused an increase in the specific interfacial area values for 38%, 36%, and 36% obtained with the BC, the riser zone, and the down-comer zone

of ILALR, respectively. It can be observed that the increase in the specific interfacial area obtained with the BC and ILALR were closed.

As presented previously, the terminal rising bubble velocity (U_B) in down-comer zone of ILALR decreased with the gas flow rates. The U_B values varied between 2.42-0.70 and 2.36-0.49 m/min for no media and 15% of PP addition, respectively while gas flow rates can change between 2.5-20 L/min. From the equation 3.9;

$$Q_G = f_B \times V_B = a \times \frac{U_B}{H_L} \times \frac{AH_L + N_B V_B}{\pi D_B^2} \times V_B$$

It can be stated that the increase in specific interfacial area and U_B values caused an increase in the Q_G in down-comer zone. Therefore, the next section the effect of plastic media on the gas flow rate (Q_G) in down-comer zone of ILALR will be studied.

- **Effect of plastic media on the gas flow rate in down-comer zone (Q_G) of ILALR**

Figure 4.52 presents the variation of gas flow rate (Down-comer zone) with gas flow rates (Riser zone) obtained in the ILALR for no media and 15% of PP.

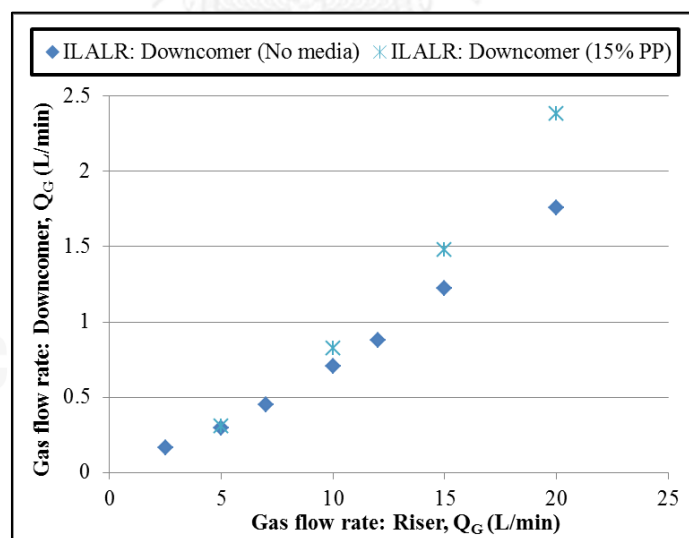


Figure 4.52 Gas flow rate (Down-comer zone) versus gas flow rates (Riser zone) in the ILALR

From the Figure, it can be show that the Q_G (Down-comer zone) was lower than Q_G (Riser zone); the ratios of Q_G (Down-comer zone) to Q_G (Riser zone) were in range of 0.07-0.09 and 0.06-0.11 L/min for no media and 15% PP addition,

respectively. Therefore, it can be observed from the Figure that the addition of 15% PP media provided an increase in the Q_G values (Down-comer zone). The flow of gas (bubble) phase and liquid phase through the suspended plastic media porous caused an increase in Q_G values (Down-comer zone) which consequently decreased the terminal rising bubble velocity and increased the specific interfacial area in the down-comer zone.

In conclusion, the addition of 15% PP media provides the positive effect on oxygen mass transfer in tap water; these effects can be explained below:

- The PP addition not modified the bubble size.
- The PP particles increased the gas flow rate in down-comer zone, increased the flow-path distance of bubble in the reactor and momentarily hindered the rising-up of bubble. These results related to the decreased in the U_B values in the down-comer zone.
- This decrease in the U_B value related to an increase in specific interfacial area in the down-comer zone, which related to an increase in the specific interfacial area in the total of ILALR.

- **Liquid film mass transfer coefficient (K_L) in BC and ILALR**

Figure 4.53 presents the variation of liquid film mass transfer coefficient (K_L) with gas flow rates obtained in the BC and ILALR for no media and 15% of PP.

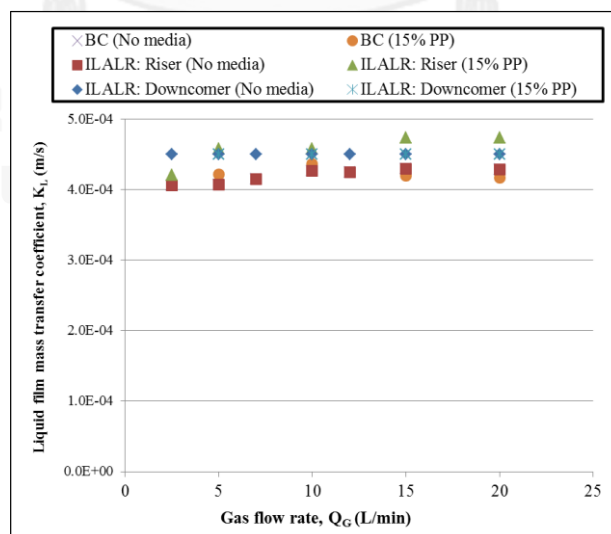


Figure 4.53 Liquid film mass transfer coefficient versus gas flow rate in BC and ILALR

From the Figure 4.53, the K_L values of tap water obtained with BC and ILALR (Riser and down-comer zone) were ranged between 4.09×10^{-4} and 4.74×10^{-4} m/s. The K_L values of tap water obtained in this work were acceptable. This result can proved that an increase in $K_L a$ values must be primarily conformed to an increase in specific interfacial area.

The overall results obtained with oxygen absorption part were show in the Table 4.1. The effect of 15% plastic media addition on the overall mass transfer coefficient ($K_L a$), bubble diameter (D_B), terminal rising bubble velocity (U_B), specific interfacial area (a), and liquid film mass transfer coefficient (K_L) comparing to no media addition in BC and ILALR were concluded.

Table 4.1 The overall results obtained in oxygen absorption part.

Parameter	BC			ILALR			Remark
	PVC	ABS	PP	PVC	ABS	PP	
K_{La}	↓ at low Q_G ↑ at high Q_G	↓ at low Q_G ↑ at high Q_G	↑	↓ at low Q_G ↑ at high Q_G	↓ at low Q_G ↑ at high Q_G	↑	<ul style="list-style-type: none"> For high plastic media loading, at low gas flow rate, the K_{La} values for PVC loading lower than those for ABS loading.
D_B	↑ at low Q_G ≈ at high Q_G	↑ at low Q_G ≈ at high Q_G	≈	↑ at low Q_G ≈ at high Q_G	↑ at low Q_G ≈ at high Q_G	≈	<ul style="list-style-type: none"> For high plastic media loading, at low gas flow rate, the bubble diameter for PVC loading larger than those for ABS loading.
U_B	↑ at low Q_G ↓ at high Q_G	↑ at low Q_G ↓ at high Q_G	↓	↑ at low Q_G ↓ at high Q_G	↑ at low Q_G ↓ at high Q_G	↓	<ul style="list-style-type: none"> For high plastic media loading, at low gas flow rate, the U_B values for PVC loading higher than those for ABS loading.
a	↓ at low Q_G ↑ at high Q_G	↓ at low Q_G ↑ at high Q_G	↑	↓ at low Q_G ↑ at high Q_G	↓ at low Q_G ↑ at high Q_G	↑	<ul style="list-style-type: none"> For high plastic media loading, at low gas flow rate, the specific interfacial area for PVC loading lower than those for ABS loading.
K_L	≈	≈	≈	≈	≈	≈	

From the experimental results in part 4.5, it can be concluded that the best condition (reactor, and types and concentration of plastic media) was observed with the addition of 15% PP loading in the ILALR. This result was due to the decrease in the U_B value, which related to an increase in the specific interfacial area and the $K_L a$ coefficients. The next part, the best condition will be applied for remove the benzene gas from the gas stream.

4.6 Application for benzene gas absorption.

The aim of this part was to study the application of the best condition obtained from the previously part for benzene gas absorption. The effects of surfactant, plastic media addition, and granular activated carbon (GAC) addition on the overall mass transfer coefficient for benzene absorption were investigated in the ILALR.

Benzene gas generator was applied in order to generate the benzene gas at room temperature. The air was injected into the 100 mL of pure benzene in the flask in order to generating benzene gas stream from their volatilization. Due to the low boiling point of benzene (80.1 °C), it proved that the benzene was evaporated. The benzene gas stream was added into the bottom of the ILALR.

4.6.1 Overall mass transfer coefficient ($K_L a$) for benzene absorption

The $K_L a$ values from this section were calculated by measured the concentration of benzene in liquid phases with time using the UV/Visible Spectroscopy technique. The liquid samples were collected at 1-25 minutes. In this work, the absorbents were referred to the concentration of benzene in liquid phase. Figure 4.49 presents the variation of absorbent with time obtained in the ILALR for benzene absorption with different condition (different liquid phases, media addition, and GAC addition).

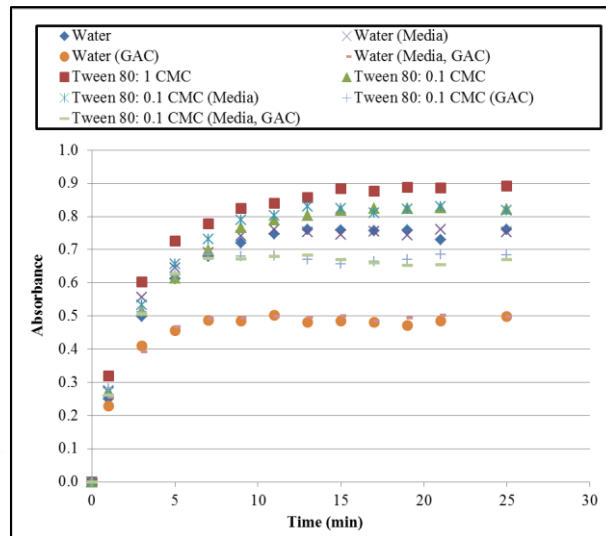


Figure 4.54 Absorbent versus time for benzene absorption

Concerning to Figure 4.54, it can be found that, the benzene concentrations rapidly increased in first step, and then nearly to the constant values (saturated concentration, C_S) with increasing times. From the Figure, it can be stated that the values of saturated benzene concentration were related to types and concentration of liquid phases, and GAC addition.

$$C_{S \text{ Tween } 80:1 \text{ CMC}} > C_{S \text{ Tween } 80:0.1 \text{ CMC}} > C_{S \text{ Water}} > C_{S \text{ Tween } 80:0.1 \text{ CMC (GAC)}} > C_{S \text{ Water (GAC)}}$$

Note that, the effect of plastic media addition on the values of C_S was not observed. The experimental results shown that the addition of GAC

Table 4.2 Summary of $K_L a$ values for benzene absorption

Condition	$K_L a$ (min^{-1})
Surfactant (No media)	
• Water	0.3213
• Tween 80: 1 CMC	0.3501
• Tween 80: 0.1 CMC	0.3323
Surfactant (Media)	
• Water (Media)	0.3642
• Tween 80: 0.1 CMC (Media)	0.3688
Surfactant (GAC)	
• Water (GAC)	0.2683
• Tween 80: 0.1 CMC (GAC)	0.2905
Surfactant (Media, and GAC)	
• Water (Media, GAC)	0.2105
• Tween 80: 0.1 CMC (Media, GAC)	0.2613

Table 4.2 presents the values of overall mass transfer coefficient obtained in the ILALR for benzene absorption. From the Table, it can be concluded that:

- Concerning to the different types and concentrations of surfactant (2nd row), it can be shown that the $K_L a$ values depended on the concentration of surfactant: $K_L a$ (1 CMC) > $K_L a$ (0.1 CMC) > $K_L a$ (Water). However, for Tween 80, the $K_L a$ coefficient obtained with 1 CMC was not much higher than those obtained with 0.1 CMC.

- For surfactant with media (3rd row), the $K_L a$ coefficients obtained for both liquid phases with 15% of PP loading were higher than those obtained with no media. The increase in the $K_L a$ value by adding the plastic media obtained with water (13% increased) was higher than those obtained with 0.1 CMC Tween 80 (11% increased) compared with no media. This was due to large number of bubble foam generated at the surface of the liquid phase (0.1 CMC Tween 80), led the PP particles out of the liquid phase. Therefore, the number of PP particles suspended in the liquid phase was decreased, and related to an increase in U_B values.

- For surfactant with GAC (4th row), the $K_L a$ coefficients obtained for both liquid phases with GAC were lower than those obtained with no GAC. This result can be explained that the benzene gas in liquid phase was reduced by adsorbing into the GAC; thus, the decrease in $K_L a$ values was observed. Moreover, the $K_L a$ value obtained with water (0.2683 min^{-1}) was lower than those obtained with 0.1 CMC Tween 80 (0.2905). This is to say the benzene gas adsorption in GAC obtained with 0.1 CMC Tween 80 was lower than those obtained with water. The surfactant may block the adsorption efficiency of GAC.

- For surfactant with 15% of PP media and GAC (5th row), the $K_L a$ coefficients obtained for both liquid phases with media and GAC were lower than those obtained with only media and with only GAC. The decrease in the $K_L a$ value due to the decrease in U_B values.

4.6.2 Benzene removal efficiency

In this section, the inlet and outlet benzene concentrations in the gas phase were sampled and collected at 5 to 5.5 minutes using air bag, and measured by using the GC-FID equipment. The benzene removal efficiency (%Eff) was calculated by using the equation 3.10.

Table 4.3 presents the values of overall mass transfer coefficient obtained in the ILALR for benzene absorption.

Table 4.3 Summary of $K_L a$ benzene removal efficiency.

Condition	Average peak area	Benzene removal efficiency (%Eff)
Benzene gas inlet	40419.97	-
Benzene gas outlet		
Surfactant (No media)		
• Water	28248.00	30
• Tween 80: 1 CMC	18249.80	55
• Tween 80: 0.1 CMC	16297.60	60
Surfactant (Media)		
• Water (Media)	20307.80	50
• Tween 80: 0.1 CMC (Media)	12422.90	69
Surfactant (GAC)		
• Water (GAC)	7263.30	82
• Tween 80: 0.1 CMC (GAC)	10175.36	75
Surfactant (Media, and GAC)		
• Water (Media, GAC)	4790.07	88
• Tween 80: 0.1 CMC (Media, GAC)	8954.40	78

From the Table 4.3, it can be concluded that:

- For no GAC addition, for all cases, the addition of Tween 80 into the tap water provide the increased in benzene removal efficiency. By considering the Figure 4.49, the saturated benzene concentration obtained with Tween 80 was higher than

those obtained with tap water. Therefore, at the same period of time, the benzene gas can absorb in Tween 80 more than in tap water.

- The addition of 15% PP media increased the benzene removal efficiency at 5 to 5.5 min. This result was agreeable with the Figure 4.49 and Table 4.1. According to the Figure 4.49, the benzene concentration in liquid phase was not reached the saturated benzene concentration. And from the Table 4.1, the $K_L a$ values obtained with media addition were higher than those obtain with no media. Therefore, the benzene gas can absorption obtained with media addition was higher than those obtained with no media.

- For GAC addition, for all cases, the benzene removal efficiency was higher than those obtained with no GAC addition. Moreover, the %Eff obtained with tap water was higher than those obtained with Tween 80. This result can explained that Tween 80 blocked the benzene gas adsorption into the GAC.

- The highest value of the %Eff was observed with the addition of 15% PP media and GAC in tap water.

In conclusion, it can be expressed that the best condition for hydrophobic VOCs absorption in this work observed with the 15% PP and GAC addition in water within the ILALR.

CHAPTER V

CONCLUSIONS AND RECOMMENDATIONS

5.1 Conclusions

The emission of volatile organic compounds (VOCs) into the air has been an environmental concern. Benzene is one of toxic VOC; it is known to be a human carcinogen based on sufficient evidence of carcinogenicity from studies in humans. Therefore, the objective of this work was to study the absorption system for controlling benzene emissions. The effect of plastic media on oxygen mass transfer and bubble hydrodynamic parameters at a variety of gas flow rate in a bubble column (BC) and an internal loop airlift reactor (ILALR) was studied. The different types and amount of small size plastic particles were added into the reactors in order to increase the liquid-gas surface contact, which improve mass transfer rates. The best condition system from the experimental results was applied for designing a high-efficiency benzene absorption system.

In this research work, the experiments were carried out in laboratory scale at atmospheric pressure and liquid temperature 26 (± 1) °C. The BC was made of Plexiglas with 14 cm in diameter and 100 cm in height. For ILALR system, the rectangular Plexiglas baffle (with 13 cm width, 80 cm height, and 0.5 cm thickness) was installed within the BC in order to divide the cross section into a riser zone and a down-comer zone. Gas diffuser used in this work is rigid orifice diffuser, it was injected at the bottom of reactors: in the middle and in the riser zone for BC and ILALR, respectively. In this study, the experiments can be divided into two parts; oxygen absorption and benzene absorption parts.

For the oxygen absorption part, the effect of small plastic media particles on overall mass transfer coefficient ($K_L a$), bubble diameter (D_B), terminal rising bubble velocity, specific interfacial area (a), and liquid film mass transfer coefficient (K_L) in BC and ILALR were investigated. The operating conditions were as follows: liquid phase is tap water, liquid height (H_L) = 86.5 cm (13 L) and gas flow rate of 2.5, 5, 7, 10, 12, 15 and 20 L/min. The three different plastic media particles (PVC, ABS, and PP) with different concentration (2, 5, 10, 15 (%v/v)) were used.

In this part, the following results have been obtained;

1. For no plastic media, the overall mass transfer coefficient ($K_L a$) seemed to be higher in ILALR than in BC because of the gas and liquid recirculation from the riser zone to the down-comer zone in ILALR.

2. The same trendline of bubble diameter in BC and ILALR without plastic media was observed due to the similar diffuser applied in this work. The K_L values of tap water calculated in this study were acceptable.

3. For both reactors, the similar effect of plastic media loading on the $K_L a$ value was found. The following results were observed:

- For PVC addition, by the large amount of media loadings (10-15%), the PVC blocked or modified the bubble generation, which caused the negative effect on the $K_L a$ value. This adverse effect was smaller in ILALR than in BC because the liquid and bubble recirculation in the ILALR enhanced the suspension and reduced the accumulation of PVC.
- The addition of ABS insignificantly changed the $K_L a$ value. However, similar to the case of PVC, the slight decrease in the $K_L a$ value was observed at high amount of ABS loading (15%).
- The PP addition significantly enhanced the $K_L a$ value due to the increase of specific interfacial area.

4. The effect of plastic media on bubble diameter in the BCR and ILALR was concluded as follows:

- At high amount of PVC loading, the accumulated of PVC particles performed as the large orifice diffuser, which generated the large size of bubble.
- For ABS addition, the bubble size was not significantly changed, except the large amount of ABS particles (15%); the large size of bubble was observed.
- The increase in PP loading not significantly changed bubble diameter.

5. The similar effect of plastic media loading on the U_b value in BC and the riser zone was found. The following results were observed:

- At high amount of PVC loading, the large size bubbles were generated. An increase in bubble size increased the U_B value.
- For ABS addition, there was no significantly change in U_B value, except the high amount of ABS particles (15%).
- The increase in PP loading not significantly changed the U_B value.

For the down-comer zone, for all types of plastic media addition, the U_B value slightly decreased with the gas flow rate. The U_B values (Down-comer zone) were in range: No plastic media > PVC > ABS > PP. An increase in the amount plastic media particles suspended within the reactor caused the decreased in U_B value in the down-comer zone.

6. The similar effect of plastic media loading on the specific interfacial area in BC and the riser zone was found. The following results were observed:

- At high amount of PVC loading, the large size bubbles were generated. An increase in bubble size and U_B value caused an increase in the specific interfacial area.
- For ABS addition, there was no significantly change in specific interfacial area, except the high amount of ABS particles (15%); the specific interfacial area was lower than those obtained with no media.
- The increase in PP loading not significantly changed the specific interfacial area value.

For the down-comer zone, the specific interfacial area increased with the decrease in U_B value.

In conclusion for the oxygen absorption part, the ILALR provides higher oxygen mass transfer rate than BC. Moreover, the highest specific interfacial area and overall mass transfer coefficient was observed with 15% of PP media. Therefore, the best condition for oxygen absorption part is the 15% of PP media addition in ILALR.

The best condition obtained from the oxygen absorption part (15% of PP media addition in ILALR) was applied for benzene absorption part. For the benzene

absorption part, the $K_L a$ values and the benzene removal efficiency was analyzed. The operating conditions were as follows: liquid phase is tap water and Tween 80 (0.1 and 1 CMC), liquid height (H_L) = 86.5 cm (13 L), and gas flow rate of 10 L/min. The 100 mL of pure benzene was added in to the benzene gas generator in order to generating benzene gas stream from their volatilization. The 15 % of PP was added into the ILALR. Moreover, the granular activated carbon (GAC) was added into the reactor in order to increase the benzene removal efficiency.

In this part, the following results have been obtained;

1. The values of saturated benzene concentration were in ranged:

$$C_{S \text{ Tween } 80:1 \text{ CMC}} > C_{S \text{ Tween } 80:0.1 \text{ CMC}} > C_{S \text{ Water}} > C_{S \text{ Tween } 80:0.1 \text{ CMC (GAC)}} > C_{S \text{ Water (GAC)}}.$$

2. The addition of 15% PP media increased the $K_L a$ values of benzene absorption.

3. For no GAC addition, the benzene removal efficiency obtained with Tween 80 was higher than those obtained with tap water.

4. For GAC addition, the benzene removal efficiency obtained with tap water was higher than those obtained with Tween 80. This results can be explained that the Tween 80 hindrance the mass transfer of benzene from liquid phase into the GAC.

In conclusion, the best condition for benzene absorption in this work was observed with the 15% PP media and GAC addition into tap water in the ILALR.

The absorption system obtained in this work can be applied for VOCs gas removal and also for water treatment. The advantages of this system over other techniques are simple construction and low operation costs.

5.2 Recommendations for future work

In the future, the development of a continuous system internal loop airlift reactor should be studied in order to provide a high hydrophobic VOCs removal efficiency system. Figure 5.1 shows a schematic diagram of the design continuously internal loop airlift reactor. According to the Figure, the VOC gas (absorbate) is injected at the base of the reactor through a single gas rigid orifice and the rest of VOC gas out at the top of the column. The liquid phase (absorbent) is flow in and out at the lower- and upper- of the riser zone and down-comer zone of the ILALR, respectively.

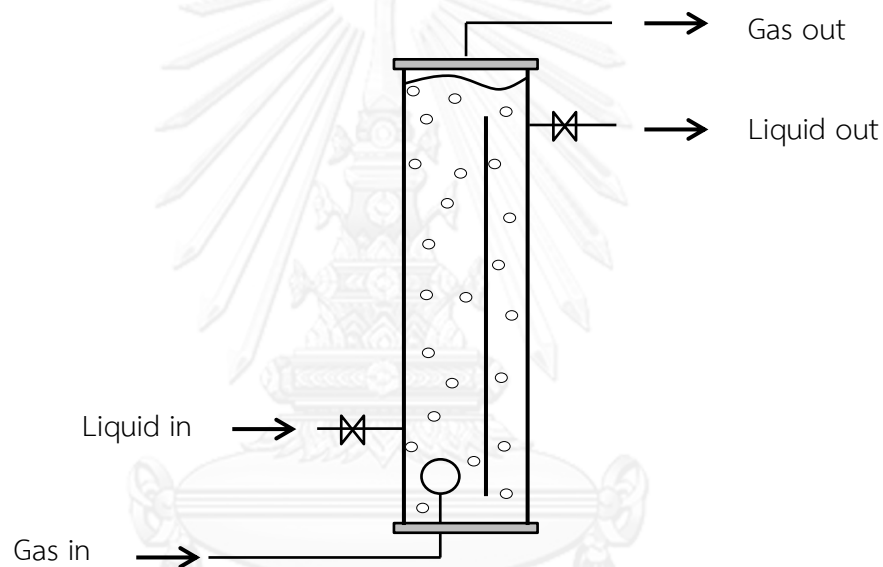


Figure 5.1 Schematic diagram of continuous ILALR system

More different types of small plastic media particle should be investigated in order to increase the mass transfer rate of the hydrophobic VOCs absorption. Noted that the density (ρ) of plastic media should be similar to density of water (ρ_{water}). Furthermore, the effect of different shapes of plastic media (for a similar density) on mass transfer rate is interested to investigate.

From the results of this work, the addition of GAC increased the benzene removal efficiency; therefore, the activated carbon may be used as media particles for VOCs removal system.

Moreover, more different types and concentration of surfactant used should be investigated in order to increase the overall mass transfer coefficient and removal efficiency of hydrophobic VOCs.

REFERENCES

- Chisti, Y., Kasper, M., & Moo-Young, M. (1990). Mass transfer in external-loop airlift bioreactors using static mixers. *Chemical Engineering Science*, *68*(45-50).
- Deckwer, W. (1992). *Bubble column reactors* (Vol. 38): Institution of Chemical Engineers
- Deithorn, R. T. & Mazzoni, A. F. (2014). The Story of Activated Carbon. from <http://www.tigg.com/what-is-activated-carbon.html>
- EPA, U. S. (1998). Toxicological review of benzene (Noncancer effects). Retrieved september 1998
- EPA, U. S. (2009). Benzene TEACH Chemical Summary. Retrieved 2/27/2009, from Toxicity and Exposure Assessments for Children's Health
- Erto, A. & Lancia, A. (2012). Solubility of benzene in copolymer aqueous solutions for the design of gas absorption unit operations. *Chemical Engineering Journal*, *187*, 166-171.
- Freitas, C. & José, T. A. (2001). Oxygen mass transfer in a high solids loading three-phase internal-loop airlift reactor. *Chemical Engineering Journal*, *84*, 57-61.
- Gourich, B., Vial, C., El Azher, N., Belhaj Soulami, M., & Ziyad, M. (2006). Improvement of oxygen mass transfer estimation from oxygen concentration measurements in bubble column reactors. *Chemical Engineering Science*, *61*(18), 6218-6222.
- Han, S. J., Tan, R. B. H., & Loh, K. C. (2000). Hydrodynamic Behaviour in a New Gas-Liquid-Solid Inverse Fluidization Airlift Bioreactor. *Food and Bioproducts Processing*, *78*(4), 207-215.
- Hasanen, A., Orivuori, P., & Aittamaa, J. (2006). Measurements of local bubble size distributions from various flexible membrane diffusers. *Chemical Engineering and Processing: Process Intensification*, *45*(4), 291-302.
- Higbie, R. (1935). The Rate of Absorption of a Pure Gas Into Still Liquid During Short Periods of Exposure. *Transactions of the American Institute of Chemical Engineers*, *31* 365-378.
- Kracht, W., Gomez, C. O., & Finch, J. A. (2008). Controlling bubble size using a frit and sleeve sparger. *Minerals Engineering*, *21*(9), 660-663.
- Meng, A. X., Hill, G. A., & Dalai, A. K. (2002). Hydrodynamic Characteristics in an External Loop Airlift Bioreactor Containing a Spinning Sparger and a Packed Bed. *Industrial & Engineering Chemistry Research*, *41*2124-2128.

- Moraveji, M. K., Mohsenzadeh, E., Fakhari, M. E., & Davarnejad, R. (2012). Effects of surface active agents on hydrodynamics and mass transfer characteristics in a split-cylinder airlift bioreactor with packed bed. *chemical engineering research and design*, 90(7), 899-905.
- Nikakhtari, H. & Hill, G. A. (2005). Volatile Organic Chemical Mass Transfer in an External Loop Airlift Bioreactor with a Packed Bed. *Industrial & Engineering Chemistry Research*, 44, 9299-9306.
- Painmanakul, P. & Hébrard, G. (2008). Effect of different contaminants on the α -factor: Local experimental method and modeling. *chemical engineering research and design*, 86(11), 1207-1215.
- Painmanakul, P., Loubière, K., Hébrard, G., Mietton-Peuchot, M., & Roustan, M. (2005). Effect of surfactants on liquid-side mass transfer coefficients. *Chemical Engineering Science*, 60(22), 6480-6491.
- Peevaa, L., Ben-zvi Yonab, S., & Merchukb, J. C. (2001). Mass transfer coefficients of decane to emulsions in a bubble column reactor. *Chemical Engineering Science*, 56, 5201-5206.
- Pjontek, D., Parisien, V., & Macchi, A. (2014). Bubble characteristics measured using a monofibre optical probe in a bubble column and freeboard region under high gas holdup conditions. *Chemical Engineering Science*, 111, 153-169.
- Polli, M., Stanislao, M. D., Bagatin, R., Bakr, E. A., & Masi, M. (2002). Bubble size distribution in the sparger region of bubble columns. *Chemical Engineering Science*, 57(1), 197-205.
- Sardeing, R., Painmanakul, P., & Hébrard, G. (2006). Effect of surfactants on liquid-side mass transfer coefficients in gas-liquid systems: A first step to modeling. *Chemical Engineering Science*, 61(19), 6249-6260.
- Whitman, W. G. (1962). THE TWO-FILM THEORY OF GAS ABSORPTION. *International Journal of Heat and Mass Transfer*, 5, 429-433.



APPENDIX

จุฬาลงกรณ์มหาวิทยาลัย
CHULALONGKORN UNIVERSITY

Table 1-2 Overall mass transfer coefficient (min^{-1}) in riser zone of ILALR

Flow rate (L/min)	No media	Flow rate (L/min)	PVC				ABS				PP			
			2%	5%	10%	15%	2%	5%	10%	15%	2%	5%	10%	15%
2.5	0.894	2.5	0.930	0.993	0.060	0.057	0.948	1.005	1.014	0.240	0.930	0.990	0.936	0.942
5	1.338	5	1.398	1.518	0.300	0.288	1.422	1.554	1.650	1.326	1.404	1.530	1.656	1.860
7	1.734	10	2.382	2.640	1.860	1.410	2.412	2.658	2.814	2.922	2.394	2.580	2.874	3.270
10	2.208	15	3.300	3.630	3.060	2.820	3.312	3.678	3.936	4.158	3.300	3.600	3.888	4.254
12	2.634	20	3.774	4.230	4.140	3.660	3.804	4.296	4.710	4.980	3.786	4.230	4.890	5.328
15	3.054													
20	3.474													



Table 1-3 Overall mass transfer coefficient (min^{-1}) in down-comer zone of ILALR

Flow rate (L/min)	No media	Flow rate (L/min)	PVC				ABS				PP			
			2%	5%	10%	15%	2%	5%	10%	15%	2%	5%	10%	15%
2.5	0.912	2.5	0.924	0.999	-	-	0.960	1.014	1.026	-	0.948	1.032	-	-
5	1.362	5.0	1.404	1.530	-	-	1.434	1.560	1.674	1.332	1.428	1.560	1.638	1.848
7	1.740	10.0	2.388	2.658	1.920	-	2.418	2.664	2.814	2.940	2.400	2.658	2.874	3.318
10	2.250	15.0	3.312	3.648	3.120	-	3.324	3.684	3.966	4.140	3.318	3.666	3.924	4.296
12	2.634	20.0	3.780	4.248	4.170	-	3.816	4.290	4.722	5.010	3.768	4.278	4.932	5.340
15	3.060													
20	3.480													



2. Bubble diameter at different gas flow rate in BC and ILALR

Table 2-1 Bubble diameter (mm) at different gas flow rate in the BC

Flow rate (L/min)	No media	Flow rate (L/min)	PVC				ABS				PP			
			2%	5%	10%	15%	2%	5%	10%	15%	2%	5%	10%	15%
2.5	2.65	2.5	2.64	2.65	17.01	27.88	2.64	2.60	2.58	6.03	2.63	2.56	2.64	2.65
5	2.90	5	2.88	2.85	13.75	21.31	2.87	2.85	2.83	4.43	2.88	2.87	2.88	2.87
7	3.15	10	3.42	3.42	5.86	6.10	3.42	3.36	3.37	3.97	3.46	3.44	3.45	3.45
10	3.43	15	4.04	4.00	4.21	4.20	4.03	3.97	3.93	4.15	4.03	4.02	4.02	4.02
12	3.72	20	4.56	4.55	4.61	4.59	4.46	4.40	4.27	4.38	4.56	4.53	4.56	4.53
15	4.05													
20	4.57													

Table 2-2 Bubble diameter (mm) at different gas flow rate in the riser zone of ILALR

Flow rate (L/min)	No media	Flow rate (L/min)	PVC				ABS				PP			
			2%	5%	10%	15%	2%	5%	10%	15%	2%	5%	10%	15%
2.5	2.64	2.5	2.62	2.64	10.68	15.25	2.59	2.58	2.58	5.26	2.64	2.64	2.64	2.65
5	2.90	5	2.87	2.86	7.71	10.07	2.83	2.81	2.83	3.90	2.90	2.88	2.88	2.87
7	3.22	10	3.42	3.42	4.02	4.91	3.39	3.36	3.35	3.80	3.46	3.42	3.44	3.43
10	3.43	15	4.01	4.02	4.18	4.46	4.00	3.93	3.92	3.81	4.02	4.03	4.04	4.02
12	3.72	20	4.39	4.41	4.42	4.40	4.39	4.30	4.27	4.17	4.59	4.54	4.56	4.54
15	4.02													
20	4.55													



Table 2-3 Bubble diameter (mm) at different gas flow rate in the down-comer zone of ILALR

Flow rate (L/min)	No media	Flow rate (L/min)	PVC				ABS				PP			
			2%	5%	10%	15%	2%	5%	10%	15%	2%	5%	10%	15%
2.5	2.61	2.5	2.66	2.62	-	-	2.57	2.54	2.59	-	2.64	2.61	-	-
5	2.82	5	2.83	2.82	-	-	2.82	2.82	2.82	3.86	2.87	2.84	2.87	2.80
7	3.16	10	3.42	3.42	3.68	-	3.36	3.36	3.34	3.79	3.45	3.42	3.43	3.43
10	3.28	15	3.98	3.98	4.13	-	3.99	3.90	3.90	3.88	4.01	4.00	4.02	4.01
12	3.58	20	4.38	4.39	4.38	-	4.28	4.30	4.26	4.26	4.55	4.53	4.55	4.52
15	4.01													
20	4.39													

3. Terminal rising bubble velocity (U_b) in BC and ILALR

Table 3-1 Terminal rising bubble velocity (m/min) in the BC

Flow rate (L/min)	No media	Flow rate (L/min)	PVC				ABS				PP			
			2%	5%	10%	15%	2%	5%	10%	15%	2%	5%	10%	15%
2.5	16.80	2.5	15.59	15.27	29.94	23.59	15.51	15.23	14.98	17.90	15.56	15.28	15.29	14.75
5	16.85	5	15.75	15.64	27.71	19.73	15.63	15.26	15.05	15.73	15.69	15.32	15.37	14.89
7	17.40	10	17.11	16.69	15.75	17.22	16.74	16.69	15.86	15.39	16.95	16.52	16.38	15.44
10	18.54	15	18.51	17.41	18.30	19.14	18.46	17.41	16.36	15.34	18.47	17.52	16.69	15.71
12	19.32	20	19.43	18.33	18.86	20.28	19.95	17.54	17.50	16.75	19.01	17.65	16.71	15.82
15	19.77													
20	22.17													

Table 3-2 Terminal rising bubble velocity (m/min) the riser zone of ILALR

Flow rate (L/min)	No media	Flow rate (L/min)	PVC				ABS				PP			
			2%	5%	10%	15%	2%	5%	10%	15%	2%	5%	10%	15%
2.5	16.75	2.5	15.59	15.31	20.46	22.56	15.49	15.23	15.02	20.42	15.50	15.30	15.34	14.78
5	16.81	5	15.74	15.64	20.21	20.31	15.66	15.30	15.10	17.50	15.70	15.33	15.47	14.96
7	17.41	10	17.11	16.87	19.60	19.18	16.71	16.76	15.97	15.60	16.94	16.82	16.45	15.48
10	18.54	15	18.51	17.54	18.43	18.08	18.46	17.44	16.41	16.79	18.49	17.51	16.69	15.74
12	19.37	20	19.41	18.71	19.03	20.93	19.98	17.54	17.59	17.49	19.01	17.77	16.74	15.84
15	19.75													
20	22.18													



Table 3-3 Terminal rising bubble velocity (m/min) the down-comer zone of ILALR

Flow rate (L/min)	No media	Flow rate (L/min)	PVC				ABS				PP			
			2%	5%	10%	15%	2%	5%	10%	15%	2%	5%	10%	15%
2.5	2.42	2.5	2.40	2.35	-	-	2.30	2.23	2.18	-	2.36	2.35	2.24	-
5	1.59	5	1.58	1.55	-	-	1.50	1.45	1.39	1.82	1.50	1.50	1.50	1.41
7	1.46	10	1.27	1.22	1.31	-	1.22	1.15	1.09	1.28	1.25	1.20	1.15	1.09
10	1.32	15	0.79	0.78	0.79	-	0.75	0.71	0.66	0.65	0.76	0.75	0.72	0.66
12	1.10	20	0.68	0.64	0.70	-	0.66	0.60	0.54	0.49	0.67	0.63	0.59	0.49
15	0.81													
20	0.70													

4. Benzene concentration (Absorbent) in liquid phases for different condition

Table 4-1 Outlet benzene concentration (Absorbent) in liquid phases for different condition at gas flow rate 10 L/min with time

Time (min)	Surfactant (No media)			Surfactant (Media)		Surfactant (GAC)		Surfactant (Media, GAC)	
	Water	Tween 80: 1 CMC	Tween 80: 0.1 CMC	Water (Media)	Tween 80: 0.1 CMC (Media)	Water (GAC)	Tween 80: 0.1 CMC (GAC)	Water (Media, GAC)	Tween 80: 0.1 CMC (Media, GAC)
0	0.000	0.000	0.000	0.000	0.000	0.000	0.000	0.000	0.000
1	0.249	0.319	0.272	0.271	0.275	0.228	0.281	0.255	0.261
3	0.499	0.602	0.515	0.557	0.532	0.410	0.511	0.392	0.507
5	0.612	0.726	0.614	0.644	0.656	0.456	0.621	0.468	0.627
7	0.680	0.777	0.698	0.691	0.731	0.487	0.683	0.492	0.674
9	0.721	0.824	0.766	0.741	0.789	0.485	0.679	0.495	0.672
11	0.748	0.839	0.789	0.760	0.802	0.502	0.681	0.499	0.680
13	0.760	0.856	0.802	0.752	0.829	0.482	0.670	0.497	0.683
15	0.758	0.883	0.818	0.746	0.825	0.484	0.656	0.500	0.670
17	0.757	0.877	0.824	0.754	0.810	0.482	0.664	0.484	0.660
19	0.759	0.888	0.825	0.743	0.823	0.472	0.670	0.494	0.652
21	0.730	0.886	0.827	0.760	0.829	0.484	0.685	0.502	0.654
25	0.760	0.891	0.823	0.753	0.819	0.499	0.683	0.499	0.670
$K_L a$ (min^{-1})	0.3213	0.3501	0.3323	0.3642	0.3688	0.5026	0.4639	0.5492	0.4873

VITA

Name: Miss. Nawaporn Thaphet
Date of Birth: May 14, 1990
Nationality: Thai
University Education: 2008-2012 Bachelor Degree of Chemical
Science, Faculty of Science, Chulalongkorn
University, Bangkok, Thailand

Presentation:

Nawaporn Thaphet, Prajak Sastaravet, Waralee Wisanpoka, Suriyapong Sasiwanapong, Passaworn Warunyuwong and Pisut Painmanakul. Effect of plastic media on mass transfer and bubble hydrodynamic parameters in bubble column and internal loop airlift reactor. The Proceedings of the 6th ASEAN Civil Engineering Conference (ACEC)/ the 6th ASEN Environmental Engineering Conference (AEEC), November 21-22, 2013, Pratumwan Princess Hotel, Bangkok, Thailand, Organized by Department of Civil Engineering and Department of Environmental Engineering, Faculty of Engineering, Chulalongkorn University



จุฬาลงกรณ์มหาวิทยาลัย
CHULALONGKORN UNIVERSITY